



## **Hong Kong Fine Particulate Matter (PM<sub>2.5</sub>) Chemical Compositions**

**January 1, 2020 – December 31, 2020**

*(Tender Ref. AS 19-03555)*

---

### **Final Report**

#### **PREPARED BY:**

Dr. John G. Watson  
Dr. Judith C. Chow  
Dr. Xiaoliang Wang  
Mr. Steven D. Kohl

DESERT RESEARCH INSTITUTE  
2215 Raggio Parkway  
Reno, NV 89512  
USA

#### **PREPARED FOR:**

Environmental Protection Department  
The Government of Hong Kong Special Administrative Region  
33/F, Revenue Tower  
5 Gloucester Rd.  
Wan Chai  
Hong Kong

October 31, 2021

## Contents

1	Introduction.....	1-1
1.1	Study Objectives.....	1-1
1.2	Background.....	1-1
1.3	Technical Approach.....	1-1
1.4	Guide to Report.....	1-2
2	Sampling Network.....	2-1
2.1	Ambient PM <sub>2.5</sub> Speciation Network.....	2-1
2.1	Ambient Particulate Measurements.....	2-1
2.2	Sample Delivery and Filter Condition.....	2-3
3	Database and Data Validation.....	3-1
3.1	Database Structures and Features.....	3-1
3.2	Measurement and Analytical Specifications.....	3-1
3.2.1	Definitions of Measurement Attributes.....	3-1
3.2.2	Definitions of Measurement Precision.....	3-4
3.2.3	Analytical Specifications.....	3-5
3.3	Quality Assurance.....	3-6
3.4	Data Validation.....	3-19
3.4.1	Sum of Chemical Species versus PM <sub>2.5</sub> Mass.....	3-19
3.4.2	Physical and Chemical Consistency.....	3-22
3.4.3	Anion and Cation Balance.....	3-29
3.4.4	IMPROVE_A TOR versus TOT Protocol for Carbon Measurements.....	3-31
3.4.5	Reconstructed versus Measured Mass.....	3-31
3.5	Collocated Comparisons.....	3-34
3.6	PM <sub>2.5</sub> Continuous and Filter Measurements 2017.....	3-34
4	PM <sub>2.5</sub> Components and Trends.....	4-1
5	Summary.....	5-1
6	References.....	6-1

## List of Figures

	<u>Page</u>
Figure 2-1. Monitoring sites in the Hong Kong PM <sub>2.5</sub> speciation network. ....	2-1
Figure 3-1. Flow diagram of data base management. ....	3-2
Figure 3-2. Sum of species vs. measured mass comparisons. ....	3-21
Figure 3-3. Comparison of sulfate by IC with sulfur by XRF. ....	3-23
Figure 3-4. Comparison of chloride by IC with chlorine by XRF. ....	3-25
Figure 3-5. Comparison of soluble potassium by IC with potassium by XRF. ....	3-26
Figure 3-6. Calculated vs measured ammonium ion. ....	3-28
Figure 3-7. Anion vs. cation balance. ....	3-30
Figure 3-8. OC by TOT vs. OC by TOR. ....	3-32
Figure 3-9. EC by TOT vs. EC by TOR. ....	3-33
Figure 3-10. Comparisons of reconstructed with measured mass. ....	3-35
Figure 3-11. Comparisons of selected species from collocated and primary quartz filter sampler concentrations.....	3-37
Figure 3-12. Comparisons of selected species from collocated and primary Teflon filter sampler concentrations.....	3-38
Figure 4-1. Trends in PM <sub>2.5</sub> annual averages at the five speciation sites. ....	4-8
Figure 4-2. Contributions of major components to 2020 PM <sub>2.5</sub> average concentrations. ....	4-9
Figure 4-3. Monthly average contributions from major PM <sub>2.5</sub> components at each site. ..	4-10
Figure 4-4. Trends in contributions from major components to PM <sub>2.5</sub> . ....	4-11

## List of Tables

Table 2-1. PM <sub>2.5</sub> sampler locations and site descriptions. ....	2-2
Table 2-2. Arrangement of collocated PM <sub>2.5</sub> samplers in the monitoring sites. ....	2-2
Table 2-3. Valid sampling dates for 2020 PM <sub>2.5</sub> speciation samples. ....	2-4
Table 2-4. Invalid samples for 2020. ....	2-4
Table 3-1. Summary of data files in the Hong Kong PM <sub>2.5</sub> data archive. ....	3-3
Table 3-2. Dynamic field blank concentration averages and standard deviations in µg/47 mm filter for: a) January-June 2020; b) July-December 2020; and c) January- December 2020. ....	3-7
Table 3-3. Minimum Detectable Limits (MDL), and Lower Quantifiable Limits (LQL), and samples exceeding them for: a) January-June, 2020; b) July-December, 2020; c) January-December, 2020. ....	3-13
Table 3-4. Statistics for sum of species vs. measured mass. Averages are in µg/m <sup>3</sup> .....	3-22
Table 3-5. Statistics for sulfate/sulfur comparisons. Averages are in µg/m <sup>3</sup> .....	3-24
Table 3-6. Samples outside of the EPA comparison tolerances for ratios<2.22.....	3-24
Table 3-7. Statistics for chloride/chlorine comparisons. Averages are in µg/m <sup>3</sup> . ....	3-26
Table 3-8. Statistics for potassium ion/total potassium comparisons. Averages in µg/m <sup>3</sup> ..	3-27
Table 3-9. Statistics for ammonium balance comparisons. Averages are in µg/m <sup>3</sup> . ....	3-29
Table 3-10. Statistics for anion/cation comparisons. Averages are in µg/m <sup>3</sup> . ....	3-31
Table 3-11. Statistics for TOT/TOR comparisons. Average concentrations in µg/m <sup>3</sup> .....	3-34
Table 3-12. Statistics for reconstructed and measured PM <sub>2.5</sub> mass. Average in µg/m <sup>3</sup> .....	3-36
Table 3-13. Samples with reconstructed mass exceeding measured mass. ....	3-36
Table 4-1. Annual averages for PM <sub>2.5</sub> mass and chemical constituents (µg/m <sup>3</sup> ) at MK. ....	4-3
Table 4-2. Annual averages for PM <sub>2.5</sub> mass and chemical constituents (µg/m <sup>3</sup> ) at YL. ....	4-4
Table 4-3. . Annual averages for PM <sub>2.5</sub> mass and chemical constituents(µg/m <sup>3</sup> ) at TW.....	4-5
Table 4-4. Annual averages for PM <sub>2.5</sub> mass and chemical constituents(µg/m <sup>3</sup> ) at KC. ....	4-6
Table 4-5. Annual averages for PM <sub>2.5</sub> mass and chemical constituents(µg/m <sup>3</sup> ) at WB.. ....	4-7
Table 4-6. 2020 annual average contributions of major PM <sub>2.5</sub> components (µg/m <sup>3</sup> ). ....	4-8
Table 4-7. 2020 annual average relative contributions (%) of major PM <sub>2.5</sub> components.....	4-9
Table 4-8. Change in annual average contributions from 2019 to 2020 (µg/m <sup>3</sup> ). ....	4-11

## Acronyms, Abbreviations and Chemical Symbols

AAE: absorption Angstrom exponent

Ag: Silver

Al: Aluminum

AQMS: Air Quality Monitoring Site

AQO: Air Quality Objective

AQRS: Air Quality Research Site

As: Arsenic

Au: Gold

Ba: Barium

BC: black carbon

$b_{\text{ext}}$ : light extinction coefficient

BLK: blank

Br: Bromine

Ca: Calcium

$\text{Ca}^{2+}$ : Calcium ion

Cd: Cadmium

Ce: Cerium

Cl: Chlorine

$\text{Cl}^-$ : Chloride ion

Co: Cobalt

Cr: Chromium

Cs: Cesium

CSN: Chemical Speciation Network

Cu: Copper

DRI: Desert Research Institute

dV: deciview =  $10 \times \ln(b_{\text{ext}}/10)$

EAF: DRI's Environmental Analysis Facility

EC: Elemental carbon

EC1, EC2, and EC3: Elemental carbon evolved at 580 °C, 740 °C, and 840 °C, respectively, in a 98% He/2% O<sub>2</sub> atmosphere

ECR: Elemental carbon reflectance

ECT: Elemental carbon transmittance

ED-XRF: Energy-Dispersive X-Ray Fluorescence Spectroscopy

Eu: Europium

F(RH): relative humidity growth factor

Fe: Iron

FID: Flame ionization detector

Ga: Gallium

He: Helium

Hf: Hafnium

Hg: Mercury

HKEPD: Hong Kong Environmental Protection Department

IC: Ion chromatography

ID: Identification number

IMPROVE: Interagency Monitoring of Protected Visual Environments

IMPROVE\_A: IMPROVE\_A thermal/optical carbon analysis protocol temperature protocol

In: Indium

Ir: Iridium

K: Potassium

$\text{K}^+$ : Potassium ion

KC: Kwai Chung

La: Lanthanum

LQL: Lower quantifiable limit

MDL: Minimum detectable limit

Mg: Magnesium

MK: Mong Kok

Mn: Manganese

Mo: Molybdenum

MU: Makeup

Na: Sodium

$\text{Na}^+$ : Sodium ion

$\text{Na}_2\text{SO}_4$ : Sodium sulfate

NAAQS: U.S. National Ambient Air Quality Standards

Nb: Niobium

$\text{NH}_4^+$ : Ammonium

$\text{NH}_4\text{NO}_3$ : Ammonium nitrate

$(\text{NH}_4)_2\text{SO}_4$ : Ammonium sulfate

$\text{NH}_4\text{HSO}_4$ : Ammonium bisulfate

Ni: Nickel

$\text{NO}_3^-$ : Nitrate

O<sub>2</sub>: Oxygen

OC: Organic carbon

OC1, OC2, OC3, and OC4: Organic carbon evolved at 140 °C, 280 °C, 480 °C, and 580 °C, respectively, in a 100% He atmosphere

OCR: Organic carbon reflectance

OCT: Organic carbon transmittance

OM: Organic matter

OP: Pyrolyzed carbon

OPR: Pyrolyzed organic carbon by reflection

OPT: Pyrolyzed organic carbon by transmittance

P: Phosphorous

Pb: Lead

Pd: Palladium

PM: Particulate matter

$\text{PM}_{2.5}$ : Particles with aerodynamic diameter  $\leq 2.5 \mu\text{m}$

PTFE: Polytetrafluoroethylene

QA: Quality assurance

QC: Quality control

Rb: Rubidium

S: Sulfur

Sb: Antimony

Sc: Scandium

Se: Selenium

Si: Silicon

Sm: Samarium

Sn: Tin

SNAQS: Southern Nevada Air Quality Study

SO<sub>4</sub><sup>2-</sup>: Sulfate  
Sr: Strontium  
Ta: Tantalum  
Tb: Terbium  
TC: Total carbon or Tung Chung site  
Ti: Titanium  
Tl: Thallium  
TOR: Thermal optical reflectance  
TOT: Thermal optical transmittance  
TW: Tsuen Wan  
U: Uranium  
U.S.EPA: United States Environmental Protection  
Agency

V: Vanadium  
V<sub>r</sub>: visual range  
VSCC: Very Sharp Cut Cyclone  
W: Wolfram  
WB: Clear Water Bay  
WHO: World Health Organization  
XRF: X-ray fluorescence  
Y: Yttrium  
YL: Yuen Long  
Zn: Zinc  
Zr: Zirconium

# 1 Introduction

## 1.1 Study Objectives

Under direction of the Hong Kong Environmental Protection Department (HKEPD), the Desert Research Institute (DRI) of the Nevada System of Higher Education (NSHE) has analyzed PM<sub>2.5</sub> (particles with aerodynamic diameters <2.5 µm) samples acquired during calendar year 2020. The objectives of these measurements are to:


- Determine PM<sub>2.5</sub> organic and inorganic chemical compositions and how they differ by season and proximity to different source types.
- Use ambient concentrations of marker compounds, source measurements performed elsewhere, and available Hong Kong emissions inventories, to determine which sources are probable contributors to Hong Kong PM<sub>2.5</sub> levels.
- Investigate and understand the influences of meteorological/atmospheric conditions on PM<sub>2.5</sub> episodic events.
- Evaluate PM<sub>2.5</sub> mass and chemical concentrations for inter-annual variability and long-term trends in urban and rural areas.

Specific DRI tasks are:

- Receive filter samples from the HKEPD and analyze them for elements, water-soluble anions and cations, and organic and elemental carbon (OC and EC).
- Compare and evaluate the OC/EC measurements for Thermal Optical Reflectance (TOR) and Thermal Optical Transmittance (TOT) pyrolysis adjustments.
- Validate data and compare with HKEPD previous data sets.

## 1.2 Background

HKEPD (2021a) Air Quality Objectives (AQOs) set PM<sub>2.5</sub> concentration limits to 75 µg/m<sup>3</sup> with a maximum of 9 exceedance days for 24-hour averages and 35 µg/m<sup>3</sup> for annual averages. To attain these AQOs, the HKEPD has been implementing a wide range of air quality improvement measures, including reducing emissions from land and sea transport, power plants, and non-road machinery. Recent real-world emission measurements are demonstrating the effectiveness of several of these efforts (Cui et al., 2018; Niu et al., 2020; Wang et al., 2018; Wang et al., 2021) and revealing the limitations of other strategies (Lyu et al., 2016; Yao et al., 2019). The governments of Guangdong, Hong Kong, and Macao are strengthening collaborations to reduce regional air pollution.

The HKEPD initiated PM<sub>2.5</sub> chemical speciation in 2000 (Louie et al., 2002; Louie et al., 2005a; Louie et al., 2005b) and currently operates five sites, including collocated comparisons. PM<sub>2.5</sub> mass is used to determine AQO compliance while chemical compositions can be used to determine reasons for elevated levels. The long-term composition record permits tracking of trends in response to emission reduction strategies. This report documents PM<sub>2.5</sub> measurements and data validation from January to December 2020. Data from previous years are described in earlier reports (HKEPD, 2021b). 

## 1.3 Technical Approach

Twenty-four hour samples were acquired every sixth day (U.S.EPA, 2021) from midnight to midnight local standard time (LST) on collocated Teflon membrane- and quartz fiber-filters at roadside-source-dominated Mong Kok (MK), new town Yuen Long (YL), urban Tsuen Wan (TW) and Kwai Chung (KC), and suburban Clear Water Bay (WB) monitoring

stations. The Teflon-membrane and quartz-fiber filters were analyzed by an HKEPD contractor for mass by gravimetry (Watson et al., 2017), then transferred to DRI for chemical analyses for: 1) elements with atomic number ranging from 11 (Sodium) to 92 (Uranium) by Energy-Dispersive X-Ray Fluorescence (ED-XRF) Spectroscopy; 2) water-soluble anions (i.e., chloride, nitrate, and sulfate) and cations (i.e., sodium, ammonium, and potassium) using Ion Chromatography (IC); and 3) organic, elemental, and total carbon (OC, EC, and TC) and thermal fractions following the IMPROVE\_A protocol (Chow et al., 2007).

#### **1.4 Guide to Report**

This section states the objectives and background for PM<sub>2.5</sub> chemical analysis. Section 2 documents the ambient monitoring network and the unified database compiled from these measurements. The ambient database is assembled, validated, and documented in Section 3. Section 4 assesses the multi-year trends and seasonal variations of PM<sub>2.5</sub> and chemical compositions. Findings are summarized in Section 5 with reference citations in Section 6.



## 2 Sampling Network

### 2.1 Ambient PM<sub>2.5</sub> Speciation Network

Twenty-four-hour PM<sub>2.5</sub> filter samples were acquired at five sites every sixth day from beginning on January 6, 2020 with the final sample on December 25, 2020. The PM<sub>2.5</sub> speciation network sites shown in Figure 2-1 represent roadsides (MK), urban (TW and KC), new town (YL), and suburban (WB) areas with descriptions of their surroundings in Table 2-1.

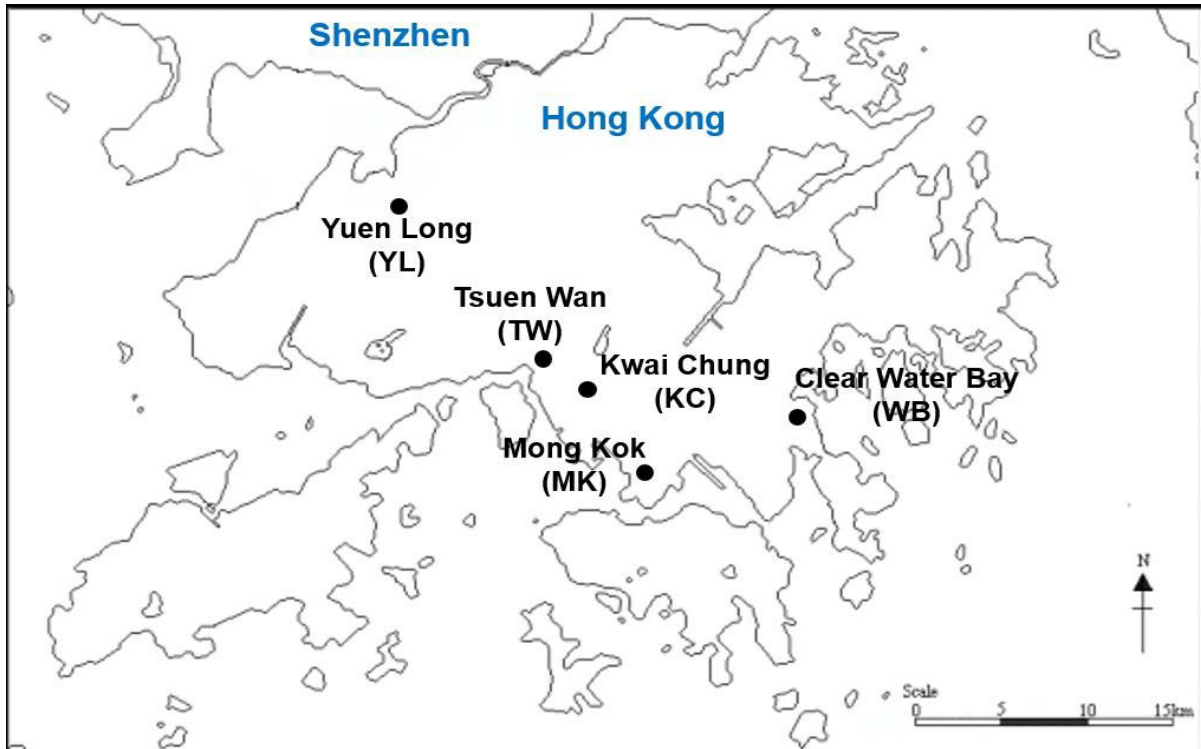


Figure 2-1. Monitoring sites in the Hong Kong PM<sub>2.5</sub> speciation network.

### 2.1 Ambient Particulate Measurements

Two BGI PQ200 filter samplers were located at the MK, TW, and YL sites with two Partisol samplers located at the KC and WB sites so that the Teflon and quartz filters could be sampled simultaneously (Yu et al., 2020). Collocated measurements were acquired at the locations specified in Table 2-2 to estimate collocated precisions for the measurements. Each filter sampler is equipped with an Andersen PM<sub>10</sub> inlet (Watson and Chow, 2011) followed by a Very Sharp Cut Cyclone (VSCC) (Kenny et al., 2004) to sample PM<sub>2.5</sub> at a flow rate of 16.7 L/min. At this flow rate, a nominal volume of 24.0 m<sup>3</sup> of ambient air is obtained over a 24-hour period. Lippmann (1989), Lee and Ramamurthi (1993), Watson and Chow (1993, 1994), and Chow (1995) evaluated substrates for different sampling and analyses. Based on these evaluations, filters used for this study were: 1) Whatman PTFE filters (Piscataway, NJ, USA) PM<sub>2.5</sub> membrane 46.2 mm with support ring (#7592-104) for mass and elemental analysis; and 2) Pall (#7202) quartz-fiber filter for ion and carbon analyses. Filter preparation, operation and maintenance of the Partisol samplers, and gravimetric analysis were conducted by HKEPD's contractor throughout the study period.

Table 2-1. PM<sub>2.5</sub> sampler locations and site descriptions.

Site Name	Site Code	Site Location	Site Description
Mong Kok	MK	Junction of Lai Chi Kok Road and Nathan Road, Kowloon	Urban roadside in mixed residential/commercial area with heavy traffic and surrounded by many tall buildings
Yuen Long	YL	Rooftop of Yuen Long District Branch Office Building, 269 Castle Peak Road, New Territories	Residential town, about 15 km southwest of Shenzhen
Tsuen Wan	TW	Rooftop of Princess Alexandra Community Center, 60 Tai Ho Road, New Territories	Urban, densely populated, residential site with mixed commercial and industrial developments. Located northwest of the MK site
Kwai Chung	KC	Rooftop of the Kwai Chung Police Station, 999 Kwai Chung Road	Urban, densely populated residential site with mixed commercial and industrial developments, close to the Kwai Tsing Container Terminals
Clear Water Bay	WB	Rooftop of a pump house next to Coastal Marine Lab, HKUST Campus, Clear Water Bay	Clean rural area with little residential and commercial development on the east coast of Sai Kung

Table 2-2. Arrangement of collocated PM<sub>2.5</sub> samplers in the monitoring sites.

Location	No. of Samplers	Collocated Samples
MK AQMS	3	Teflon-membrane filters
YL AQMS	2	None
TW AQMS	2	None
KC AQMS	2	None
WB AQRS	3	Quartz-fiber filters

At DRI, Teflon-membrane filters were analyzed for 51 elements (Na, Mg, Al, Si, P, S, Cl, K, Ca, Sc, Ti, V, Cr, Mn, Fe, Co, Ni, Cu, Zn, Ga, As, Se, Br, Rb, Sr, Y, Zr, Nb, Mo, Pd, Ag, Cd, In, Sn, Sb, Cs, Ba, La, Ce, Sm, Eu, Tb, Hf, Ta, W, Ir, Au, Hg, Tl, Pb, and U) by energy dispersive x-ray fluorescence (XRF) (Watson et al., 1999). Portions of the quartz-fiber filters were analyzed for water-soluble anions (i.e., chloride [Cl<sup>-</sup>], nitrate [NO<sub>3</sub><sup>-</sup>], and sulfate [SO<sub>4</sub><sup>2-</sup>] and cations (i.e., sodium [Na<sup>+</sup>], ammonium [NH<sub>4</sub><sup>+</sup>], and potassium [K<sup>+</sup>]) by IC (Chow and Watson, 1999, 2017), and for carbon by thermal/optical reflectance and transmittance (TOR and TOT) following the IMPROVE\_A protocol (Chow et al., 1993; Chow et al., 2007; Chow et al., 2011; Chow et al., 2015b; Chow et al., 2021).

Uncertainty in determining total carbon (TC) using thermal evolution methods results from differences in adsorption and volatilization of certain organic compounds during sampling and storage (Chow et al., 2010; Fitz, 1990; Turpin et al., 1994; Watson et al., 2009). The division of TC into OC and EC depends on temperature set-points, temperature ramping rates, residence time at each temperature step, and carrier gas composition (Watson et al., 2005). At higher temperatures in an oxygen-free atmosphere, samples visibly darken as OC pyrolyzes to EC. To overcome this artifact, a laser is used to monitor changes in filter darkness during the thermal evolution process by detecting filter reflectance ([TOR] method) and/or transmittance ([TOT] method) (Birch and Cary, 1996; Chow et al., 2001; Chow et al., 2004). OC and EC TOR and TOT separations of OC from EC differ due to charring of particles on the filter surface and organic gases adsorbed within the filter. TOR is more sensitive to

particulate OC charring than TOT which is dominated by adsorbed gas charring (Chow et al., 2004).

The IMPROVE\_A protocol (Chow et al., 2007) has been used for OC, EC, and carbon fractions in the U.S. National Park Service's Interagency Monitoring of Protected Visual Environments (IMPROVE) network since 2005 and the U.S.EPA's Chemical Speciation Network (CSN) since 2007. This protocol measures seven well-defined OC and EC thermal fractions and OC-charring by both TOR and TOT, allowing OC and EC comparability with other methods through appropriate sums of these fractions. The temperature in a pure helium (He) atmosphere ramps from 25 to 140 °C (OC1), from 140 to 280 °C (OC2), from 280 to 480 °C (OC3), and from 480 to 580 °C (OC4). Then, a 98% He/2% O<sub>2</sub> atmosphere is introduced and peaks are integrated at 580 °C (EC1), 740 °C (EC2), and 840 °C (EC3). The IMPROVE\_A protocol requires the optical signal to return to baseline before advancing to the next set-point. The fraction of pyrolyzed organic carbon by reflection of transmittance (OPR or OPT) is detected in the He/O<sub>2</sub> atmosphere at 580 °C prior to the return of reflectance or transmittance to its original value. In the IMPROVE\_A protocol, OC is defined as the sum of OC1 + OC2 + OC3 + OC4 + OPR (or OPT), and EC is defined as the sum of EC1+EC2+EC3-OPR (or OPT). In cases where the laser reflectance or transmittance returns to its initial value before O<sub>2</sub> is introduced, a negative OPR or OPT is reported. The carbon analyses were performed with the DRI Model 2015 multiwavelength thermal/optical carbon analyzer (Magee Scientific, Berkeley, CA, USA). Chow et al. (2015b; 2018) demonstrated that the replacement of DRI Model 2001 with Model 2015 analyzers return equivalent results while adding multiwavelength optical information (i.e., 405, 445, 532, 635, 780, 808, and 980 nm) that separates brown carbon (BrC) from EC (Chen et al., 2015; Chen et al., 2021).

## **2.2 Sample Delivery and Filter Condition**

A total of 792 filter samples were collected during the study period. Two of these were invalidated by the field operations, leaving 790 filter samples for analysis, including 396 Teflon filters and 394 quartz fiber filters. Valid sample dates are summarized in Table 2-3 with the reasons for the two invalid samples given in Table 2-4. This is an improvement over the previous year when seven samples were invalidated, mostly due to power failures (Yu et al., 2020). Complete routine operations data are available for 298 Teflon/quartz pairs.

Table 2-3. Valid sampling dates for 2020 PM<sub>2.5</sub> speciation samples.

<b>January</b>	<b>February</b>	<b>March</b>	<b>April</b>	<b>May</b>	<b>June</b>
6-Jan	5-Feb	6-Mar	5-Apr	5-May <sup>a</sup>	4-Jun
12-Jan	11-Feb	12-Mar <sup>a</sup>	11-Apr	11-May	10-Jun
18-Jan	17-Feb	18-Mar	17-Apr	17-May	16-Jun
24-Jan	23-Feb	24-Mar	23-Apr	23-May	22-Jun
30-Jan	26-Feb <sup>a,b</sup>	30-Mar	29-Apr	29-May	28-Jun
	29-Feb				
<b>July</b>	<b>August</b>	<b>September</b>	<b>October</b>	<b>November</b>	<b>December</b>
4-Jul <sup>a</sup>	3-Aug	2-Sep	2-Oct	1-Nov	1-Dec
10-Jul	9-Aug	8-Sep <sup>a</sup>	8-Oct	7-Nov	7-Dec
16-Jul	15-Aug	14-Sep	14-Oct	13-Nov <sup>a</sup>	13-Dec
22-Jul	21-Aug	20-Sep	20-Oct	19-Nov	19-Dec
28-Jul	27-Aug	26-Sep	26-Oct	25-Nov	25-Dec

<sup>a</sup>Both regular and blank samples were collected. <sup>b</sup>Sample day not on 1-in-6 day schedule.

Table 2-4. Invalid samples for 2020.

<b>Sample ID</b>	<b>Comments</b>
YL200511SF011Q	Voided by EPD
WB201020PF03Q	Sampler failed, external leak

### 3 Database and Data Validation

This section describes the data base and evaluates the precision, accuracy, and validity of the Hong Kong PM<sub>2.5</sub> filter data measurements in 2020. Lioy et al. (1980), Chow and Watson (1989, 1994), and Watson and Chow (1992) summarize the requirements, limitations, and current availability of ambient and source databases in the United States. The Hong Kong PM<sub>2.5</sub> data set intends to meet these requirements.

#### 3.1 Database Structures and Features

An electronic database for the analytical results was established for Hong Kong PM<sub>2.5</sub> data archive. Figure 3-1 illustrates the processes followed to compile this data base. Raw HKEPD data were unified with laboratory measurements using a relational database and converted to Microsoft Excel format for reporting and general use purposes. Table 3-1 lists the contents of the final data files. Each observable is identified by a field name which follows a pattern for that type of observable. For example, in the filter-based aerosol concentration file, the first two characters represent the measured species (e.g., AL for aluminum, SI for silicon, and CA for calcium), the third character designates the analysis method (i.e., “G” for gravimetric weighing, “X” for X-ray fluorescence analysis, “I” for ion chromatography, “T” for thermal/optical carbon analysis), and the last character uses a “C” to identify a species concentration or a “U” to identify the uncertainty (i.e., precision) of the corresponding measurement. Each measurement method is associated with a separate validation field to document the sample validity for that method. Missing or invalidated measurements have been removed and replaced with -99. Each record is tagged with “RO” for routine operations, “CO” for a collocated measurement, or “FB” for field blank.

#### 3.2 Measurement and Analytical Specifications

Every measurement consists of: 1) a value; 2) a precision; 3) an accuracy; and 4) a validity (Hidy, 1985; Watson et al., 1989; 2001). The measurement/analysis methods described in Section 2 are used to obtain the value. Performance testing via regular submission of standards, blank analysis, and replicate analysis are used to estimate precision. These precisions are reported in the data files so that they can be propagated through air quality models and used to evaluate how well different values compare with one another. The submission and evaluation of independent standards through quality audits are used to estimate accuracy. Validity applies both to the measurement method and to each measurement taken with that method. The validity of each measurement is indicated by appropriate flagging within the data base.

##### 3.2.1 Definitions of Measurement Attributes

The precision, accuracy, and validity of the PM<sub>2.5</sub> measurements are defined as follows (Watson et al., 2001):

- A **measurement** is an observation at a specific time and place which possesses: 1) value – the center of the measurement interval; 2) precision – the width of the measurement interval; 3) accuracy – the difference between measured and reference values; and 4) validity – the compliance with assumptions made in the measurement method.
- A **measurement method** is the combination of equipment, reagents, and procedures, which provide the value of a measurement. The full description of the measurement method requires substantial documentation. For example, two methods may use the same sampling systems and the same analysis systems. These are not identical methods,

however, if one performs acceptance testing on filter media and the other does not. Seemingly minor differences between methods can result in major differences between measurement values.

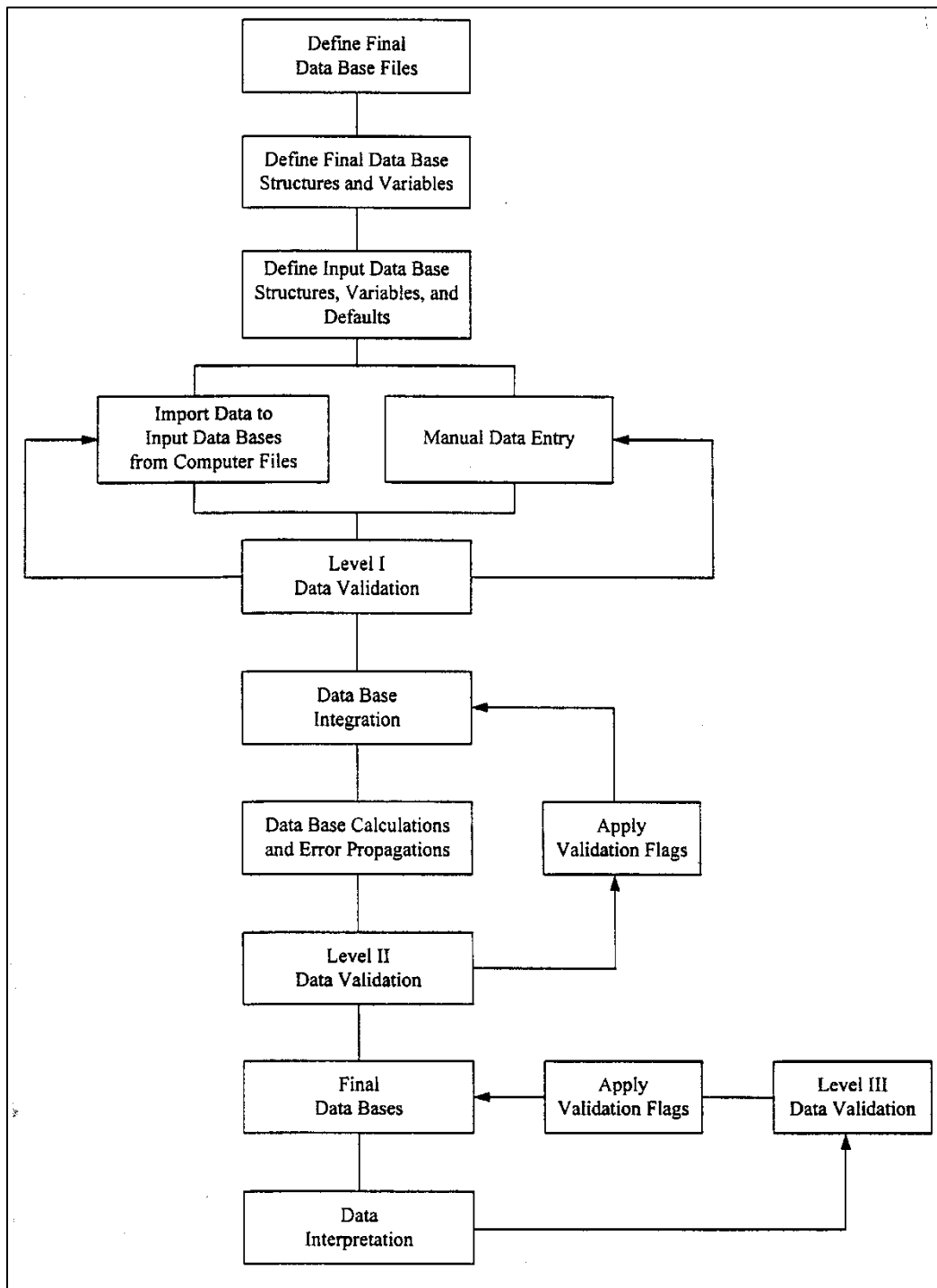


Figure 3-1. Flow diagram of data base management

Table 3-1. Summary of data files in the Hong Kong PM<sub>2.5</sub> data archive.

Category	Database File	Database Description
I. DATABASE DOCUMENTATION		
	HKEPD Field Names.xlsx	Defines the field names, measurement units, and formats used in the ambient database
II. MASS AND CHEMICAL DATA		
	HKEPD2020- PM25.xlsx	Contains 24-hour PM <sub>2.5</sub> mass and chemical data <sup>a,b</sup> collected with Partisol filter samplers at five sites on every sixth day between January 6, 2020 and December 25, 2020
III. DATABASE VALIDATION		
	FLDFLAGS.xlsx	Contains the field sampling data validation flags
	CHEMFLAG.xlsx	Contains the chemical analysis data validation flags

<sup>a</sup> Includes 51 elements (Na, Mg, Al, Si, P, S, Cl, K, Ca, Sc, Ti, V, Cr, Mn, Fe, Co, Ni, Cu, Zn, Ga, As, Se, Br, Rb, Sr, Y, Zr, Nb, Mo, Pd, Ag, Cd, In, Sn, Sb, Cs, Ba, La, Ce, Sm, Eu, Tb, Hf, Ta, W, Ir, Au, Hg, Tl, Pb, and U) by X-ray fluorescence.

<sup>b</sup> Includes water-soluble chloride, nitrate, sulfate, sodium, ammonium, and potassium by ion chromatography; and organic carbon (OCR and OCT), elemental carbon (ECR and ECT), nine carbon fractions (OC1, OC2, OC3, OC4, OPR, OPT, EC1, EC2, and EC3) and total carbon (TC) by thermal/optical reflectance and transmittance following the IMPROVE\_A protocol at 635 nm. Initial and final reflectance and transmittance at 405, 445, 532, 635, 780, 808, and 980 nm are reported.

- **Measurement method validity** is the identification of measurement method assumptions, the quantification of effects of deviations from those assumptions, the evaluation that deviations are within reasonable tolerances for the specific application, and the creation of procedures to quantify and minimize those deviations during a specific application.
- **Sample validation** is accomplished by procedures that identify deviations from measurement assumptions and the assignment of flags to individual measurements for potential deviations from assumptions.
- The **comparability and equivalence of sampling and analysis methods** are established by the comparison of values and precisions for the same measurement obtained by different measurement methods. Interlaboratory and intralaboratory comparisons are usually made to establish this comparability. Simultaneous measurements of the same observable are considered equivalent when more than 90% of the values differ by no more than the sum of two one-sigma precision intervals for each measurement.
- **Completeness** measures how many environmental measurements with specified values, precisions, accuracies, and validities were obtained out of the total number attainable. It measures the practicability of applying the selected measurement processes throughout the measurement period. Databases which have excellent precision, accuracy, and validity may be of little use if they contain so many missing values that data interpretation is impossible.

A total of 298 routine sample pairs (each sample pair includes a Teflon-membrane filter and a quartz-fiber filter) were acquired, of which the two quartz filters identified in Table 2-4 were excluded. Elemental results from the Teflon filter are available for these samples. No

samples from the TW site during January were submitted for analysis and non-routine samples were acquired at MK, YL, and WB on 2/26/2020. Thirty-six field blank pairs and 121 collocated Teflon and quartz filters were analyzed. The total filters submitted for chemical analysis included 396 Teflon-membrane filters (for 51 elements) and 394 quartz-fiber filters (for 6 ions and 14 carbon fractions as a function of 7 wavelengths).

### 3.2.2 Definitions of Measurement Precision

Measurement precisions were propagated from precisions of the volumetric measurements, the chemical composition measurements, and the field blank variability using the methods of Bevington (1969) and Watson et al. (2001). The following equations are applied to calculate the precision associated with filter-based measurements:

$$C_i = (M_i - B_i)/V \quad (3-1)$$

$$V = F \times t \quad (3-2)$$

$$B_i = \frac{1}{n} \sum_{j=1}^n B_{ij} \quad \text{for } B_i > \sigma_{Bi} \quad (3-3)$$

$$B_i = 0 \quad \text{for } B_i \leq \sigma_{Bi} \quad (3-4)$$

$$\sigma_{Bi} = \text{STD}_{Bi} = \left[ \frac{1}{n-1} \sum_{j=1}^n (B_{ij} - B_i)^2 \right]^{1/2} \quad \text{for } \text{STD}_{Bi} > \text{SIG}_{Bi} \quad (3-5)$$

$$\sigma_{Bi} = \text{SIG}_{Bi} = \left[ \frac{1}{n} \sum_{j=1}^n (\sigma_{Bij})^2 \right]^{1/2} \quad \text{for } \text{STD}_{Bi} \leq \text{SIG}_{Bi} \quad (3-6)$$

$$\sigma_{Ci} = \left[ \frac{\sigma_{Mi}^2 + \sigma_{Bi}^2}{V^2} + \frac{\sigma_V^2 (M_i - B_i)^2}{V^4} \right]^{1/2} \quad (3-7)$$

$$\sigma_V/V = 0.05 \quad (3-8)$$

where:

$B_i$  = average amount of species i on field blanks

$B_{ij}$  = amount of species i found on field blank j

$C_i$  = the ambient concentration of species i

$F$  = flow rate throughout sampling period

$M_i$  = amount of species i on the substrate

$n$  = total number of samples in the sum

$\text{SIG}_{Bi}$  = root mean square error (RMSE), the square root of the averaged sum of the squared of  $\sigma_{Bij}$ .

$\text{STD}_{Bi}$  = standard deviation of the blank

$\sigma_{Bi}$  = blank precision for species i

$\sigma_{Bij}$  = precision of the species i found on field blank j

$\sigma_{Ci}$  = propagated precision for the concentration of species i

$\sigma_{Mi}$  = precision of amount of species i on the substrate

$\sigma_V$  = precision of sample volume

$t$  = sample duration



$V$  = volume of air sampled

Dynamic field blanks were periodically placed in each sampling system without air being drawn through them to estimate the magnitude of passive deposition for the period of time that filter packs remained in a sampler (typically 24 hours). The uncertainty of the measured value and the average uncertainty of the field blanks for each species are used to propagate the overall precision for each blank subtracted concentration value. The final value is propagated by taking the square root of the sum of the squares of the calculated uncertainty and the average field blank uncertainty for each measurement.

### 3.2.3 Analytical Specifications

The average field blank concentrations (with outliers removed) were calculated for each species on each substrate (i.e., Teflon-membrane and quartz-fiber), irrespective of the sites. For the 2020 data, average blank concentrations and their standard deviations were applied to samples taken from January–June 2020 and July–December 2020 and applied to routine samples for each of these periods. These are summarized in Table 3-2.

Blank precisions ( $\sigma_{Bi}$ ) are defined as the higher value of the standard deviation of the blank measurements,  $STD_{Bi}$ , or the square root of the averaged squared uncertainties of the blank concentrations,  $SIG_{Bi}$ . If the average blank for a species was less than its precision, the blank was set to zero (as shown in Equation 3-4).

The precisions ( $\sigma_{Mi}$ ) for IC and carbon analyses were determined from replicate measurements as the average fractional difference between original and replicate analysis concentrations. Concentration uncertainty is the fractional precision times sample concentration. The precisions for XRF analysis were determined from counting statistics unique to each sample. Hence, the  $\sigma_{Mi}$  is a function of the energy-specific peak area, the background, and the area under the baseline. Filter mass and blank mass analysis was performed by the HKEPD's contractor. Blank subtractions and calculated uncertainties were not examined by DRI and were thus not included in data in this report.

Table 3-3 summarizes the analytical specifications for the 24-hour  $PM_{2.5}$  measurements obtained during the study. Minimum detectable limits (MDL) and lower quantifiable limits (LQL) are given. The MDL is defined as the concentration at which the instrument response equals three times the standard deviation of the response to a known concentration of zero. The LQL is defined as a concentration corresponding to three times the standard deviation of the dynamic field blank. The LQLs in Table 3-3 were divided by  $24.0\text{ m}^3$ , nominal 24-hour volume, for the filter samplers. Actual volumes varied from sample to sample, but were typically within  $\pm 5\%$  of the pre-set volume. The LQLs should always be equal to or larger than the analytical MDLs because they include the standard deviation of the field blank and flow rate precision (Watson et al., 2001). This was the case for most of the chemical compounds noted in Table 3-3.

The number of reported (non-void, non-missing) concentrations for each species and the number of reported concentrations greater than the MDLs and LQLs are also summarized in Table 3-3. For routine samples, ions (e.g., nonvolatilized nitrate, sulfate, ammonium, sodium, and potassium), OC and EC, Na, Si, S, Cl, K, Ca, V, Mn, Fe, Ni, Cu, Zn, and Br were detected ( $> \text{MDL}$ ) in most of the samples. No concentrations were detected for EC3, P, Sc, Ga, Ba, La, Hf, Ta, Ir, Hg, and Tl, with the exception of 1% for Ga and Ba during the first six months and 5% during the final six months. Elements with  $<10\%$  of samples above MDLs include Co, As, Nb, Cd, Ag, Cd, Cs, Ce, Sm, Eu, W, Au, and U. For all of these cases

concentrations were only slightly above the MDL and the values should be considered upper limits only

These results are typical for urban and non-urban sites in most regions of the world. Residual-oil-related species, such as Ni and V, were detected in 90-97% and 79-83% of the samples, respectively. Se, often associated with coal fly ash, exceeded MDLs in only 28-45% of the samples. Mineral markers, often derived from road dust and construction, include Al, Si, K, Ca, Ti, and Fe, and most of these were detected in most samples. Although Pb was once prominent when leaded additives were used in gasoline, Pb was still measured in more than 76-81% of the samples. It is suspected that tire weights (Root, 2000) that are lost during driving and ground down by traffic. Na, Cl, K, and Br ions are also prominent in marine aerosols and were detected in most of the samples.

These fractions above MDLs and LQLs imply that PM<sub>2.5</sub> samples have sufficient loadings and the analytical methods have sufficient sensitivity to accomplish the network objectives.

### **3.3 Quality Assurance**

Quality control (QC) and quality auditing establish the precision, accuracy, and validity of measured values. Quality assurance (QA) integrates quality control, quality auditing, measurement method validation, and sample validation into the measurement process. The results of QA are data values with specified precisions, accuracies, and validities.

QC is intended to prevent, identify, correct, and define the consequences of difficulties that might affect the precision and accuracy, and or validity of the measurements. Quality auditing consisted of systems and performance audits. The system audit should include a review of the operational and QC procedures to assess whether they were adequate for assuring valid data that met the specified levels of accuracy and precision. Quality auditing should also examine all phases of the measurement activity to determine that procedures were followed and that operators were properly trained. Performance audits should establish whether the predetermined specifications were achieved in practice. The performance audits should challenge the measurement/analysis systems with known transfer standards traceable to primary standards. Quality Control and Quality Auditing procedures were carried out by the HKEPD for the samplers and for filter mass analyses. Both system and performance audits were performed in DRI's Environmental Analysis Facility (EAF) on an annual basis to assure data quality. Auditors acquired and reviewed the standard operating procedures and examined all phases of measurement activities to assure that procedures were followed and that operators were properly trained.

Table 3-2. Dynamic field blank concentration averages and standard deviations in µg/47 mm filter for: a) January-June 2020; b) July-December 2020; and c) January- December 2020.

<b>a) Species, January-June 2020</b>	<b>Blank Subtracted (B<sub>i</sub>)</b>	<b>Average Field Blank</b>	<b>Blank Precision (S<sub>Bi</sub>)</b>	<b>Blank Std. Dev. (STD<sub>Bi</sub>)</b>	<b>Root Mean Squared Blank Precision (SIG<sub>Bi</sub>)</b>	<b>No. of Blanks</b>
Chloride (Cl <sup>-</sup> )	0.1631	0.1631	0.0674	0.0674	0.0045	18
Nitrate (NO <sub>3</sub> <sup>-</sup> )	0.5854	0.5854	0.3095	0.3095	0.1182	18
Sulfate (SO <sub>4</sub> <sup>=</sup> )	0.3637	0.3637	0.2289	0.2289	0.0242	18
Ammonium (NH <sub>4</sub> <sup>+</sup> )	0.0392	0.0392	0.0295	0.0261	0.0295	18
Sodium (Na <sup>+</sup> )	0.0000	0.0427	0.2064	0.0141	0.2064	18
Potassium (K <sup>+</sup> )	0.0429	0.0429	0.0184	0.0174	0.0184	18
O1TC	4.9498	4.9498	0.9554	0.7569	0.9554	18
O2TC	4.3704	4.3704	1.0394	1.0394	0.2878	18
O3TC	8.9437	8.9437	6.6888	6.6888	1.4602	18
O4TC	1.9400	1.9400	1.5503	1.5503	0.7169	18
OPTTC	0.0000	1.5247	2.2085	2.2085	0.5971	18
OPTRC	0.0000	0.2974	1.1050	1.1050	0.6702	18
OCTTC	21.7285	21.7285	10.5491	10.5491	1.9646	18
OCTRC	20.5012	20.5012	9.3566	9.3566	2.3268	18
E1TC	0.0000	0.3594	0.7921	0.7921	0.1618	18
E2TC	0.0000	1.1779	1.4354	1.4354	1.3931	18
E3TC	0.0000	0.0000	0.0405	0.0000	0.0405	18
ECTTC	0.0000	0.0125	0.1385	0.0486	0.1385	18
ECTRC	0.0000	1.2398	1.3556	1.3556	0.3765	18
TCTC	21.7411	21.7411	10.5385	10.5385	2.2276	18
Sodium (Na)	0.0000	0.0788	1.0147	0.1513	1.0147	18
Magnesium (Mg)	0.0000	0.0367	0.7872	0.1421	0.7872	18
Aluminum (Al)	0.0000	0.0247	0.3827	0.0727	0.3827	18
Silicon (Si)	0.0000	0.0671	0.0829	0.0829	0.0683	18
Phosphorus (P)	0.0000	0.0072	0.0317	0.0131	0.0317	18
Sulfur (S)	0.0000	0.0000	0.0167	0.0000	0.0167	18
Chlorine (Cl)	0.0000	0.0000	0.1250	0.0000	0.1250	18
Potassium (K)	0.0000	0.0000	0.0034	0.0000	0.0034	18
Calcium (Ca)	0.0000	0.0000	0.1516	0.0000	0.1516	18
Scandium (Sc)	0.0000	0.0000	0.9245	0.0000	0.9245	18
Titanium (Ti)	0.0000	0.0098	0.0283	0.0156	0.0283	18
Vanadium (V)	0.0000	0.0011	0.0100	0.0024	0.0100	18
Chromium (Cr)	0.0000	0.0013	0.0317	0.0025	0.0317	18
Manganese (Mn)	0.0000	0.0148	0.0334	0.0153	0.0334	18
Iron (Fe)	0.0000	0.0348	0.1049	0.0447	0.1049	18
Cobalt (Co)	0.0000	0.0024	0.0083	0.0028	0.0083	18

Table 3-2 (continued). Dynamic field blank concentration averages and standard deviations in µg/47 mm filter from January-June 2020.

<b>a) Species, January-June 2020</b>	<b>Blank Subtracted (B<sub>i</sub>)</b>	<b>Average Field Blank</b>	<b>Blank Precision (S<sub>Bi</sub>)</b>	<b>Blank Std. Dev. (STD<sub>Bi</sub>)</b>	<b>Root Mean Squared Blank Precision (SIG<sub>Bi</sub>)</b>	<b>No. of Blanks</b>
Nickel (Ni)	0.0000	0.0003	0.0167	0.0006	0.0167	18
Copper (Cu)	0.0000	0.0059	0.0850	0.0094	0.0850	18
Zinc (Zn)	0.0000	0.0020	0.6614	0.0051	0.6614	18
Gallium (Ga)	0.0000	0.0000	0.0283	0.0000	0.0283	18
Arsenic (As)	0.0000	0.0002	0.0167	0.0008	0.0167	18
Selenium (Se)	0.0000	0.0081	0.0283	0.0093	0.0283	18
Bromine (Br)	0.0000	0.0000	0.0335	0.0000	0.0335	18
Rubidium (Rb)	0.0000	0.0062	0.0199	0.0105	0.0199	18
Strontium (Sr)	0.0000	0.0059	0.0233	0.0098	0.0233	18
Yttrium (Y)	0.0000	0.0024	0.0150	0.0062	0.0150	18
Zirconium (Zr)	0.0000	0.0055	0.0484	0.0093	0.0484	18
Niobium (Nb)	0.0000	0.0012	0.0334	0.0031	0.0334	18
Molybdenum (Mo)	0.0000	0.0038	0.0400	0.0103	0.0400	18
Palladium (Pd)	0.0000	0.0204	0.1168	0.0281	0.1168	18
Silver (Ag)	0.0000	0.0347	0.1318	0.0375	0.1318	18
Cadmium (Cd)	0.0000	0.0154	0.0882	0.0229	0.0882	18
Indium (In)	0.0000	0.0202	0.0783	0.0283	0.0783	18
Tin (Sn)	0.0000	0.0040	0.1051	0.0108	0.1051	18
Antimony (Sb)	0.0000	0.0067	0.0833	0.0119	0.0833	18
Cesium (Cs)	0.0000	0.0162	0.2326	0.0530	0.2326	18
Barium (Ba)	0.0000	0.0157	0.3810	0.0558	0.3810	18
Lanthanum (La)	0.0000	0.0000	0.3361	0.0000	0.3361	18
Cerium (Ce)	0.0000	0.0317	0.4055	0.0921	0.4055	18
Samarium (Sm)	0.0000	0.2052	0.7999	0.2569	0.7999	18
Europium (Eu)	0.0000	0.0941	0.7886	0.2281	0.7886	18
Terbium (Tb)	0.0000	0.1787	1.1412	0.2692	1.1412	18
Hafnium (Hf)	0.0000	0.0000	0.4998	0.0000	0.4998	18
Tantalum (Ta)	0.0000	0.0000	0.4998	0.0000	0.4998	18
Tungsten (W)	0.0000	0.0291	0.1259	0.0341	0.1259	18
Iridium (Ir)	0.0000	0.0000	0.1666	0.0000	0.1666	18
Gold (Au)	0.0000	0.0101	0.0700	0.0191	0.0700	18
Mercury (Hg)	0.0000	0.0079	0.0702	0.0158	0.0702	18
Thallium (Tl)	0.0000	0.0091	0.0467	0.0128	0.0467	18
Lead (Pb)	0.0000	0.0186	0.0516	0.0212	0.0516	18
Uranium (U)	0.0000	0.0152	0.1049	0.0225	0.1049	18

Table 3-2 (continued). Dynamic field blank concentration averages and standard deviations in µg/47 mm filter from July-December 2020.

<b>b) Species, July-December 2020</b>	<b>Blank Subtracted (B<sub>i</sub>)</b>	<b>Average Field Blank</b>	<b>Blank Precision (S<sub>Bi</sub>)</b>	<b>Blank Std. Dev. (STD<sub>Bi</sub>)</b>	<b>Root Mean Squared Blank Precision (SIG<sub>Bi</sub>)</b>	<b>No. of Blanks</b>
Chloride (Cl <sup>-</sup> )	0.1196	0.1196	0.0810	0.0810	0.0030	18
Nitrate (NO <sub>3</sub> <sup>-</sup> )	0.0000	0.0000	0.0040	0.0000	0.0040	18
Sulfate (SO <sub>4</sub> <sup>=</sup> )	0.0000	0.0000	0.0008	0.0000	0.0008	18
Ammonium (NH <sub>4</sub> <sup>+</sup> )	0.0000	0.0030	0.0112	0.0046	0.0112	18
Sodium (Na <sup>+</sup> )	0.0000	0.0400	0.2069	0.0193	0.2069	18
Potassium (K <sup>+</sup> )	0.0000	0.0103	0.0197	0.0197	0.0097	18
O1TC	5.6133	5.6133	1.3035	1.0450	1.3035	18
O2TC	5.7241	5.7241	0.7986	0.7986	0.4019	18
O3TC	9.5062	9.5062	2.0775	2.0775	1.1419	18
O4TC	2.5374	2.5374	1.0759	1.0759	0.5568	18
OPTTC	1.9524	1.9524	1.4969	1.4969	0.9628	18
OPTRC	0.0000	0.5182	1.3677	1.3677	0.5336	18
OCTTC	25.3334	25.3334	4.0431	4.0431	1.9228	18
OCTRC	23.8992	23.8992	3.7491	3.7491	1.7039	18
E1TC	0.0000	0.2916	0.5469	0.5469	0.2544	18
E2TC	1.6608	1.6608	1.1174	1.0511	1.1174	18
E3TC	0.0000	0.0000	0.1215	0.0000	0.1215	18
ECTTC	0.0000	0.0000	0.4155	0.0000	0.4155	18
ECTRC	1.4342	1.4342	1.1995	1.1995	0.9158	18
TCTC	25.3334	25.3334	4.0431	4.0431	1.8316	18
Sodium (Na)	0.0000	0.0525	1.0152	0.1389	1.0152	18
Magnesium (Mg)	0.0000	0.0524	0.7887	0.0962	0.7887	18
Aluminum (Al)	0.0000	0.0000	0.3824	0.0000	0.3824	18
Silicon (Si)	0.0000	0.0347	0.0684	0.0592	0.0684	18
Phosphorus (P)	0.0000	0.0062	0.0317	0.0143	0.0317	18
Sulfur (S)	0.0000	0.0000	0.0167	0.0000	0.0167	18
Chlorine (Cl)	0.0000	0.0007	0.1250	0.0027	0.1250	18
Potassium (K)	0.0000	0.0000	0.0034	0.0000	0.0034	18
Calcium (Ca)	0.0000	0.0000	0.1516	0.0000	0.1516	18
Scandium (Sc)	0.0000	0.0000	0.9245	0.0000	0.9245	18
Titanium (Ti)	0.0000	0.0162	0.0283	0.0162	0.0283	18
Vanadium (V)	0.0000	0.0016	0.0100	0.0029	0.0100	18
Chromium (Cr)	0.0000	0.0003	0.0317	0.0011	0.0317	18
Manganese (Mn)	0.0000	0.0172	0.0334	0.0174	0.0334	18
Iron (Fe)	0.0000	0.0287	0.1049	0.0386	0.1049	18
Cobalt (Co)	0.0000	0.0004	0.0083	0.0013	0.0083	18

Table 3-2 (continued). Dynamic field blank concentration averages and standard deviations in µg/47 mm filter from July-December 2020.

<b>b) Species, July-December 2020</b>	<b>Blank Subtracted (B<sub>i</sub>)</b>	<b>Average Field Blank</b>	<b>Blank Precision (S<sub>Bi</sub>)</b>	<b>Blank Std. Dev. (STD<sub>Bi</sub>)</b>	<b>Root Mean Squared Blank Precision (SIG<sub>Bi</sub>)</b>	<b>No. of Blanks</b>
Nickel (Ni)	0.0000	0.0008	0.0167	0.0017	0.0167	18
Copper (Cu)	0.0000	0.0051	0.0850	0.0110	0.0850	18
Zinc (Zn)	0.0000	0.0018	0.6614	0.0047	0.6614	18
Gallium (Ga)	0.0000	0.0001	0.0283	0.0003	0.0283	18
Arsenic (As)	0.0000	0.0012	0.0167	0.0034	0.0167	18
Selenium (Se)	0.0000	0.0113	0.0283	0.0150	0.0283	18
Bromine (Br)	0.0000	0.0000	0.0335	0.0000	0.0335	18
Rubidium (Rb)	0.0000	0.0026	0.0199	0.0042	0.0199	18
Strontium (Sr)	0.0000	0.0045	0.0233	0.0100	0.0233	18
Yttrium (Y)	0.0000	0.0021	0.0150	0.0053	0.0150	18
Zirconium (Zr)	0.0000	0.0197	0.0484	0.0259	0.0484	18
Niobium (Nb)	0.0000	0.0058	0.0334	0.0098	0.0334	18
Molybdenum (Mo)	0.0000	0.0105	0.0400	0.0140	0.0400	18
Palladium (Pd)	0.0000	0.0213	0.1168	0.0356	0.1168	18
Silver (Ag)	0.0000	0.0339	0.1317	0.0458	0.1317	18
Cadmium (Cd)	0.0000	0.0125	0.0882	0.0288	0.0882	18
Indium (In)	0.0000	0.0178	0.0783	0.0257	0.0783	18
Tin (Sn)	0.0000	0.0196	0.1052	0.0282	0.1052	18
Antimony (Sb)	0.0000	0.0195	0.0833	0.0274	0.0833	18
Cesium (Cs)	0.0000	0.0167	0.2326	0.0293	0.2326	18
Barium (Ba)	0.0000	0.0082	0.3808	0.0316	0.3808	18
Lanthanum (La)	0.0000	0.0210	0.3365	0.0557	0.3365	18
Cerium (Ce)	0.0000	0.0223	0.4062	0.0602	0.4062	18
Samarium (Sm)	0.0000	0.1202	0.7996	0.1759	0.7996	18
Europium (Eu)	0.0000	0.1039	0.7880	0.1720	0.7880	18
Terbium (Tb)	0.0000	0.2235	1.1440	0.2988	1.1440	18
Hafnium (Hf)	0.0000	0.0000	0.4998	0.0000	0.4998	18
Tantalum (Ta)	0.0000	0.0000	0.4998	0.0000	0.4998	18
Tungsten (W)	0.0000	0.0163	0.1256	0.0338	0.1256	18
Iridium (Ir)	0.0000	0.0000	0.1666	0.0000	0.1666	18
Gold (Au)	0.0000	0.0201	0.0700	0.0230	0.0700	18
Mercury (Hg)	0.0000	0.0137	0.0705	0.0209	0.0705	18
Thallium (Tl)	0.0000	0.0120	0.0467	0.0129	0.0467	18
Lead (Pb)	0.0000	0.0135	0.0516	0.0221	0.0516	18
Uranium (U)	0.0000	0.0204	0.1049	0.0224	0.1049	18

Table 3-2 (continued). Dynamic field blank concentration averages and standard deviations in µg/47 mm filter from January-December 2020.

<b>c) Species, January-December 2020</b>	<b>Blank Subtracted (B<sub>i</sub>)</b>	<b>Average Field Blank</b>	<b>Blank Precision (S<sub>Bi</sub>)</b>	<b>Blank Std. Dev. (STD<sub>Bi</sub>)</b>	<b>Root Mean Squared Blank Precision (SIG<sub>Bi</sub>)</b>	<b>No. of Blanks</b>
Chloride (Cl <sup>-</sup> )	0.1414	0.1414	0.0742	0.0742	0.0038	36
Nitrate (NO <sub>3</sub> <sup>-</sup> )	0.2927	0.2927	0.1568	0.1548	0.0611	36
Sulfate (SO <sub>4</sub> <sup>-</sup> )	0.1819	0.1819	0.1149	0.1145	0.0125	36
Ammonium (NH <sub>4</sub> <sup>+</sup> )	0.0196	0.0211	0.0204	0.0153	0.0204	36
Sodium (Na <sup>+</sup> )	0.0000	0.0413	0.2067	0.0167	0.2067	36
Potassium (K <sup>+</sup> )	0.0214	0.0266	0.0191	0.0186	0.0140	36
O1TC	5.2815	5.2815	1.1294	0.9010	1.1294	36
O2TC	5.0473	5.0473	0.9190	0.9190	0.3448	36
O3TC	9.2250	9.2250	4.3831	4.3831	1.3011	36
O4TC	2.2387	2.2387	1.3131	1.3131	0.6368	36
OPTTC	0.9762	1.7386	1.8527	1.8527	0.7800	36
OPTRC	0.0000	0.4078	1.2364	1.2364	0.6019	36
OCTTC	23.5310	23.5310	7.2961	7.2961	1.9437	36
OCTRC	22.2002	22.2002	6.5529	6.5529	2.0154	36
E1TC	0.0000	0.3255	0.6695	0.6695	0.2081	36
E2TC	0.8304	1.4193	1.2764	1.2432	1.2553	36
E3TC	0.0000	0.0000	0.0810	0.0000	0.0810	36
ECTTC	0.0000	0.0063	0.2770	0.0243	0.2770	36
ECTRC	0.7171	1.3370	1.2775	1.2775	0.6462	36
TCTC	23.5372	23.5372	7.2908	7.2908	2.0296	36
Sodium (Na)	0.0000	0.0656	1.0150	0.1451	1.0150	36
Magnesium (Mg)	0.0000	0.0445	0.7879	0.1192	0.7879	36
Aluminum (Al)	0.0000	0.0123	0.3825	0.0363	0.3825	36
Silicon (Si)	0.0000	0.0509	0.0757	0.0711	0.0684	36
Phosphorus (P)	0.0000	0.0067	0.0317	0.0137	0.0317	36
Sulfur (S)	0.0000	0.0000	0.0167	0.0000	0.0167	36
Chlorine (Cl)	0.0000	0.0004	0.1250	0.0014	0.1250	36
Potassium (K)	0.0000	0.0000	0.0034	0.0000	0.0034	36
Calcium (Ca)	0.0000	0.0000	0.1516	0.0000	0.1516	36
Scandium (Sc)	0.0000	0.0000	0.9245	0.0000	0.9245	36
Titanium (Ti)	0.0000	0.0130	0.0283	0.0159	0.0283	36
Vanadium (V)	0.0000	0.0014	0.0100	0.0026	0.0100	36
Chromium (Cr)	0.0000	0.0008	0.0317	0.0018	0.0317	36
Manganese (Mn)	0.0000	0.0160	0.0334	0.0163	0.0334	36
Iron (Fe)	0.0000	0.0317	0.1049	0.0417	0.1049	36
Cobalt (Co)	0.0000	0.0014	0.0083	0.0021	0.0083	36

Table 3-2 (continued). Dynamic field blank concentration averages and standard deviations in µg/47 mm filter from January-December 2020.

<b>c) Species, January- December 2020</b>	<b>Blank Subtracted (B<sub>i</sub>)</b>	<b>Average Field Blank</b>	<b>Blank Precision (S<sub>Bi</sub>)</b>	<b>Blank Std. Dev. (STD<sub>Bi</sub>)</b>	<b>Root Mean Squared Blank Precision (SIG<sub>Bi</sub>)</b>	<b>No. of Blanks</b>
Nickel (Ni)	0.0000	0.0005	0.0167	0.0011	0.0167	36
Copper (Cu)	0.0000	0.0055	0.0850	0.0102	0.0850	36
Zinc (Zn)	0.0000	0.0019	0.6614	0.0049	0.6614	36
Gallium (Ga)	0.0000	0.0000	0.0283	0.0002	0.0283	36
Arsenic (As)	0.0000	0.0007	0.0167	0.0021	0.0167	36
Selenium (Se)	0.0000	0.0097	0.0283	0.0122	0.0283	36
Bromine (Br)	0.0000	0.0000	0.0335	0.0000	0.0335	36
Rubidium (Rb)	0.0000	0.0044	0.0199	0.0074	0.0199	36
Strontium (Sr)	0.0000	0.0052	0.0233	0.0099	0.0233	36
Yttrium (Y)	0.0000	0.0023	0.0150	0.0058	0.0150	36
Zirconium (Zr)	0.0000	0.0126	0.0484	0.0176	0.0484	36
Niobium (Nb)	0.0000	0.0035	0.0334	0.0065	0.0334	36
Molybdenum (Mo)	0.0000	0.0071	0.0400	0.0122	0.0400	36
Palladium (Pd)	0.0000	0.0208	0.1168	0.0319	0.1168	36
Silver (Ag)	0.0000	0.0343	0.1318	0.0416	0.1318	36
Cadmium (Cd)	0.0000	0.0139	0.0882	0.0258	0.0882	36
Indium (In)	0.0000	0.0190	0.0783	0.0270	0.0783	36
Tin (Sn)	0.0000	0.0118	0.1052	0.0195	0.1052	36
Antimony (Sb)	0.0000	0.0131	0.0833	0.0196	0.0833	36
Cesium (Cs)	0.0000	0.0165	0.2326	0.0411	0.2326	36
Barium (Ba)	0.0000	0.0119	0.3809	0.0437	0.3809	36
Lanthanum (La)	0.0000	0.0105	0.3363	0.0278	0.3363	36
Cerium (Ce)	0.0000	0.0270	0.4059	0.0761	0.4059	36
Samarium (Sm)	0.0000	0.1627	0.7998	0.2164	0.7998	36
Europium (Eu)	0.0000	0.0990	0.7883	0.2001	0.7883	36
Terbium (Tb)	0.0000	0.2011	1.1426	0.2840	1.1426	36
Hafnium (Hf)	0.0000	0.0000	0.4998	0.0000	0.4998	36
Tantalum (Ta)	0.0000	0.0000	0.4998	0.0000	0.4998	36
Tungsten (W)	0.0000	0.0227	0.1258	0.0339	0.1258	36
Iridium (Ir)	0.0000	0.0000	0.1666	0.0000	0.1666	36
Gold (Au)	0.0000	0.0151	0.0700	0.0210	0.0700	36
Mercury (Hg)	0.0000	0.0108	0.0704	0.0184	0.0704	36
Thallium (Tl)	0.0000	0.0105	0.0467	0.0129	0.0467	36
Lead (Pb)	0.0000	0.0161	0.0516	0.0217	0.0516	36
Uranium (U)	0.0000	0.0178	0.1049	0.0224	0.1049	36





Table 3-3. Minimum Detectable Limits (MDL), and Lower Quantifiable Limits (LQL), and samples exceeding them for: a) January-June, 2020; b) July-December, 2020; c) January-December, 2020.

<b>a) Species, January-June, 2020</b>	<b>Method</b>	<b>MDL<sup>b</sup></b>	<b>LQL<sup>c</sup></b>	<b>No of Values</b>	<b>No.&gt; MDL</b>	<b>%&gt; MDL</b>	<b>No.&gt; LQL</b>	<b>%&gt; LQL</b>
Chloride (Cl <sup>-</sup> )	IC	0.0043	0.0084	148	141	95%	131	89%
Nitrate (NO <sub>3</sub> <sup>-</sup> )	IC	0.0028	0.0387	148	148	100%	148	100%
Sulfate (SO <sub>4</sub> <sup>-</sup> )	IC	0.0051	0.0286	148	148	100%	148	100%
Ammonium (NH <sub>4</sub> <sup>+</sup> )	IC	0.0008	0.0033	148	148	100%	148	100%
Sodium (Na <sup>+</sup> )	IC	0.0018	0.0018	148	148	100%	148	100%
Potassium (K <sup>+</sup> )	IC	0.0024	0.0022	148	145	98%	146	99%
OC1	TOR/TOT	0.0829	0.0946	148	54	36%	48	32%
OC2	TOR/TOT	0.0829	0.1299	148	148	100%	148	100%
OC3	TOR/TOT	0.0829	0.8361	148	147	99%	52	35%
OC4	TOR/TOT	0.0829	0.1938	148	147	99%	143	97%
OPT	TOT	0.0829	0.2761	148	147	99%	123	83%
OPR	TOR/TOT	0.0829	0.1381	148	88	59%	76	51%
OCT	TOT	0.0829	1.3186	148	148	100%	126	85%
OCR	TOR	0.0829	1.1696	148	148	100%	127	86%
EC1	TOR/TOT	0.0104	0.0990	148	148	100%	148	100%
EC2	TOR/TOT	0.0104	0.1794	148	148	100%	72	49%
EC3	TOR/TOT	0.0104	0.0001	148	0	0%	2	1%
ECT	TOT	0.0104	0.0061	148	148	100%	148	100%
ECR	TOR	0.0104	0.1695	148	148	100%	148	100%
Total Carbon (TC)	TOR/TOT	0.0833	1.3173	148	148	100%	139	94%
Sodium (Na)	XRF	0.0287	0.0189	149	149	100%	149	100%
Magnesium (Mg)	XRF	0.0280	0.0178	149	58	39%	74	50%
Aluminum (Al)	XRF	0.0106	0.0091	149	73	49%	80	54%
Silicon (Si)	XRF	0.0015	0.0104	149	138	93%	126	85%
Phosphorus (P)	XRF	0.0007	0.0016	149	0	0%	0	0%
Sulfur (S)	XRF	0.0004	0.0001	149	149	100%	149	100%
Chlorine (Cl)	XRF	0.0004	0.0001	149	149	100%	149	100%
Potassium (K)	XRF	0.0004	0.0001	149	149	100%	149	100%
Calcium (Ca)	XRF	0.0024	0.0001	149	149	100%	149	100%
Scandium (Sc)	XRF	0.0097	0.0001	149	0	0%	0	0%
Titanium (Ti)	XRF	0.0009	0.0019	149	128	86%	109	73%
Vanadium (V)	XRF	0.0002	0.0003	149	117	79%	112	75%
Chromium (Cr)	XRF	0.0008	0.0003	149	63	42%	102	68%
Manganese (Mn)	XRF	0.0011	0.0019	149	143	96%	134	90%
Iron (Fe)	XRF	0.0040	0.0056	149	149	100%	149	100%
Cobalt (Co)	XRF	0.0003	0.0004	149	5	3%	0	0%

Table 3-3 (continued). Minimum Detectable Limits (MDL), and Lower Quantifiable Limits (LQL), and samples exceeding them for January-June, 2020.

<b>a) Species, January-June, 2020</b>	<b>Method</b>	<b>MDL<sup>b</sup></b>	<b>LQL<sup>c</sup></b>	<b>No of Values</b>	<b>No.&gt; MDL</b>	<b>%&gt; MDL</b>	<b>No.&gt; LQL</b>	<b>%&gt; LQL</b>
Nickel (Ni)	XRF	0.0009	0.0001	149	134	90%	148	99%
Copper (Cu)	XRF	0.0039	0.0012	149	48	32%	106	71%
Zinc (Zn)	XRF	0.0019	0.0006	149	149	100%	149	100%
Gallium (Ga)	XRF	0.0009	0.0001	149	1	1%	10	7%
Arsenic (As)	XRF	0.0004	0.0001	149	6	4%	13	9%
Selenium (Se)	XRF	0.0007	0.0012	149	41	28%	28	19%
Bromine (Br)	XRF	0.0010	0.0001	149	105	70%	117	79%
Rubidium (Rb)	XRF	0.0005	0.0013	149	73	49%	26	17%
Strontium (Sr)	XRF	0.0005	0.0012	149	124	83%	78	52%
Yttrium (Y)	XRF	0.0005	0.0008	149	11	7%	3	2%
Zirconium (Zr)	XRF	0.0014	0.0012	149	45	30%	55	37%
Niobium (Nb)	XRF	0.0011	0.0004	149	6	4%	17	11%
Molybdenum (Mo)	XRF	0.0011	0.0013	149	23	15%	14	9%
Palladium (Pd)	XRF	0.0022	0.0035	149	22	15%	7	5%
Silver (Ag)	XRF	0.0050	0.0047	149	7	5%	12	8%
Cadmium (Cd)	XRF	0.0029	0.0029	149	10	7%	12	8%
Indium (In)	XRF	0.0025	0.0035	149	13	9%	0	0%
Tin (Sn)	XRF	0.0033	0.0014	149	13	9%	40	27%
Antimony (Sb)	XRF	0.0016	0.0015	149	25	17%	27	18%
Cesium (Cs)	XRF	0.0068	0.0066	149	5	3%	5	3%
Barium (Ba)	XRF	0.0136	0.0070	149	2	1%	7	5%
Lanthanum (La)	XRF	0.0104	0.0001	149	4	3%	21	14%
Cerium (Ce)	XRF	0.0098	0.0115	149	4	3%	2	1%
Samarium (Sm)	XRF	0.0234	0.0321	149	10	7%	0	0%
Europium (Eu)	XRF	0.0236	0.0285	149	4	3%	1	1%
Terbium (Tb)	XRF	0.0170	0.0336	149	45	30%	19	13%
Hafnium (Hf)	XRF	0.0208	0.0001	149	0	0%	0	0%
Tantalum (Ta)	XRF	0.0208	0.0001	149	0	0%	0	0%
Tungsten (W)	XRF	0.0047	0.0043	149	9	6%	11	7%
Iridium (Ir)	XRF	0.0094	0.0001	149	0	0%	0	0%
Gold (Au)	XRF	0.0022	0.0024	149	11	7%	8	5%
Mercury (Hg)	XRF	0.0029	0.0020	149	0	0%	8	5%
Thallium (Tl)	XRF	0.0021	0.0016	149	0	0%	4	3%
Lead (Pb)	XRF	0.0014	0.0026	149	120	81%	100	67%
Uranium (U)	XRF	0.0030	0.0028	149	9	6%	12	8%

<sup>a</sup> IC=ion chromatography. TOR= thermal/optical reflectance. TOT= thermal/optical transmittance. XRF=X-ray fluorescence.

<sup>b</sup> Minimum detectable limit (MDL) is the concentration at which instrument response equals three times the standard deviation of the lab blank concentrations. Typical sample volumes are 24.0 m<sup>3</sup>.

<sup>c</sup> Lower quantifiable limit (LQL) is three times the standard deviation of the field blank concentrations. LQL is expressed here in terms of mass per cubic meter after dividing by 24.0 m<sup>3</sup> for 16.7 L/min flow rates.

Table 3-3 (continued). Minimum Detectable Limits (MDL), and Lower Quantifiable Limits (LQL), and samples exceeding them for July-December, 2020.

<b>b) Species, July-December, 2020</b>	<b>Method<sup>a</sup></b>	<b>MDL<sup>b</sup></b>	<b>LQL<sup>c</sup></b>	<b>No of Values</b>	<b>No.&gt; MDL</b>	<b>%&gt; MDL</b>	<b>No.&gt; LQL</b>	<b>%&gt; LQL</b>
Chloride (Cl <sup>-</sup> )	IC	0.0043	0.0101	150	143	95%	129	86%
Nitrate (NO <sub>3</sub> <sup>-</sup> )	IC	0.0028	0.0100	150	149	99%	149	99%
Sulfate (SO <sub>4</sub> <sup>=</sup> )	IC	0.0051	0.0100	150	150	100%	150	100%
Ammonium (NH <sub>4</sub> <sup>+</sup> )	IC	0.0008	0.0006	150	150	100%	150	100%
Sodium (Na <sup>+</sup> )	IC	0.0018	0.0024	150	150	100%	150	100%
Potassium (K <sup>+</sup> )	IC	0.0024	0.0025	150	148	99%	148	99%
OC1	TOR/TOT	0.0829	0.1306	150	72	48%	57	38%
OC2	TOR/TOT	0.0829	0.0998	150	150	100%	150	100%
OC3	TOR/TOT	0.0829	0.2597	150	147	98%	136	91%
OC4	TOR/TOT	0.0829	0.1345	150	149	99%	147	98%
OPT	TOT	0.0829	0.1871	150	143	95%	126	84%
OPR	TOR/TOT	0.0829	0.1710	150	118	79%	103	69%
OCT	TOT	0.0829	0.5054	150	150	100%	148	99%
OCR	TOR	0.0829	0.4686	150	150	100%	146	97%
EC1	TOR/TOT	0.0104	0.0684	150	150	100%	150	100%
EC2	TOR/TOT	0.0104	0.1314	150	148	99%	93	62%
EC3	TOR/TOT	0.0104	0.0001	150	0	0%	0	0%
ECT	TOT	0.0104	0.0005	150	149	99%	149	99%
ECR	TOR	0.0104	0.1499	150	150	100%	149	99%
Total Carbon (TC)	TOR/TOT	0.0833	0.5054	150	150	100%	150	100%
Sodium (Na)	XRF	0.0287	0.0174	150	149	99%	150	100%
Magnesium (Mg)	XRF	0.0280	0.0120	150	33	22%	56	37%
Aluminum (Al)	XRF	0.0106	0.0050	150	84	56%	87	58%
Silicon (Si)	XRF	0.0015	0.0074	150	140	93%	129	86%
Phosphorus (P)	XRF	0.0007	0.0018	150	8	5%	8	5%
Sulfur (S)	XRF	0.0004	0.0001	150	150	100%	150	100%
Chlorine (Cl)	XRF	0.0004	0.0003	150	150	100%	150	100%
Potassium (K)	XRF	0.0004	0.0001	150	150	100%	150	100%
Calcium (Ca)	XRF	0.0024	0.0001	150	150	100%	150	100%
Scandium (Sc)	XRF	0.0097	0.0001	150	0	0%	0	0%
Titanium (Ti)	XRF	0.0009	0.0020	150	133	89%	124	83%
Vanadium (V)	XRF	0.0002	0.0004	150	124	83%	114	76%
Chromium (Cr)	XRF	0.0008	0.0001	150	98	65%	124	83%
Manganese (Mn)	XRF	0.0011	0.0022	150	143	95%	122	81%
Iron (Fe)	XRF	0.0040	0.0048	150	149	99%	149	99%
Cobalt (Co)	XRF	0.0003	0.0002	150	2	1%	8	5%

Table 3-2 (continued). Dynamic field blank concentration averages and standard deviations in µg/47 mm filter from July-December 2020.

<b>b) Species, July-December, 2020</b>	<b>Method<sup>a</sup></b>	<b>MDL<sup>b</sup></b>	<b>LQL<sup>c</sup></b>	<b>No of Values</b>	<b>No.&gt; MDL</b>	<b>%&gt; MDL</b>	<b>No.&gt; LQL</b>	<b>%&gt; LQL</b>
Nickel (Ni)	XRF	0.0009	0.0002	150	145	97%	148	99%
Copper (Cu)	XRF	0.0039	0.0014	150	104	69%	130	87%
Zinc (Zn)	XRF	0.0019	0.0006	150	150	100%	150	100%
Gallium (Ga)	XRF	0.0009	0.0001	150	0	0%	7	5%
Arsenic (As)	XRF	0.0004	0.0004	150	8	5%	8	5%
Selenium (Se)	XRF	0.0007	0.0019	150	67	45%	29	19%
Bromine (Br)	XRF	0.0010	0.0001	150	99	66%	107	71%
Rubidium (Rb)	XRF	0.0005	0.0005	150	88	59%	88	59%
Strontium (Sr)	XRF	0.0005	0.0013	150	128	85%	69	46%
Yttrium (Y)	XRF	0.0005	0.0007	150	17	11%	12	8%
Zirconium (Zr)	XRF	0.0014	0.0032	150	66	44%	15	10%
Niobium (Nb)	XRF	0.0011	0.0012	150	6	4%	3	2%
Molybdenum (Mo)	XRF	0.0011	0.0018	150	28	19%	1	1%
Palladium (Pd)	XRF	0.0022	0.0045	150	16	11%	0	0%
Silver (Ag)	XRF	0.0050	0.0057	150	7	5%	0	0%
Cadmium (Cd)	XRF	0.0029	0.0036	150	8	5%	1	1%
Indium (In)	XRF	0.0025	0.0032	150	19	13%	1	1%
Tin (Sn)	XRF	0.0033	0.0035	150	25	17%	18	12%
Antimony (Sb)	XRF	0.0016	0.0034	150	20	13%	1	1%
Cesium (Cs)	XRF	0.0068	0.0037	150	6	4%	17	11%
Barium (Ba)	XRF	0.0136	0.0040	150	0	0%	6	4%
Lanthanum (La)	XRF	0.0104	0.0070	150	0	0%	2	1%
Cerium (Ce)	XRF	0.0098	0.0075	150	5	3%	7	5%
Samarium (Sm)	XRF	0.0234	0.0220	150	10	7%	13	9%
Europium (Eu)	XRF	0.0236	0.0215	150	7	5%	10	7%
Terbium (Tb)	XRF	0.0170	0.0373	150	34	23%	10	7%
Hafnium (Hf)	XRF	0.0208	0.0001	150	0	0%	0	0%
Tantalum (Ta)	XRF	0.0208	0.0001	150	0	0%	0	0%
Tungsten (W)	XRF	0.0047	0.0042	150	5	3%	8	5%
Iridium (Ir)	XRF	0.0094	0.0001	150	0	0%	0	0%
Gold (Au)	XRF	0.0022	0.0029	150	9	6%	0	0%
Mercury (Hg)	XRF	0.0029	0.0026	150	0	0%	3	2%
Thallium (Tl)	XRF	0.0021	0.0016	150	0	0%	2	1%
Lead (Pb)	XRF	0.0014	0.0028	150	114	76%	95	63%
Uranium (U)	XRF	0.0030	0.0028	150	6	4%	6	4%

<sup>a</sup> IC=ion chromatography. TOR= thermal/optical reflectance. TOT= thermal/optical transmittance. XRF=X-ray fluorescence.

<sup>b</sup> Minimum detectable limit (MDL) is the concentration at which instrument response equals three times the standard deviation of the lab blank concentrations. Typical sample volumes are 24.0 m<sup>3</sup>.

<sup>c</sup> Lower quantifiable limit (LQL) is three times the standard deviation of the field blank concentrations. LQL is expressed here in terms of mass per cubic meter after dividing by 24.0 m<sup>3</sup> for 16.7 L/min flow rates.

Table 3-3 (continued). Minimum Detectable Limits (MDL), and Lower Quantifiable Limits (LQL), and samples exceeding them for January-December, 2020.

<b>c) Species, January- December, 2020</b>	<b>Method<sup>a</sup></b>	<b>MDL<sup>b</sup></b>	<b>LQL<sup>c</sup></b>	<b>No of Values</b>	<b>No.&gt; MDL</b>	<b>%&gt; MDL</b>	<b>No.&gt; LQL</b>	<b>%&gt; LQL</b>
Chloride (Cl <sup>-</sup> )	IC	0.0043	0.0093	298	284	95%	260	87%
Nitrate (NO <sub>3</sub> <sup>-</sup> )	IC	0.0028	0.0243	298	297	100%	297	100%
Sulfate (SO <sub>4</sub> <sup>=</sup> )	IC	0.0051	0.0193	298	298	100%	298	100%
Ammonium (NH <sub>4</sub> <sup>+</sup> )	IC	0.0008	0.0019	298	298	100%	298	100%
Sodium (Na <sup>+</sup> )	IC	0.0018	0.0021	298	298	100%	298	100%
Potassium (K <sup>+</sup> )	IC	0.0024	0.0023	298	293	98%	294	99%
OC1	TOR/TOT	0.0829	0.1126	298	126	42%	105	35%
OC2	TOR/TOT	0.0829	0.1149	298	298	100%	298	100%
OC3	TOR/TOT	0.0829	0.5479	298	294	99%	188	63%
OC4	TOR/TOT	0.0829	0.1641	298	296	99%	290	97%
OPT	TOT	0.0829	0.2316	298	290	97%	249	84%
OPR	TOR/TOT	0.0829	0.1545	298	206	69%	179	60%
OCT	TOT	0.0829	0.9120	298	298	100%	274	92%
OCR	TOR	0.0829	0.8191	298	298	100%	273	92%
EC1	TOR/TOT	0.0104	0.0837	298	298	100%	298	100%
EC2	TOR/TOT	0.0104	0.1554	298	296	99%	165	55%
EC3	TOR/TOT	0.0104	0.0001	298	0	0%	2	1%
ECT	TOT	0.0104	0.0033	298	297	100%	297	100%
ECR	TOR	0.0104	0.1597	298	298	100%	297	100%
Total Carbon (TC)	TOR/TOT	0.0833	0.9113	298	298	100%	289	97%
Sodium (Na)	XRF	0.0287	0.0181	299	298	100%	299	100%
Magnesium (Mg)	XRF	0.0280	0.0149	299	91	30%	130	43%
Aluminum (Al)	XRF	0.0106	0.0070	299	157	52%	167	56%
Silicon (Si)	XRF	0.0015	0.0089	299	278	93%	255	85%
Phosphorus (P)	XRF	0.0007	0.0017	299	8	3%	8	3%
Sulfur (S)	XRF	0.0004	0.0001	299	299	100%	299	100%
Chlorine (Cl)	XRF	0.0004	0.0002	299	299	100%	299	100%
Potassium (K)	XRF	0.0004	0.0001	299	299	100%	299	100%
Calcium (Ca)	XRF	0.0024	0.0001	299	299	100%	299	100%
Scandium (Sc)	XRF	0.0097	0.0001	299	0	0%	0	0%
Titanium (Ti)	XRF	0.0009	0.0020	299	261	87%	233	78%
Vanadium (V)	XRF	0.0002	0.0003	299	241	81%	226	76%
Chromium (Cr)	XRF	0.0008	0.0002	299	161	54%	226	76%
Manganese (Mn)	XRF	0.0011	0.0020	299	286	96%	256	86%
Iron (Fe)	XRF	0.0040	0.0052	299	298	100%	298	100%
Cobalt (Co)	XRF	0.0003	0.0003	299	7	2%	8	3%

Table 3-3 (continued). Minimum Detectable Limits (MDL), and Lower Quantifiable Limits (LQL), and samples exceeding them for January-December, 2020.

<b>c) Species, January- December, 2020</b>	<b>Method<sup>a</sup></b>	<b>MDL<sup>b</sup></b>	<b>LQL<sup>c</sup></b>	<b>No of Values</b>	<b>No.&gt; MDL</b>	<b>%&gt; MDL</b>	<b>No.&gt; LQL</b>	<b>%&gt; LQL</b>
Nickel (Ni)	XRF	0.0009	0.0001	299	279	93%	296	99%
Copper (Cu)	XRF	0.0039	0.0013	299	152	51%	236	79%
Zinc (Zn)	XRF	0.0019	0.0006	299	299	100%	299	100%
Gallium (Ga)	XRF	0.0009	0.0001	299	1	0%	17	6%
Arsenic (As)	XRF	0.0004	0.0003	299	14	5%	21	7%
Selenium (Se)	XRF	0.0007	0.0015	299	108	36%	57	19%
Bromine (Br)	XRF	0.0010	0.0001	299	204	68%	224	75%
Rubidium (Rb)	XRF	0.0005	0.0009	299	161	54%	114	38%
Strontium (Sr)	XRF	0.0005	0.0012	299	252	84%	147	49%
Yttrium (Y)	XRF	0.0005	0.0007	299	28	9%	15	5%
Zirconium (Zr)	XRF	0.0014	0.0022	299	111	37%	70	23%
Niobium (Nb)	XRF	0.0011	0.0008	299	12	4%	20	7%
Molybdenum (Mo)	XRF	0.0011	0.0015	299	51	17%	15	5%
Palladium (Pd)	XRF	0.0022	0.0040	299	38	13%	7	2%
Silver (Ag)	XRF	0.0050	0.0052	299	14	5%	12	4%
Cadmium (Cd)	XRF	0.0029	0.0032	299	18	6%	13	4%
Indium (In)	XRF	0.0025	0.0034	299	32	11%	1	0%
Tin (Sn)	XRF	0.0033	0.0024	299	38	13%	58	19%
Antimony (Sb)	XRF	0.0016	0.0025	299	45	15%	28	9%
Cesium (Cs)	XRF	0.0068	0.0051	299	11	4%	22	7%
Barium (Ba)	XRF	0.0136	0.0055	299	2	1%	13	4%
Lanthanum (La)	XRF	0.0104	0.0035	299	4	1%	23	8%
Cerium (Ce)	XRF	0.0098	0.0095	299	9	3%	9	3%
Samarium (Sm)	XRF	0.0234	0.0270	299	20	7%	13	4%
Europium (Eu)	XRF	0.0236	0.0250	299	11	4%	11	4%
Terbium (Tb)	XRF	0.0170	0.0355	299	79	26%	29	10%
Hafnium (Hf)	XRF	0.0208	0.0001	299	0	0%	0	0%
Tantalum (Ta)	XRF	0.0208	0.0001	299	0	0%	0	0%
Tungsten (W)	XRF	0.0047	0.0042	299	14	5%	19	6%
Iridium (Ir)	XRF	0.0094	0.0001	299	0	0%	0	0%
Gold (Au)	XRF	0.0022	0.0026	299	20	7%	8	3%
Mercury (Hg)	XRF	0.0029	0.0023	299	0	0%	11	4%
Thallium (Tl)	XRF	0.0021	0.0016	299	0	0%	6	2%
Lead (Pb)	XRF	0.0014	0.0027	299	234	78%	195	65%
Uranium (U)	XRF	0.0030	0.0028	299	15	5%	18	6%

### 3.4 Data Validation

Data acquired from the study was submitted to several data validation levels:

- Level 0 sample validation designates data as they come off the instrument. This process ascertains that the field or laboratory instrument is functioning properly.
- Level I sample validation: 1) flags samples when significant deviations from measurement assumptions have occurred, 2) verifies computer file entries against data sheets, 3) eliminates values for measurements that are known to be invalid because of instrument malfunctions, 4) replaces data from a backup data acquisition system in the event of failure of the primary system, and 5) adjusts values for quantifiable calibration or interference biases.
- Level II sample validation applies consistency tests to the assembled data based on known physical relationships between variables.
- Level III sample validation is part of the data interpretation process. The first assumption upon finding a measurement which is inconsistent with physical expectations, is that the unusual value is due to a measurement error. If, upon tracing the path of the measurement nothing unusual is found, the value can be assumed to be a valid result of an environmental cause. Unusual values are identified during the data interpretation process as: 1) extreme values, 2) values which would otherwise normally track the values of other variables in a time series, and 3) values for observables which would normally follow a qualitatively predictable spatial or temporal pattern.

Level II data validation evaluates the chemical data for internal consistency and include: 1) sum of chemical species versus PM<sub>2.5</sub> mass, 2) physical and chemical consistency, 3) anion and cation balance, 4) carbon measurements by different thermal/optical methods, 5) reconstructed versus measured mass, and 6) collocated measurement comparison.

#### 3.4.1 Sum of Chemical Species versus PM<sub>2.5</sub> Mass

The sum of the individual chemical concentrations for PM<sub>2.5</sub> should be less than or equal to the corresponding gravimetrically measured mass concentrations. U.S.EPA (2012) specifies that the ratio of sum of species over gravimetric mass should be within the range of 0.60–1.32. This sum includes chemicals quantified on the Teflon-membrane and quartz-fiber filters. Total sulfur (S), water-soluble chloride (Cl<sup>-</sup>), and water-soluble potassium (K<sup>+</sup>) are excluded from the sum to avoid double counting since sulfate (SO<sub>4</sub><sup>2-</sup>), chlorine (Cl), and total potassium (K) are included in the sum. Chloride is a subset of chlorine, therefore, the conventional approach is to use the total chlorine in the sum of species calculations to attain mass closure. For a coastal environment, the majority of the chloride is water-soluble, therefore, including either chloride or chlorine in the sum of species will not alter the outcome. Elemental sodium (Na) and magnesium (Mg) have low atomic numbers and require detailed particle size distributions in order to completely correct for particle x-ray absorption effects, so these concentrations are also excluded from the calculation. Carbon is represented by OC and EC. Measured concentrations do not account for unmeasured oxygen associated with metal oxides in crustal material, unmeasured anions and cations, or hydrogen and oxygen associated with organic carbon (Chow et al., 2015a).

Figure 3-2 compares the sums of species at each site with the PM<sub>2.5</sub> mass from the Teflon-membrane filters. Statistical analysis reported in each plot includes simple linear regression models whereby error is assumed in the response variate (y-axis), and no error is assumed for the explanatory variate (x-axis). The trend line indicates the slope with intercept.

Regression statistics and average ratios of sums of species (Y) over gravimetric mass (X) are summarized in Table 3-4. Ratios of the sums over the measured mass are slightly higher than the regression slopes owing to the positive intercepts.



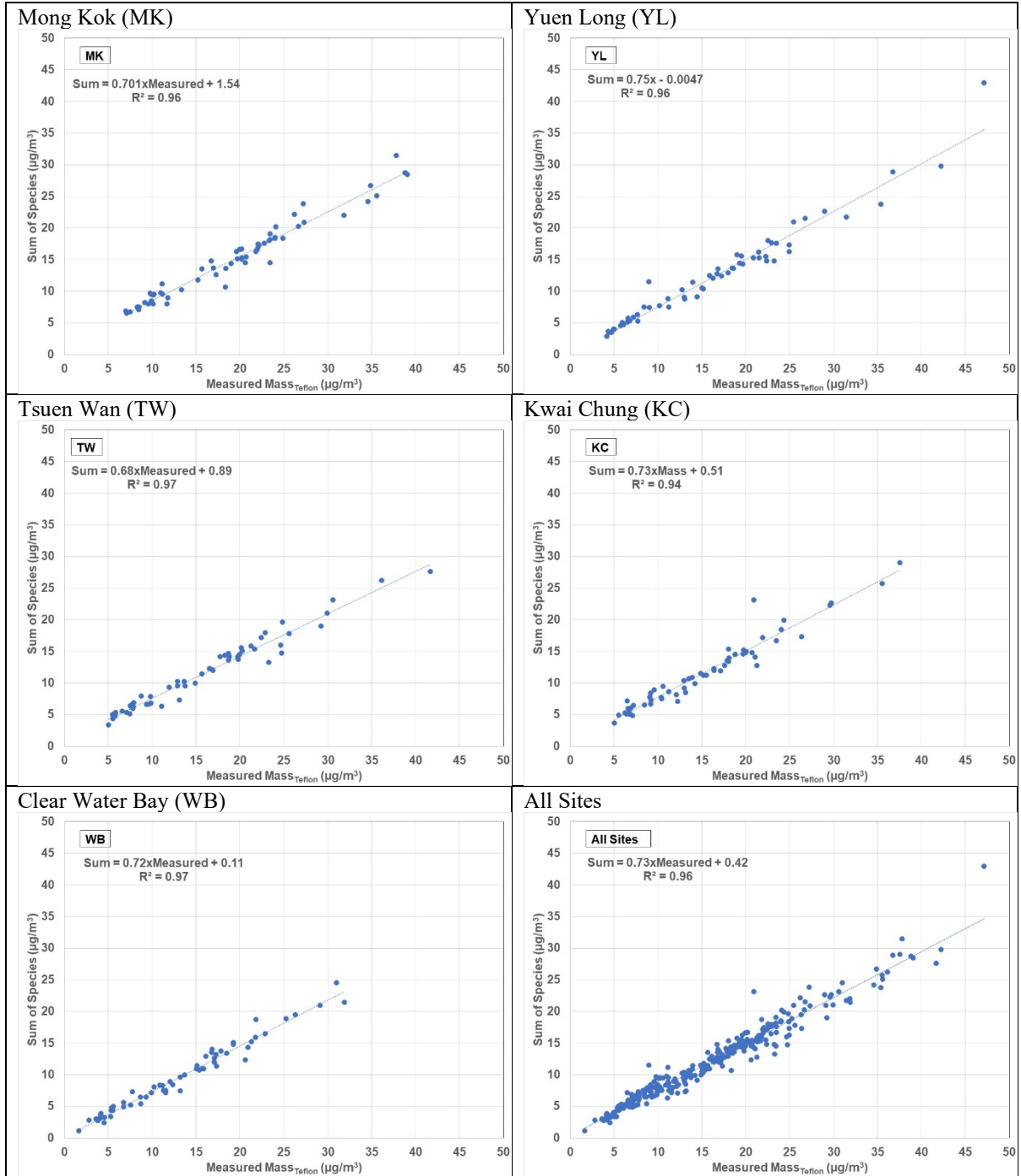


Figure 3-2. Sum of species vs. measured mass comparisons,

One of the 298 sums of species was higher than the corresponding PM<sub>2.5</sub> mass within the reported measurement precisions. The average Y/X ratio is 0.741 with minimum and maximum ratios being 0.49 and 1.03, respectively. All but 10 (17-Feb at TW; 23-Feb at TW, KC, and WB, 5-April at MK, TW, KC, and WB; 11-April at TW; and 23-May at WB) were within the 0.60–1.32 range suggested by the U.S.EPA (2012) with a minimum of 0.52 at WB. The date 5-April appears to be an unusual day at with ratios lower than the criterion at multiple

sites. A strong correlation exists between the sum of species and measured mass, with coefficients of determination ( $R^2$ ) exceeding 0.94 for all sites. Comparisons are similar across individual sites (Figure 3-2a-e). The intercept is the highest at the roadside MK site (1.42  $\mu\text{g}/\text{m}^3$ ) and the lowest at the suburban WB site (0.09  $\mu\text{g}/\text{m}^3$ ). The intercepts indicate sampling artifacts, including the positive (adsorption of vapors) and negative (volatilization of particles) organic carbon artifacts.

Table 3-4. Statistics for sum of species vs. measured mass. Averages are in  $\mu\text{g}/\text{m}^3$ .

Site	Slope	Intercept	$R^2$	N	Avg(Meas)	Avg(Sum)	Avg(Sum/Meas)
MK	0.701	1.54	0.96	61	19.3	15.1	0.78
YL	0.75	0.0047	0.96	60	16.5	12.5	0.75
TW	0.68	0.89	0.97	56	15.9	11.5	0.73
KC	0.73	0.51	0.94	60	15.5	11.8	0.76
WB	0.72	0.11	0.97	61	13.2	9.7	0.73
ALL	0.73	0.42	0.96	298	16.1	12.1	0.75

Several studies have been conducted to evaluate organic carbon artifacts using backup quartz-fiber filter and field blanks as well as different filter face velocities and passive exposure time (Chow et al., 2010; Watson et al., 2009). However, this information is not available for Hong Kong samples and corrections are not made to the OC levels aside from the field blank subtraction. Given the relatively high OC levels in the region this is not expected to result in a significant bias.

### 3.4.2 Physical and Chemical Consistency

Measurements of chemical species concentrations conducted by different methods are compared. Physical and chemical consistency was tested for: 1) sulfate ( $\text{SO}_4^{2-}$ ) versus total sulfur (S), 2) chloride ( $\text{Cl}^-$ ) versus chlorine (Cl), 3) water-soluble potassium ( $\text{K}^+$ ) versus total potassium (K), and 4) ammonium balance.

#### 3.4.2.1 Water-Soluble Sulfate ( $\text{SO}_4^{2-}$ ) vs. Total Sulfur (S)

$\text{SO}_4^{2-}$  is measured by IC analysis on quartz-fiber filters, and total S is measured by XRF analysis on Teflon-membrane filters. The ratio of sulfate to total sulfur should equal “3” if all of the S is present as soluble  $\text{SO}_4^{2-}$ . U.S.EPA (2012) specifies that the  $\text{SO}_4^{2-}/\text{S}$  ratio should be within the range of 2.22–4.00. Figure 3-3 compares  $\text{SO}_4^{2-}$  with S concentrations for each site. Regression statistics, averages, and ratios of the averages are summarized in Table 3-5 showing high correlations exceeding 0.97 in all cases. Most samples meet the EPA ratio criteria, consistent with most of the sulfur is present as water-soluble sulfate, most probably of secondary atmospheric transformation of  $\text{SO}_2$  emissions. Most sulfur is present as water-soluble sulfate in the Hong Kong atmosphere. The regression slopes range from 2.53 to 2.71 and the intercepts are low (0.03-0.08  $\mu\text{g}/\text{m}^3$ ). The average  $\text{SO}_4^{2-}/\text{S}$  ratio is 2.66 with a maximum ratio of 2.71 at WB. There are 4 samples with  $\text{SO}_4^{2-}/\text{S}$  ratio ranging from 2.11 to 2.21, slightly lower than the U.S.EPA minimum outlier criterion of 2.22. These samples and their  $\text{SO}_4^{2-}/\text{S}$  ratios are listed in Table 3-6. There are other forms of sulfur that are not sulfate, but that are sulfates with limited solubility. Examples include  $\text{SO}_2$  adsorbed onto diesel soot and minerals such as gypsum ( $\text{CaSO}_4 \cdot 2\text{H}_2\text{O}$ ) which is widely used in construction materials and as an agricultural amendment.

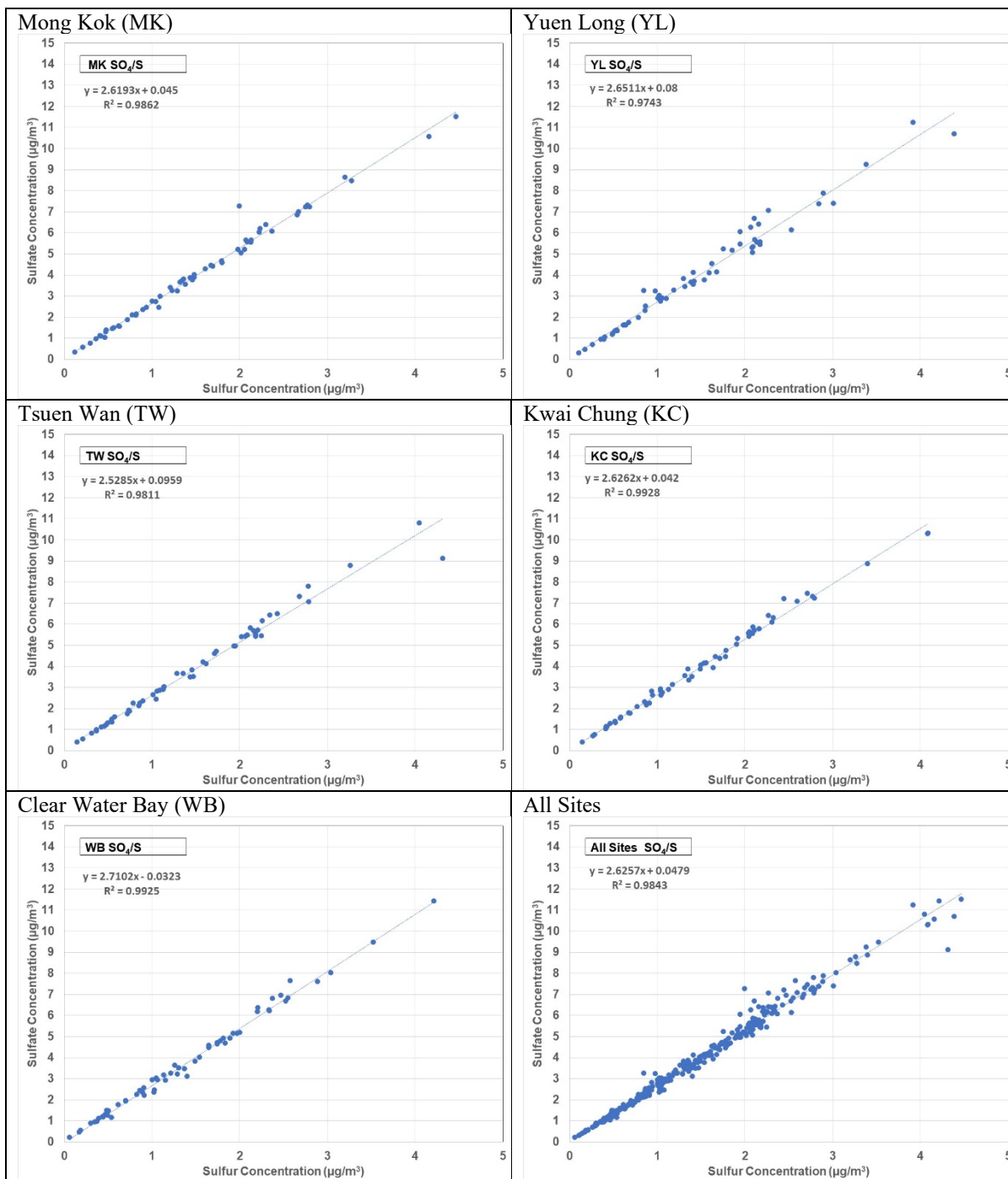


Figure 3-3. Comparison of sulfate by IC with sulfur by XRF.

Table 3-5. Statistics for sulfate/sulfur comparisons. Averages are in  $\mu\text{g}/\text{m}^3$ .

Site	Slope	Intercept	$R^2$	N	Avg( $\text{SO}_4$ )	Avg(S)	Avg( $\text{SO}_4/\text{S}$ )
<b>MK</b>	2.629	0.045	0.986	61	3.96	1.49	2.65
<b>YL</b>	2.651	0.08	0.974	60	4.05	1.53	2.65
<b>TW</b>	2.528	0.096	0.981	56	3.82	1.47	2.59
<b>KC</b>	2.626	0.042	0.992	60	3.76	1.40	2.69
<b>WB</b>	2.710	0.032	0.992	61	4.06	1.50	2.71
<b>ALL</b>	2.625	0.048	0.984	298	3.93	1.48	2.66

Table 3-6. Samples outside of the EPA comparison tolerances for ratios &lt; 2.22.

Site	Date	$\text{SO}_4^{2-}/\text{S}$ Ratio
<b>MK</b>	7/16/2020	2.21
<b>TW</b>	9/2/2020	2.11
<b>WB</b>	5/23/2020	2.13
<b>WB</b>	5/29/2020	2.21

### 3.4.2.2 Chloride ( $\text{Cl}^-$ ) vs. Chlorine (Cl)

$\text{Cl}^-$  was measured by IC on quartz-fiber filters, and Cl was measured by XRF on Teflon-membrane filters. Figure 3-4 compares  $\text{Cl}^-$  with Cl concentrations for each site with statistics summarized in Table 3-7. The slopes range from 0.91 to 1.1, indicating that most the Cl exists as water-soluble  $\text{Cl}^-$ . As Figure 3-4 shows, most of the concentrations are low, near the LQLs and with larger relative uncertainties. The slopes, which are dominated by the higher concentrations, are better indicators of the comparability than the ratios of the averages, which exceed 1 at several sites. It appears that there are periodic chloride incursions, usually due to marine aerosols, that do not occur on a regular basis.  $R^2 > 0.92$  for all of the sites, indicating a good relationship between the two measurements, an improvement over prior years in terms of correlation. The good agreement between anions and cations (see below) indicates that the IC chloride measurement is probably preferable to the XRF chlorine measurement. The Teflon filters are analyzed under a vacuum which can evaporate some of the semi-volatile compounds that might be associated with chloride compounds. The chlorine XRF peak can also be influenced by counts from nearby peaks at the low concentrations found here.

### 3.4.2.3 Water-Soluble Potassium ( $\text{K}^+$ ) vs. Total Potassium (K)

$\text{K}^+$  was measured by IC on quartz-fiber filters, and K was measured by XRF on Teflon-membrane filters. The ratio of  $\text{K}^+$  to K is expected to equal or be less than 1. Figure 3-5 compares  $\text{K}^+$  and K concentrations for each site with the statistics summarized in Table 3-8. Soluble potassium constitutes ~70% of total potassium, consistent with the soluble fraction being common in biomass burning emissions and marine aerosols. Non-soluble potassium compounds are found in many minerals and may be associated with road dust suspension and construction activities.  $R^2$  values all exceed 0.93, indicating high correlations among the two measurements.

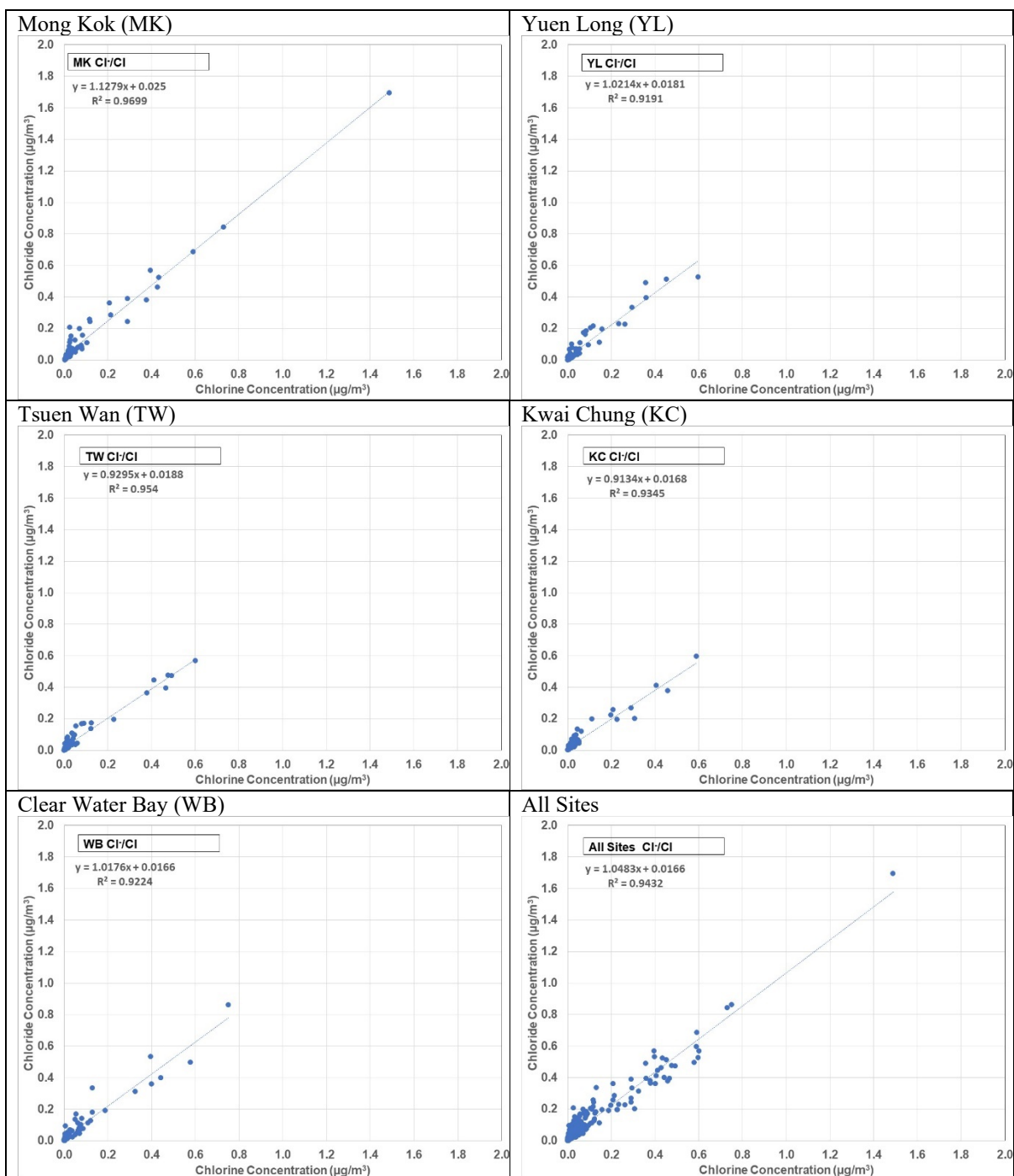


Figure 3-4. Comparison of chloride by IC with chlorine by XRF.

Table 3-7. Statistics for chloride/chlorine comparisons. Averages are in  $\mu\text{g}/\text{m}^3$ .

Site	Slope	Intercept	R <sup>2</sup>	N	Avg(Cl <sup>-</sup> )	Avg(Cl)	Avg(Cl/Cl)
<b>MK</b>	1.127	0.025	0.97	61	0.08	0.06	1.18
<b>YL</b>	1.02	0.018	0.92	60	0.16	0.12	1.34
<b>TW</b>	0.93	0.019	0.954	56	0.09	0.08	1.17
<b>KC</b>	0.913	0.017	0.935	60	0.10	0.08	1.22
<b>WB</b>	1.02	0.017	0.922	61	0.09	0.07	1.28
<b>ALL</b>	1.05	0.016	0.943	298	0.10	0.08	1.25

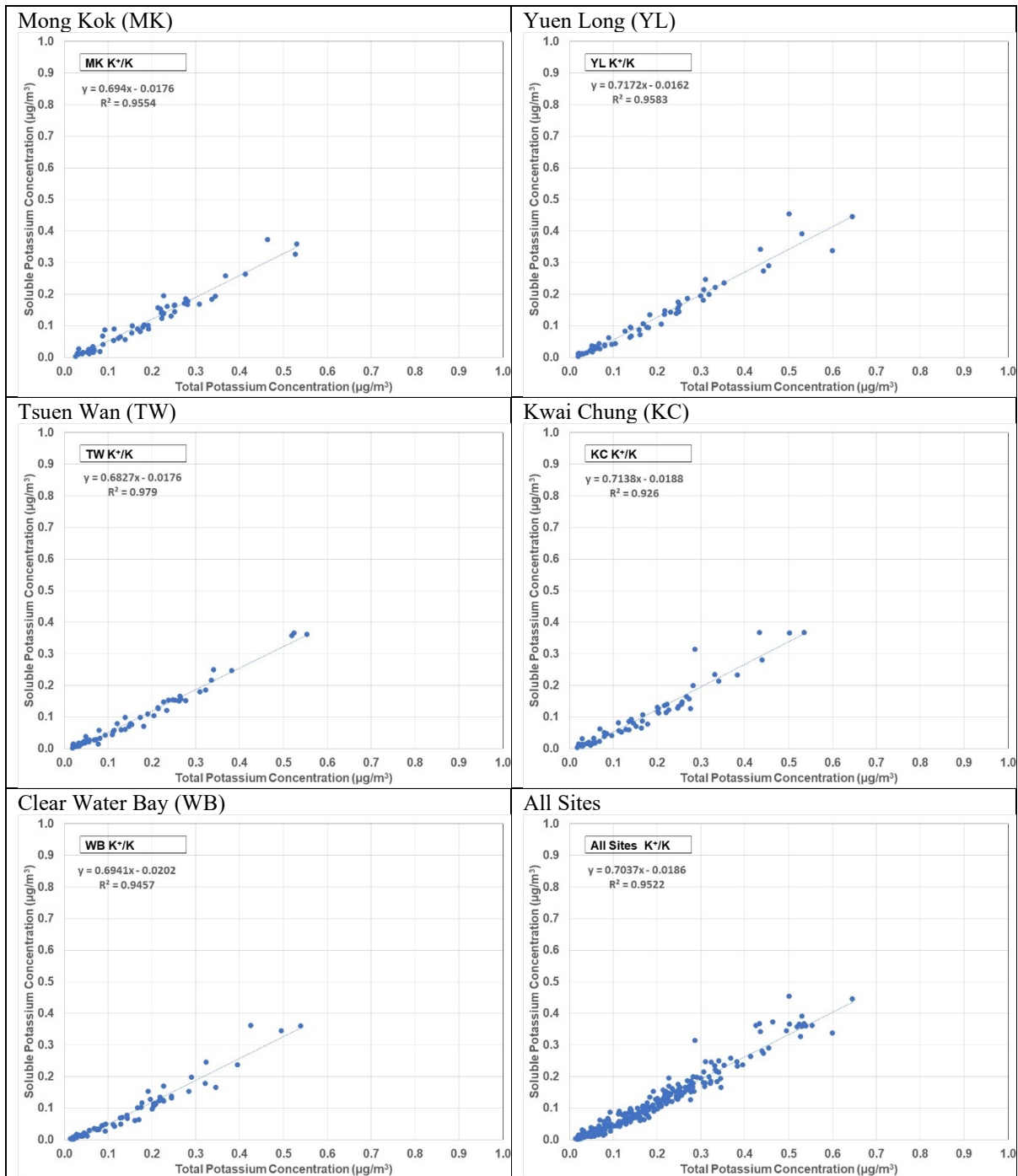


Figure 3-5. Comparison of soluble potassium by IC with potassium by XRF.

Table 3-8. Statistics for potassium ion/total potassium comparisons. Averages in  $\mu\text{g}/\text{m}^3$ .

Site	Slope	Intercept	R <sup>2</sup>	N	Avg(K <sup>+</sup> )	Avg(K)	Avg(K+/K)
<b>MK</b>	0.694	0.0176	0.955	61	0.10	0.17	0.60
<b>YL</b>	0.717	0.016	0.968	60	0.11	0.18	0.60
<b>TW</b>	0.683	0.018	0.979	56	0.09	0.16	0.58
<b>KC</b>	0.713	0.019	0.926	60	0.09	0.16	0.57
<b>WB</b>	0.694	0.020	0.946	61	0.13	0.20	0.64
<b>ALL</b>	0.704	0.019	0.952	298	0.10	0.17	0.60

#### 3.4.2.4 Ammonium Balance

Ammonium nitrate ( $\text{NH}_4\text{NO}_3$ ), ammonium sulfate ( $[\text{NH}_4]_2\text{SO}_4$ ), and ammonium bisulfate ( $\text{NH}_4\text{HSO}_4$ ) are common nitrate and sulfate compounds, although sodium nitrate ( $\text{NaNO}_3$ ) and/or sodium sulfate ( $\text{Na}_2\text{SO}_4$ ) may also be present in areas affected by marine aerosols such as Hong Kong. The large number of samples with very low chloride and chlorine concentrations is indicative of the replacement of  $\text{Cl}^-$  in the marine aerosol with  $\text{NO}_3^-$  ions resulting from the reaction of nitric acid ( $\text{HNO}_3$ ) with  $\text{NaCl}$ . Ammonium ( $\text{NH}_4^+$ ) can be calculated based on the stoichiometric ratios of the different compounds and compared with measurements. Ammonium is usually calculated from nitrate and sulfate, assuming that all nitrate was in the form of ammonium nitrate and all sulfate was in the form of either ammonium sulfate (i.e., calculated ammonium =  $[0.38 \times \text{sulfate}] + [0.29 \times \text{nitrate}]$ ) or ammonium bisulfate (i.e., ammonium =  $[0.19 \times \text{sulfate}] + [0.29 \times \text{nitrate}]$ ). This does not, however, account for the  $\text{NaCl}/\text{HNO}_3$  interaction that would dominate over the reaction of  $\text{HNO}_3$  and  $\text{NH}_3$ . In this case, the calculated ammonium would be higher than that measured, especially at low sulfate concentrations.

Figure 3-6 compares calculated and measured ammonium concentrations for each site, assuming  $(\text{NH}_4)_2\text{SO}_4$  or  $\text{NH}_4\text{HSO}_4$  with the statistics summarized in Tables 3-9 and 3-10. For both forms of sulfate the comparisons show high  $R^2$  values. The slopes for the ammonium sulfate assumption are all close to unity, indicating that most of the sulfuric acid is neutralized by ammonium. There is more scatter between calculated and measured ammonium at the lower concentrations at which the ammonium nitrate assumption is more important. For the most part, ammonium is overestimated for these values, which would be the case when sodium nitrate is displacing ammonium nitrate. Since there are many of these lower concentrations in the data set, the ratios of the calculated to measured averages exceed unity. It may also be the case that there are occasions in which there is insufficient ammonia gas to fully neutralize the sulfuric acid, resulting in the presence of ammonium bisulfate. This is often the case for less aged aerosols that have not mixed with available ammonia, typically over agricultural areas where ammonia is more abundant than in urbanized areas.

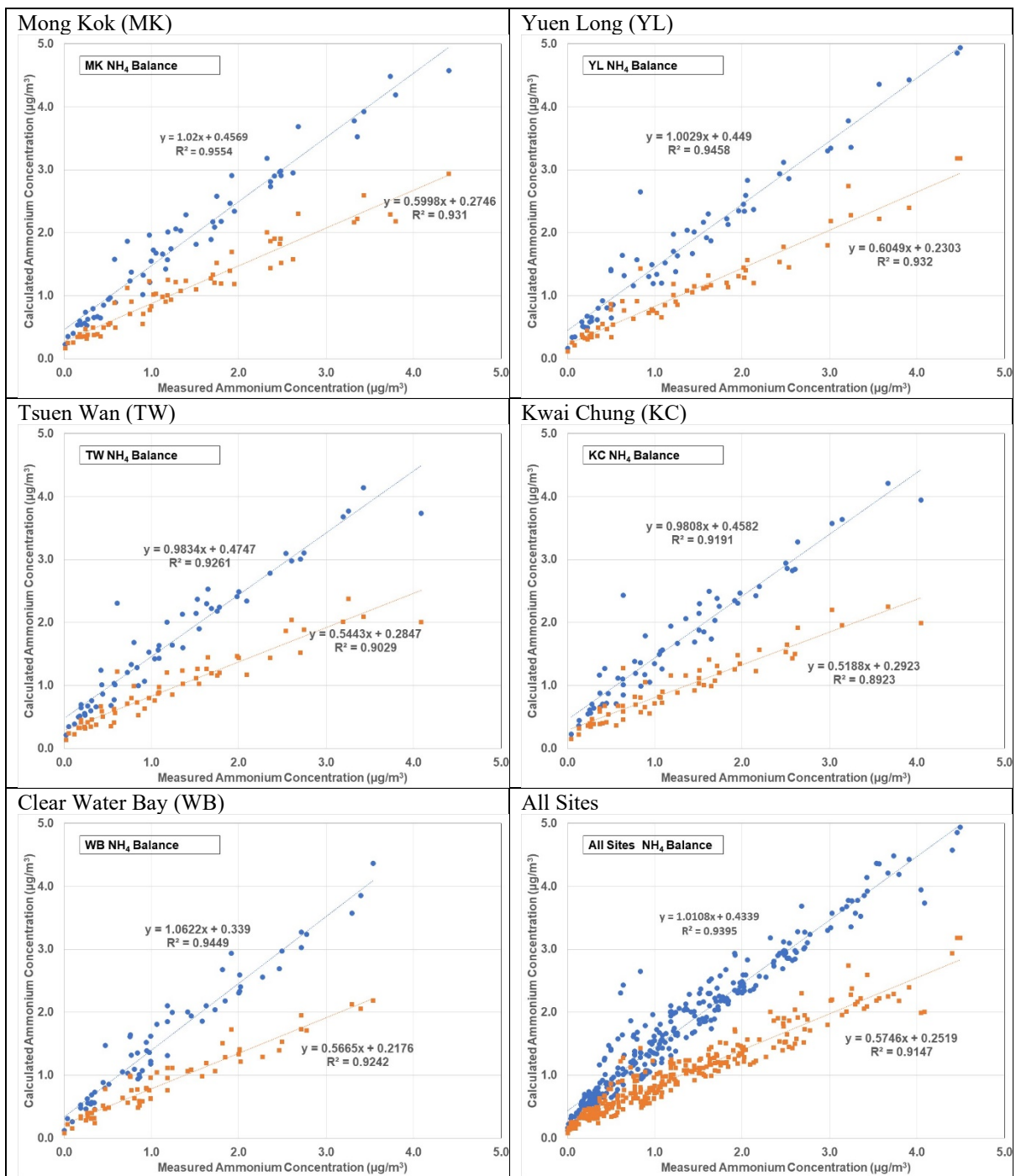


Figure 3-6. Calculated vs measured ammonium ion.



Table 3-9. Statistics for ammonium balance comparisons. Averages are in  $\mu\text{g}/\text{m}^3$ .

Ammonium Sulfate (blue dots)							
Site	Slope	Intercept	R <sup>2</sup>	N	Avg(Calc)	Avg(Meas)	Avg(Calc/Meas)
MK	1.02	0.457	0.955	61	1.70	1.27	1.70
YL	1.00	0.449	0.946	60	1.88	1.40	1.88
TW	0.983	0.474	0.926	56	1.68	1.22	1.68
KC	0.981	0.458	0.919	60	1.61	1.20	1.61
WB	1.062	0.339	0.945	61	1.84	1.39	1.84
ALL	1.010	0.434	0.940	298	1.74	1.29	1.74
Ammonium Bisulfate (brown)							
Site	Slope	Intercept	R <sup>2</sup>	N	Avg(Calc)	Avg(Meas)	Avg(Calc/Meas)
MK	0.600	0.457	0.9332	61	0.95	1.27	0.75
YL	0.605	0.230	0.959	60	1.11	1.40	0.80
TW	0.544	0.285	0.902	56	0.95	1.22	0.78
KC	0.519	0.292	0.892	60	0.90	1.20	0.75
WB	0.567	0.218	0.924	61	1.07	1.39	0.77
ALL	0.575	0.434	0.940	298	1.00	1.29	0.77

### 3.4.3 Anion and Cation Balance

Anion and cation balances compare the sum of measured  $\text{Cl}^-$ ,  $\text{NO}_3^-$ , and  $\text{SO}_4^{2-}$  to the sum of measured  $\text{NH}_4^+$ ,  $\text{Na}^+$ , and  $\text{K}^+$  in  $\mu\text{eq}/\text{m}^3$ , the product of mass concentration (in  $\mu\text{g}/\text{m}^3$ ) divided by the atomic weight of the chemical species divided by the species' charge.

$$\mu\text{eq}/\text{m}^3 \text{ for anions} = \left( \frac{[\text{Cl}^-]}{35.5} + \frac{[\text{NO}_3^-]}{62} + \frac{[\text{SO}_4^{2-}]}{96/2} \right) \quad (1)$$

$$\mu\text{eq}/\text{m}^3 \text{ for cations} = \left( \frac{[\text{NH}_4^+]}{18} + \frac{[\text{Na}^+]}{23} + \frac{[\text{K}^+]}{39.1} \right) \quad (2)$$

These are the dominant ions in typical aerosols, although others such as carbonate and phosphate compounds may also be present. Figure 3-7 shows the scatter plots of anion versus cation concentrations for each site. Regression statistics and average ratios of anion (Y) over cation (X) are summarized in Table 3-10. The correlations between anion and cation are high ( $R^2 > 0.96$ ). The regression slopes are close to unity, ranging from 0.936 to 1.012. The average anion/cation ratio is 1.12.

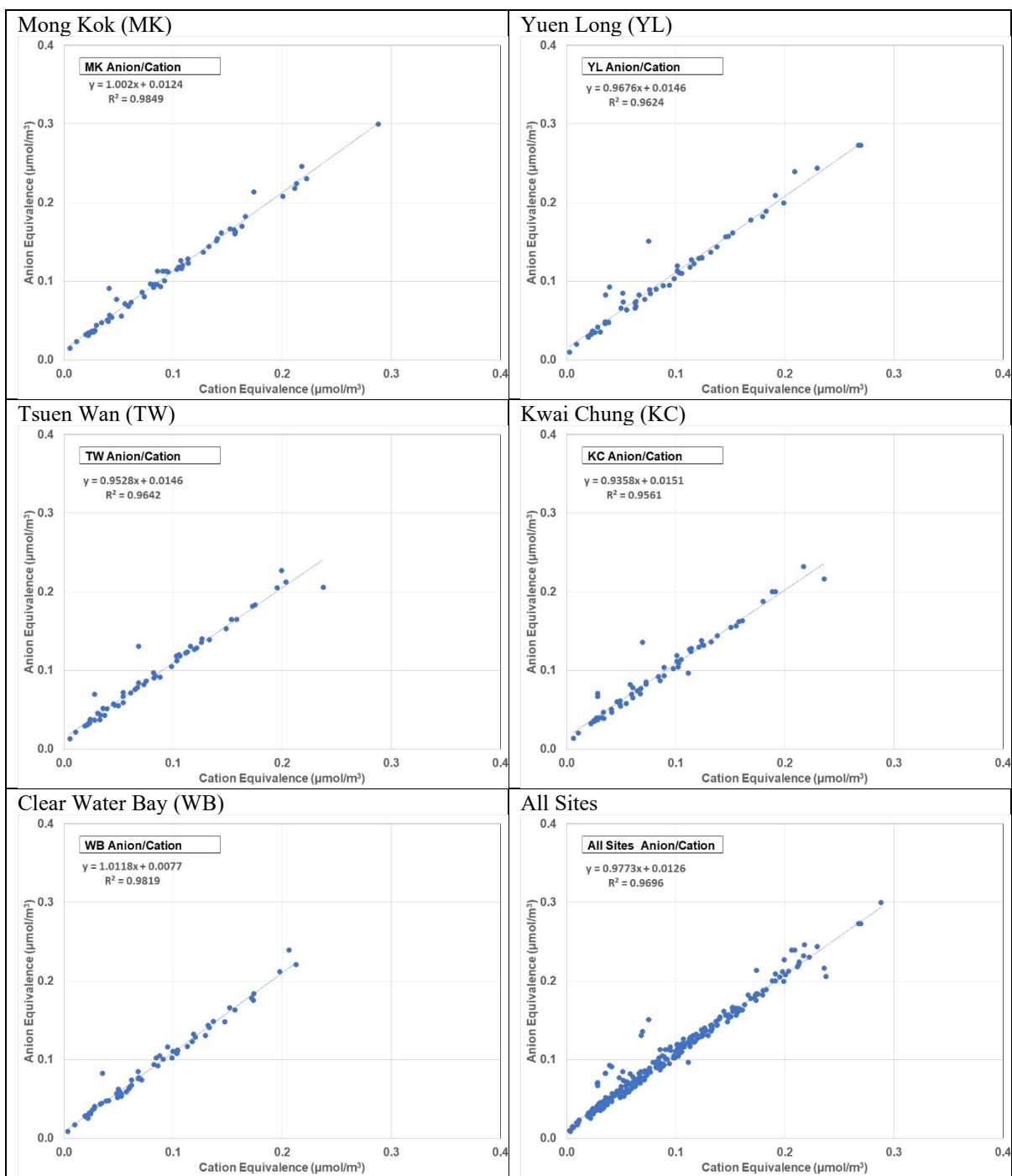


Figure 3-7. Anion vs. cation balance.

Table 3-10. Statistics for anion/cation comparisons. Averages are in  $\mu\text{g}/\text{m}^3$ .

Site	Slope	Intercept	R <sup>2</sup>	N	Avg(Anion)	Avg(Cation)	Avg(An/Cat)
<b>MK</b>	1.002	0.0124	0.985	61	0.10	0.09	1.11
<b>YL</b>	0.968	0.015	0.962	60	0.11	0.10	1.13
<b>TW</b>	0.953	0.015	0.964	56	0.09	0.08	1.13
<b>KC</b>	0.936	0.015	0.956	60	0.09	0.08	1.11
<b>WB</b>	1.012	0.008	0.982	61	0.10	0.09	1.13
<b>ALL</b>	0.977	0.011	0.970	298	0.10	0.09	1.12

The limits used for identifying outliers suggested by the U.S.EPA (2012) is  $0.86 \leq \text{anion/cation} \leq 2.82$ . Only the YL sample on 8/3/2020 exceeded this criteria with a ratio of 3.22. This sample had low ion concentrations with the highest being that for sulfate at  $0.29 \mu\text{g}/\text{m}^3$ .

#### 3.4.4 IMPROVE\_A TOR versus TOT Protocol for Carbon Measurements

OC and EC determined by IMPROVE\_A TOR and TOT methods for samples from each site and all sites combined are compared in Figures 3-8 and 3-9 with statistics in Table 3-11. TOT always yields more OC and less EC because the transmitted light is dominated by charring of the organic vapors adsorbed within the quartz-fiber filter while the TOR is dominated by charring of the aerosol deposit on the filter surface (Chow et al., 2004). Since EC is typically the smaller part of TC, it is more affected by this difference than the OC value.

#### 3.4.5 Reconstructed versus Measured Mass

Major PM components are summed compare with the measured  $\text{PM}_{2.5}$  mass (Chow et al., 2015a). The major components include: 1) organic matter (OM:  $1.4 \times \text{OC}$  to account for unmeasured hydrogen and oxygen); 2) EC (sometimes called “soot”, although soot also contains substantial amounts of OM and other materials (Akhter et al., 1985a, b)); 3) sulfate; 4) nitrate; 5) ammonium; 6) salt ( $\text{Na}^+ + \text{Cl}^-$ , which probably originates from marine aerosols in Hong Kong); 6) minerals (also called “geological” or “crustal” and estimated as  $1.89 \times [\text{Al}] + 2.14 \times [\text{Si}] + 1.4 \times [\text{Ca}] + 1.43 \times [\text{Fe}]$  to account for unmeasured oxides), and other trace elements (i.e., the sum of the remaining chemical concentrations excluding sulfur, sodium, and chloride/chlorine. The difference between the reconstructed and measured mass is termed “unidentified” and results from deviations from assumptions regarding the non-measured components which are dominated by hydrogen and oxygen in the OM. While the 1.4 OC multiplier has long been used, there is growing evidence that as OC levels decrease, mostly due to gasoline- and diesel-engine exhaust reductions, the remaining OM contains more non-carbon atoms. Secondary organic aerosols and biomass burning emissions contain OM/OC ratios on the order of  $\sim 2$  (Turpin and Lim, 2001). The new IMPROVE formula, which originally used a 1.4 OC multiplier, has been modified using a 1.8 multiplier (Pitchford et al., 2007) to better reflect the changes in sources contributing to  $\text{PM}_{2.5}$ .

Reconstructed mass is compared against the measured mass in Figure 3-10 and Table 3-12. The reconstructed mass accounts for  $\sim 70\%$  to  $\sim 80\%$  of the measured mass, indicating that a higher OC multiplier might be in order. The 1.4 multiplier is maintained here for consistency with values from prior years. Another potential cause of the discrepancy is liquid water associated with the ions that may not have been removed under the relative humidity conditions in the weighing chamber.  $\text{RH} < 30\%$  is needed to remove most of the liquid water from samples acquired in a humid environment such as Hong Kong. The higher slope for the “All” category is due to a few outliers for which the reconstructed mass exceeds the measured

mass. These are identified in Table 3-13. Each of these contains a very high OC content that is the cause of the discrepancy.

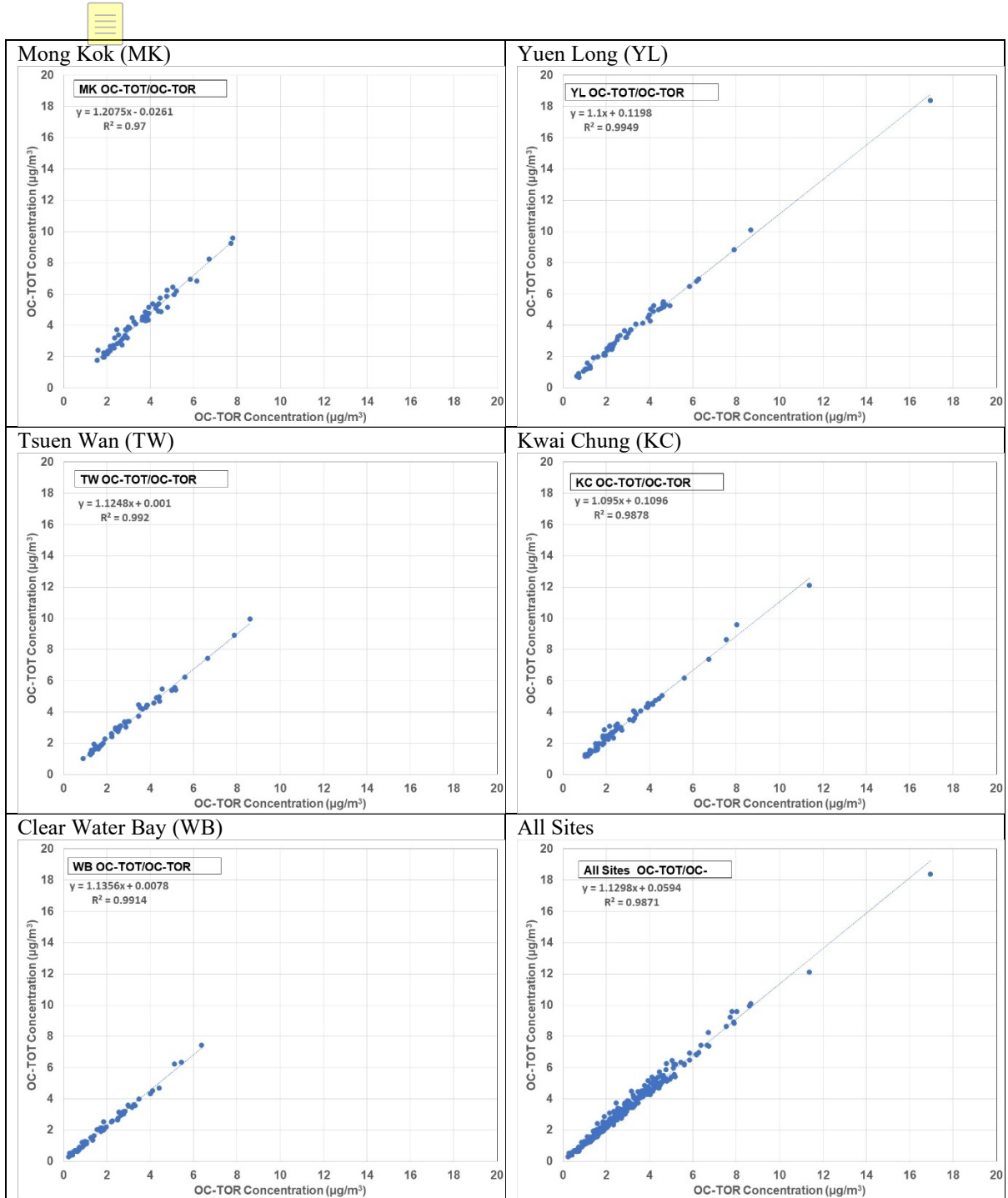


Figure 3-8. OC by TOT vs. OC by TOR.

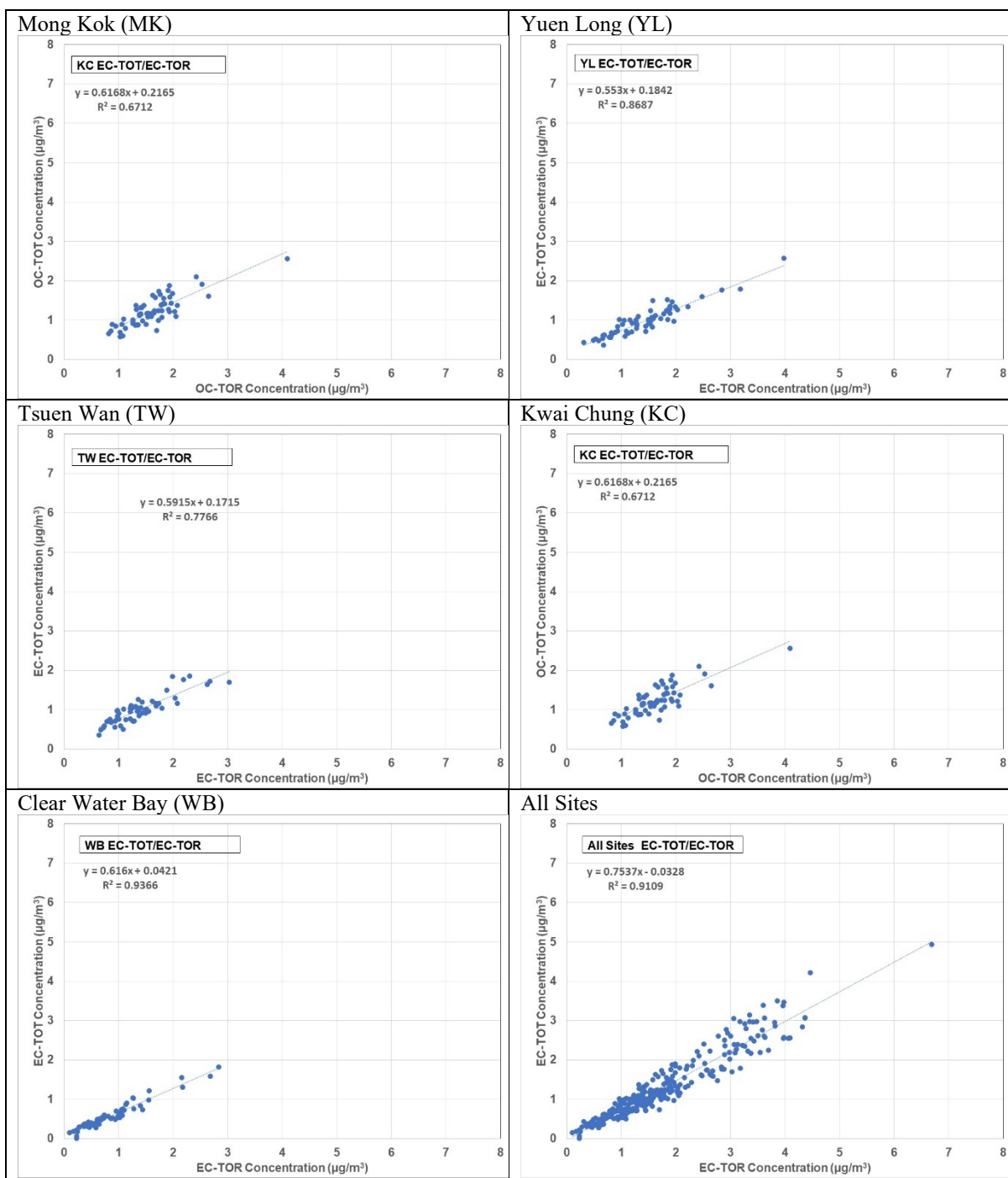


Figure 3-9. EC by TOT vs. EC by TOR.

Table 3-11. Statistics for TOT/TOR comparisons. Average concentrations in  $\mu\text{g}/\text{m}^3$ .

TOT OC vs TOR OC							
	Slope	Intercept	R <sup>2</sup>	N	Avg(TOT)	Avg(TOR)	Avg(TOT/TOR)
<b>MK</b>	1.208	0.026	0.997	61	3.24	2.86	1.13
<b>YL</b>	1.100	0.120	0.995	60	4.24	3.53	1.20
<b>TW</b>	1.125	0.001	0.992	56	3.31	2.94	1.13
<b>KC</b>	1.095	0.110	0.988	60	2.14	1.88	1.14
<b>WB</b>	1.136	0.008	0.991	61	3.57	3.14	1.14
<b>ALL</b>	1.130	0.059	0.987	298	3.30	2.87	1.15
TOT EC vs TOR EC							
Site	Slope	Intercept	R <sup>2</sup>	N	Avg(TOT)	Avg(TOR)	Avg(TOT/TOR)
<b>MK</b>	0.617	0.216	0.671	61	1.22	1.63	0.75
<b>YL</b>	0.553	0.184	0.869	60	2.54	3.27	0.78
<b>TW</b>	0.592	0.172	0.777	56	0.99	1.38	0.72
<b>KC</b>	0.617	0.217	0.671	60	0.57	0.86	0.66
<b>WB</b>	0.616	0.042	0.937	61	0.98	1.44	0.68
<b>ALL</b>	0.754	0.033	0.911	298	1.27	1.72	0.73

### 3.5 Collocated Comparisons

As shown in Table 2-2,, MK has a collocated Teflon filter while WB has a collocated quartz filter. Figures 3-11 and 3-12 compare representative species. The slopes in Figure 3-11 range are 0.9 or larger with R<sup>2</sup> exceeding 0.86, consistent with a high degree of correlation. The collocated values are slightly lower than the primary values for all of these examples. This typically occurs when there are minor differences between the flow rates of the collocated samplers. Figure 3-12 shows good agreement for all of the examples with the exception of calcium, the slope of which is biased low by three outliers that have higher concentrations on the primary sampler than the collocated sampler. This could be due to some contamination for a nearby dust source on the primary sampler. Otherwise, most of the collocated Teflon values are nearly identical among the two samplers.

### 3.6 PM<sub>2.5</sub> Continuous and Filter Measurements 2020

HKEPD conducted continuous monitoring of PM<sub>2.5</sub> concentrations at four monitoring sites during 2019. Two sites used TEOMs and two sites used BAMs. For the sites with TEOMs (MK and TW), Yu et al. (2020) found that 24-hour average PM<sub>2.5</sub> from these monitors compared well with the collocated gravimetric filter measurements with R<sup>2</sup>=0.97 at each site, slopes of 1.03-1.08, and intercepts between -1 to -3  $\mu\text{g}/\text{m}^3$ . For the BAM sites (YL and KC), R<sup>2</sup>=0.95 at each site, slopes were 0.88-0.95 and intercepts were between 1 and 2  $\mu\text{g}/\text{m}^3$ .

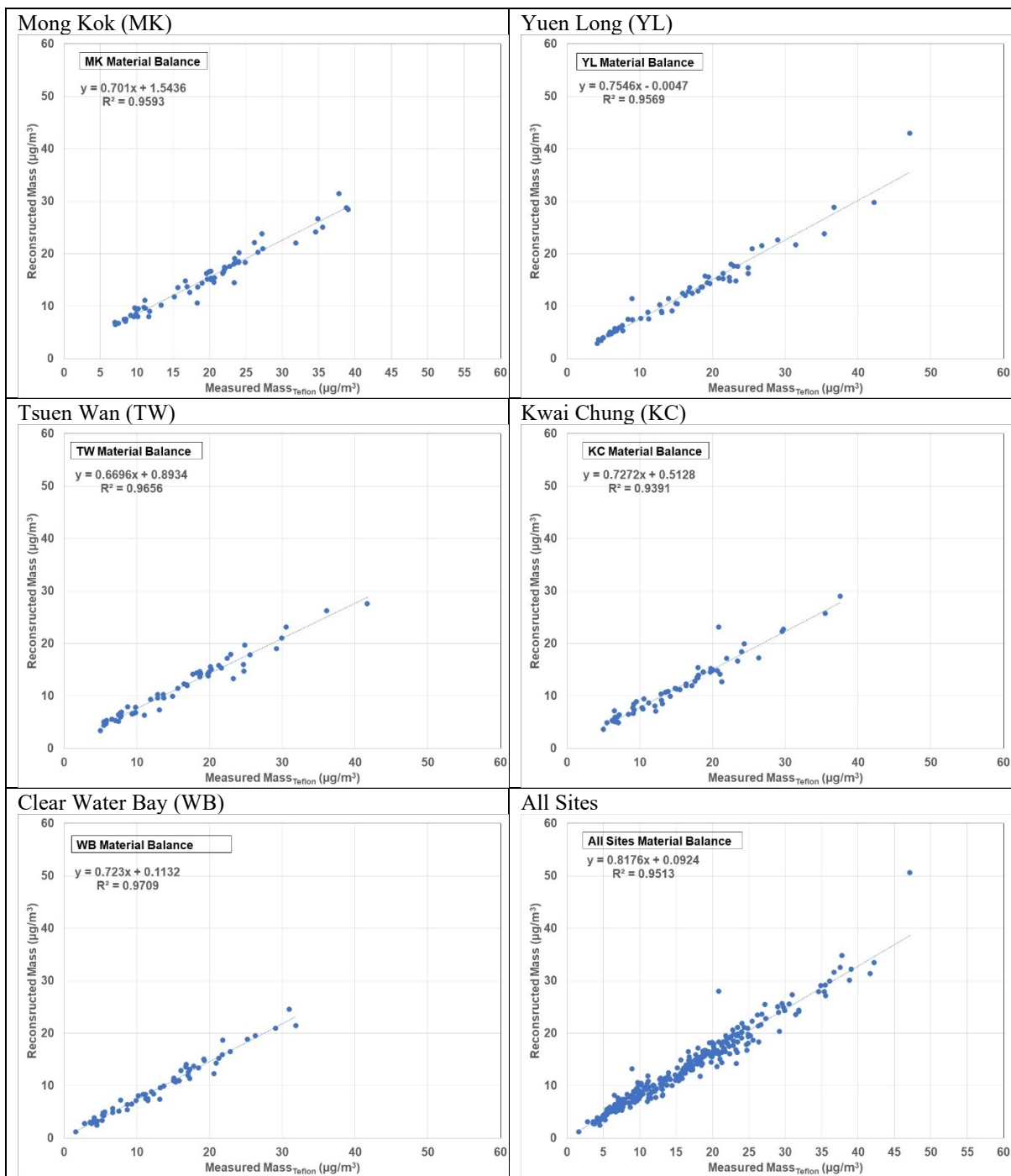


Figure 3-10. Comparisons of reconstructed with measured mass.

Table 3-12. Statistics for reconstructed and measured PM<sub>2.5</sub> mass. Average in µg/m<sup>3</sup>.

Site	Slope	Intercept	R <sup>2</sup>	N	Avg(Rec)	Avg(Meas)	Avg(Rec/Meas)
<b>MK</b>	0.701	1.534	0.960	61	16.55	19.33	0.856
<b>YL</b>	0.755	0.0.005	0.957	60	13.75	16.54	0.831
<b>TW</b>	0.670	0.893	0.966	56	12.93	15.55	0.831
<b>KC</b>	0.727	0.5130	0.940	60	12.66	15.87	0.798
<b>WB</b>	0.723	0.113	0.970	61	10.36	13.20	0.785
<b>ALL</b>	0.818	0.437	0.971	298	13.26	16.10	0.823

Table 3-13. Samples with reconstructed mass exceeding measured mass.

Site	Date	Meas	Rec	OM	EC	SO <sub>4</sub>	NO <sub>3</sub>	NH <sub>4</sub>	NaCl	Minerals	Trace	Unid
<b>MK</b>	6/4/2020	9.78	10.56	3.48	3.35	1.87	0.46	0.46	0.48	0.29	0.17	-0.78
<b>YL</b>	8/27/2020	9.00	13.22	6.20	1.90	3.25	0.36	1.03	0.15	0.20	0.13	-4.23
<b>YL</b>	12/7/2020	47.16	50.61	23.75	3.98	9.24	4.92	4.50	0.24	2.87	1.12	-3.45
<b>KC</b>	8/15/2020	6.54	8.13	3.82	1.41	1.58	0.35	0.40	0.18	0.24	0.15	-1.59
<b>KC</b>	12/19/2020	20.92	27.98	15.93	1.93	4.36	2.24	1.95	0.09	1.01	0.46	-7.06



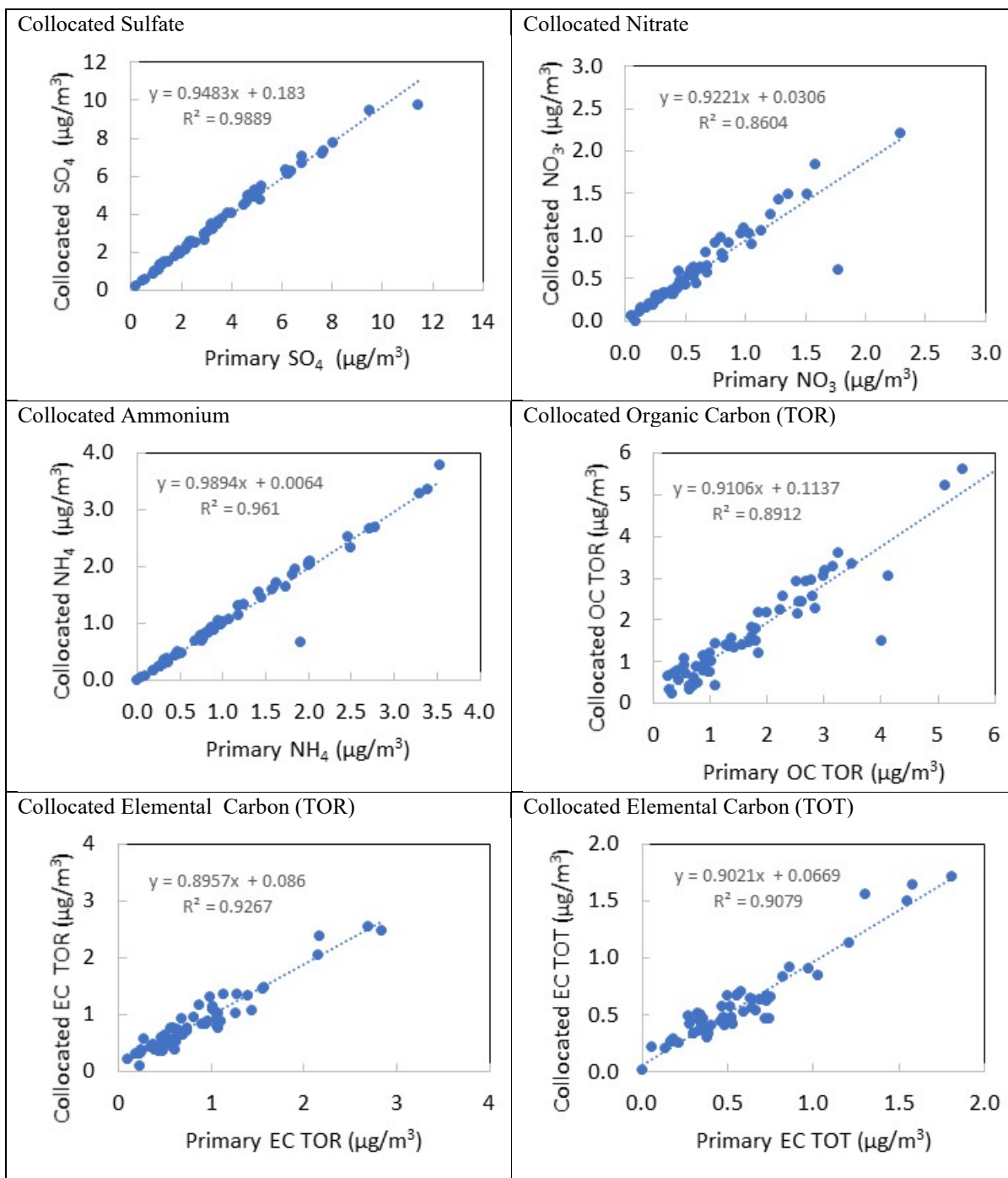


Figure 3-11. Comparisons of selected species from collocated and primary quartz filter sampler concentrations.

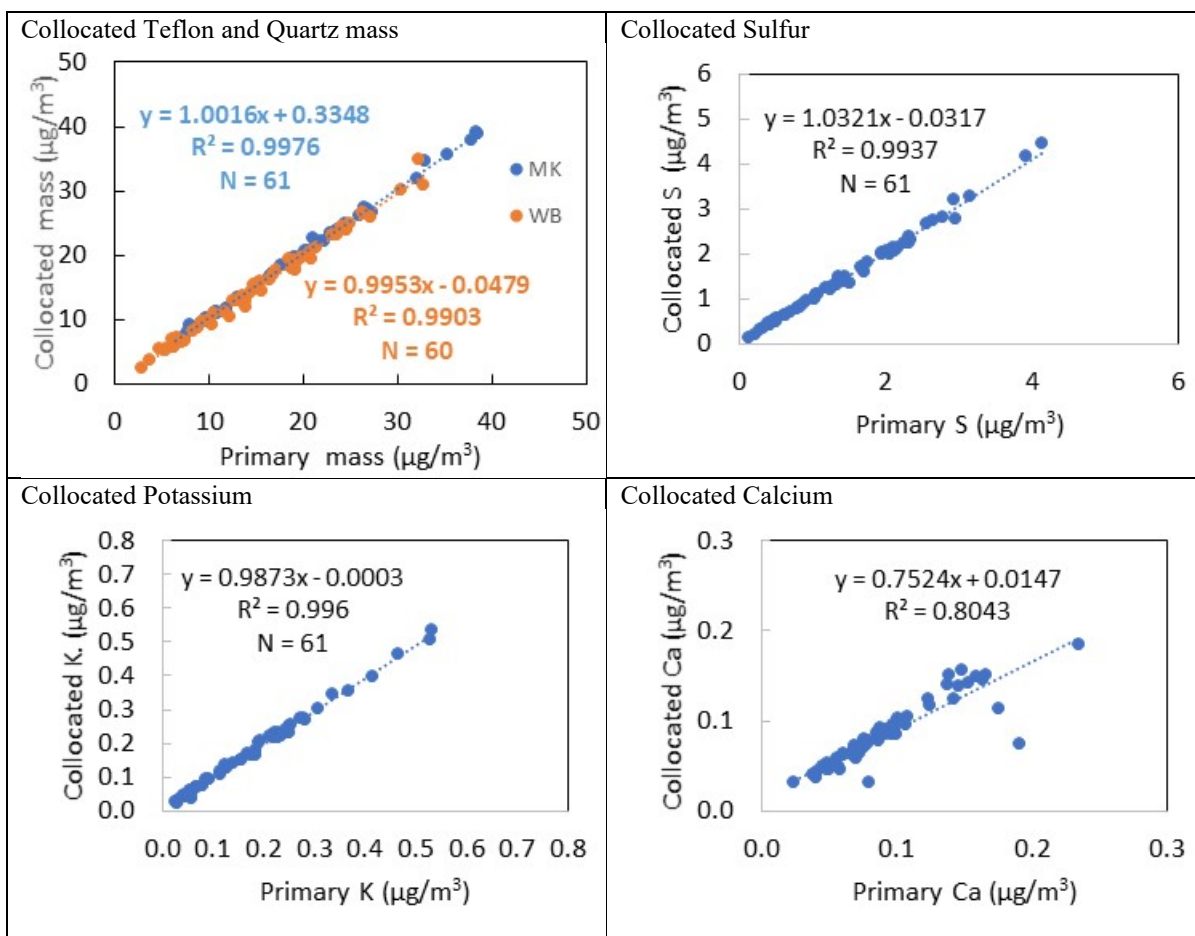


Figure 3-12. Comparisons of selected species from collocated and primary Teflon filter sampler concentrations.

## 4 PM<sub>2.5</sub> Components and Trends

Tables 4-1 through 4-5 summarize the annual averages for each measured species from 2000-2020. Figure 4-1 compares PM<sub>2.5</sub> trendlines for the five sites. Annual average PM<sub>2.5</sub> for 2020 ranged from 13.2 µg/m<sup>3</sup> at WB to 19.3 µg/m<sup>3</sup> at MK. The highest PM<sub>2.5</sub> concentrations were 31.9 µg/m<sup>3</sup> at WB, 37.6 µg/m<sup>3</sup> at KC, 39.1 µg/m<sup>3</sup> at MK, 41.7 µg/m<sup>3</sup> at TW, and 47.2 µg/m<sup>3</sup> at YL. The 2020 annual averages are well within Hong Kong's 35 µg/m<sup>3</sup> limit, but they still exceed the 12 µg/m<sup>3</sup> annual PM<sub>2.5</sub> limit followed in the U.S. and the 10 µg/m<sup>3</sup> annual average recommended by the World Health Organization.

In Figure 4-1, the most dramatic improvement is seen for the MK roadside site, indicating the success of gasoline and diesel engine exhaust reduction measures implemented by HKEPD over the past 20 years. The trend slopes indicate long-term changes ranging from 1.5 µg/m<sup>3</sup>/yr at KC to 2.9 µg/m<sup>3</sup>/yr at MK. However, there appears to be a slower rate of reduction from 2016 onward, indicating the need for additional efforts.

Annual average concentrations for the 2020 major components are compared in Table 4-6 and plotted in Figure 4-2. It is apparent that OM and sulfate are the largest contributors while the remaining trace element contributions are negligible. Sulfate levels are uniform across the network, ranging from 3.76 µg/m<sup>3</sup> at WB to 4.06 µg/m<sup>3</sup> at YL. This is consistent with the well-known regional nature of sulfate levels. Since Hong Kong has greatly reduced SO<sub>2</sub> emissions from its local power stations, the remaining sources for sulfate precursors would be coal-fired power stations on the mainland and ship emissions. OM is lowest at the non-urban WB site at 2.63 µg/m<sup>3</sup>, much lower than the 4.0 to 4.95 µg/m<sup>3</sup> OM concentrations at the more urbanized sites. This indicates that there are sources within the city, typically related to engine exhaust, that are contributing. EC is highest at the MK site, more than double the averages at the other locations, which indicates that there is still a large influence from diesel-powered engines, and to some extent the gasoline engines as well. Nitrate is also less uniform across the network with more than 1 µg/m<sup>3</sup> measured at MK and YL and lower concentrations at other locations. This indicates more local formation of the nitric acid, typically from NO<sub>x</sub> related to engine exhaust. Ammonium follows the combined levels of sulfate and nitrate, as indicated by the ammonium and ion balances in Section 3. Minerals are highest at MK and with similar concentrations at the remaining sites. This is evidence that road dust is still a noticeable contributor, although the mineral component is a small contributor. The unidentified mass is similar to or greater than contributions from nitrate, ammonium, salt, minerals, and trace materials. The unexplained mass is homogeneously distributed across the network. This implies that the 1.4 multiplier to convert OC to OM may be too low, as previously discussed. It may also be the case that the humidity conditions in the filter weighing environment may be too high to remove liquid water from the associated sulfate, nitrate, and ammonium ions.

Table 4-7 compares the fractional contributions of each component to the measured PM<sub>2.5</sub> mass. This indicates that the unidentified mass can exceed 20% of the PM<sub>2.5</sub> mass at the less polluted locations. OM and sulfate alone constitute more than or close to 50% of the mass. The importance of EC from traffic is evident from the 17% contribution to PM<sub>2.5</sub> at MK.

Figure 4-3 examines the monthly average contributions for the major components, manifesting the seasonal cycle that has been observed in previous years. Summers have the lowest levels for all components, with June and July having the lowest averages at all sites. All sites show the highest contributions from all components in December. March appears to have

higher contributions than the neighboring months at all sites. The Mineral content is higher during this period which may indicate Asian dust contributions. Monthly-averaged EC is relatively constant at MK and YL, even though OM varies more from month to month. The unidentified contributions are negligible during June and July when the ion concentrations are lowest and higher temperatures might evaporate liquid water associated with these ions during sampling. The unidentified fraction increases over the winter months

Long term trends for the major components are compared in Figure 4-4. To maintain consistency with the historical record, the Salt fraction is included with the Others category. The categories are also consistent with prior usage, with “Geological” representing “Minerals” and “Soot” representing EC. As noted earlier, these definitions are not as precise in representing the category as “Minerals” and “EC” are. Geological materials often contain important fractions of carbon in addition to minerals. Soot contains a mixture of OC and EC, although EC is usually the major component. Reductions in the Organics, Soot, and Sulfate categories are evident, although they are more pronounced in the early years than in the present situation. The Nitrate category shows improvement, but not as much as that for the other major categories. Ammonium follows the Sulfate trend. There is little change over time in the Geological and Others categories.

Table 4-8 shows the absolute changes in the annual average contributions from 2019 to 2020. The most notable improvements are at the MK and YL sites where annual average  $PM_{2.5}$  was approximately  $5 \mu g/m^3$  lower during 2020 than during 2019. Large reductions in the Organic and Sulfate categories contributed to this improvement. Sulfate decreased by  $\sim 1.5 \mu g/m^3$  across the network. The decrease in Organics and Soot contributions reflect the proximity to or distance from heavily trafficked areas. Geological and Other contributions, especially at the MK and YL sites, also showed minor reductions from the previous year. Only Soot at TW, KC, and WB showed slight increases from the prior year. These changes have not been stratified by meteorological conditions, and the fluctuations are within the year-to-year changes of previous comparisons.


Since the outbreak of COVID-19 during late January, 2020, the Hong Kong government has implemented a series of social distancing and travel restrictions. Compared to 2019, Ali et al. (2021) reported a reduction of aerosol optical depth (AOD) in the Pearl River Delta Region since February, 2020. Comparison between data collected in January-April, 2020, with those in 2017-2019, Huang et al. (2020) shows reduction of 25% to 36%  $PM_{2.5}$  at the roadside and ambient sites. This is consistent with the 28% and 35% reductions in  $PM_{2.5}$  found at the MK and YL sites. However, the corresponding changes during the COVID-19 period (February-April, 2020) varied from -16% to 38% as compared to the pre-COVID-19 period (January, 2020). More detailed analysis coupled with meteorological data is needed to evaluate the impact of the pandemic on air quality. 

Table 4-1. Annual averages for PM<sub>2.5</sub> mass and chemical constituents (µg/m<sup>3</sup>) at MK.

Site	MK	MK	MK	MK	MK	MK	MK	MK	MK	MK	MK	MK	MK
Year	2000-01	2004-05	2008-09	2011	2012	2013	2014	2015	2016	2017	2018	2019	2020
Teflon Mass	58.280	53.020	41.600	43.080	38.930	36.720	33.900	29.822	20.740	27.179	23.923	24.750	19.334
QMA Mass	62.500	54.870	45.920	47.920	58.030	41.380	35.990	32.416	22.106	29.794	25.418	27.876	22.315
Cl <sup>-</sup>	0.256	0.283	0.312	0.205	0.100	0.119	0.203	0.226	0.072	0.191	0.107	0.135	0.157
NO <sub>3</sub> <sup>-</sup>	1.650	2.400	2.810	2.450	1.320	1.310	1.530	1.600	0.612	1.356	1.261	1.433	1.183
SO <sub>4</sub> <sup>2-</sup>	9.500	12.840	10.410	10.910	10.010	9.140	8.600	7.425	6.557	6.356	5.211	5.523	4.047
NH <sub>4</sub> <sup>+</sup>	3.170	4.400	3.400	4.370	3.680	3.420	3.280	2.755	2.420	2.454	1.399	2.254	1.396
Na <sup>+</sup>	0.398	0.423	0.320	0.431	0.320	0.326	0.420	0.426	0.294	0.439	0.967	0.362	0.344
K <sup>+</sup>	0.457	0.479	0.278	0.467	0.350	0.319	0.286	0.190	0.220	0.235	0.173	0.219	0.106
OC	16.640	11.180	6.260	8.090	7.050	6.920	7.640	5.668	5.171	6.718	4.240	5.133	3.534
EC	20.290	14.120	10.660	8.480	9.200	9.420	6.910	4.959	2.604	4.946	4.339	3.576	3.272
TC	36.910	25.280	16.910	16.550	16.250	16.330	14.540	10.623	7.775	11.664	8.538	8.709	6.780
Al	0.114	0.141	0.099	0.194	0.237	0.203	0.167	0.088	0.124	0.147	0.103	0.132	0.035
Si	0.478	0.347	0.249	0.398	0.439	0.373	0.276	0.160	0.191	0.268	0.188	0.268	0.141
P	0.009	0.189	0.023	0.019	0.021	0.018	0.019	0.000	0.003	0.004	0.000	0.002	0.000
S	3.489	4.301	3.347	3.668	3.346	3.138	3.087	2.802	2.552	2.584	2.076	2.308	1.528
Cl	0.117	0.139	0.104	0.089	0.039	0.075	0.130	0.130	0.052	0.147	0.098	0.082	0.117
K	0.552	0.468	0.306	0.462	0.345	0.366	0.314	0.233	0.243	0.301	0.215	0.291	0.178
Ca	0.171	0.108	0.110	0.130	0.146	0.124	0.106	0.105	0.084	0.122	0.113	0.100	0.092
Ti	0.009	0.011	0.011	0.013	0.015	0.013	0.010	0.009	0.008	0.010	0.011	0.009	0.008
V	0.013	0.019	0.018	0.015	0.020	0.022	0.026	0.017	0.025	0.015	0.011	0.006	0.002
Cr	0.001	0.002	0.001	0.002	0.002	0.002	0.002	0.000	0.000	0.003	0.009	0.000	0.002
Mn	0.013	0.017	0.013	0.021	0.019	0.016	0.013	0.009	0.006	0.011	0.010	0.012	0.011
Fe	0.269	0.258	0.234	0.296	0.305	0.278	0.254	0.245	0.171	0.288	0.308	0.288	0.261
Co	0.000	0.000	0.000	0.001	0.000	0.000	0.001	0.000	0.000	0.000	0.000	0.000	0.000
Ni	0.006	0.006	0.005	0.005	0.007	0.007	0.007	0.005	0.006	0.004	0.004	0.002	0.004
Cu	0.011	0.011	0.021	0.025	0.021	0.023	0.022	0.021	0.016	0.018	0.012	0.015	0.008
Zn	0.179	0.240	0.158	0.216	0.189	0.157	0.135	0.096	0.076	0.104	0.060	0.076	0.055
Ga	0.000	0.002	0.000	0.000	0.000	0.000	0.000	0.000	0.000	0.000	0.000	0.000	0.000
As	0.005	0.005	0.001	0.004	0.003	0.004	0.002	0.003	0.000	0.001	0.000	0.000	0.000
Se	0.002	0.000	0.000	0.000	0.000	0.000	0.000	0.001	0.000	0.000	0.001	0.000	0.001
Br	0.013	0.011	0.017	0.017	0.013	0.013	0.013	0.011	0.005	0.011	0.007	0.000	0.006
Rb	0.004	0.002	0.001	0.001	0.001	0.001	0.000	0.001	0.000	0.001	0.001	0.000	0.001
Sr	0.001	0.001	0.002	0.003	0.002	0.002	0.001	0.002	0.001	0.001	0.003	0.001	0.002
Y	0.000	0.000	0.000	0.000	0.000	0.000	0.000	0.000	0.000	0.000	0.000	0.000	0.000
Zr	0.001	0.002	0.001	0.001	0.001	0.000	0.001	0.001	0.000	0.001	0.002	0.000	0.001
Mo	0.001	0.002	0.001	0.002	0.000	0.000	0.002	0.001	0.001	0.000	0.000	0.003	0.001
Pd	0.001	0.002	0.001	0.002	0.000	0.000	0.000	0.000	0.001	0.000	0.000	0.000	0.001
Ag	0.001	0.001	0.001	0.000	0.000	0.000	0.000	0.000	0.000	0.000	0.000	0.000	0.002
Cd	0.002	0.002	0.001	0.001	0.001	0.000	0.001	0.000	0.000	0.000	0.000	0.000	0.001
In	0.002	0.001	0.001	0.000	0.000	0.000	0.000	0.000	0.000	0.001	0.000	0.002	0.001
Sn	0.019	0.013	0.011	0.013	0.004	0.003	0.003	0.003	0.004	0.002	0.000	0.001	0.001
Sb	0.005	0.004	0.001	0.008	0.001	0.001	0.002	0.001	0.001	0.000	0.001	0.000	0.001
Ba	0.027	0.011	0.003	0.017	0.035	0.011	0.004	0.000	0.021	0.014	0.002	0.002	0.001
La	0.013	0.011	0.004	0.016	0.000	0.000	0.004	0.001	0.016	0.002	0.003	0.000	0.001
Au	0.000	0.000	0.000	0.000	0.000	0.000	0.000	0.000	0.000	0.000	0.000	0.000	0.001
Hg	0.000	0.000	0.000	0.000	0.000	0.000	0.000	0.000	0.000	0.000	0.000	0.000	0.000
Tl	0.000	0.000	0.000	0.000	0.000	0.000	0.000	0.000	0.000	0.000	0.000	0.000	0.000
Pb	0.066	0.048	0.041	0.060	0.040	0.038	0.032	0.018	0.016	0.018	0.010	0.012	0.007
U	0.000	0.001	0.001	0.004	0.000	0.000	0.000	0.000	0.000	0.000	0.000	0.000	0.001

Table 4-2. Annual averages for PM<sub>2.5</sub> mass and chemical constituents (µg/m<sup>3</sup>) at YL.

Site	YL	YL	YL	YL	YL	YL	YL	YL	YL	YL	YL	YL
Year	2004-05	2008-09	2011	2012	2013	2014	2015	2016	2017	2018	2019	2020
Teflon Mass	41.310	31.780	38.220	30.150	31.010	27.290	25.015	23.097	22.498	22.378	22.062	16.539
QMA Mass	43.910	36.340	42.890	50.230	35.370	29.800	26.700	23.962	24.211	23.783	25.195	19.323
Cl <sup>-</sup>	0.264	0.213	0.174	0.130	0.111	0.142	0.093	0.104	0.107	0.090	0.083	0.091
NO <sub>3</sub> <sup>-</sup>	2.860	2.420	2.590	1.430	1.760	1.430	1.429	1.161	1.213	1.624	1.426	1.030
SO <sub>4</sub> <sup>2-</sup>	13.910	11.040	10.850	9.580	8.960	8.630	7.283	6.659	6.516	5.425	5.722	4.056
NH <sub>4</sub> <sup>+</sup>	4.620	3.470	4.630	3.560	3.540	3.290	2.714	2.574	2.515	1.482	2.370	1.387
Na <sup>+</sup>	0.375	0.262	0.402	0.320	0.278	0.352	0.344	0.274	0.322	1.083	0.280	0.272
K <sup>+</sup>	0.562	0.365	0.590	0.370	0.385	0.348	0.234	0.298	0.260	0.219	0.248	0.126
OC	7.230	4.830	5.730	4.690	5.020	6.150	4.244	5.851	5.291	3.516	4.414	3.137
EC	6.190	3.490	4.610	3.600	3.960	2.570	2.037	2.220	1.702	2.099	1.547	1.439
TC	13.420	8.310	10.310	8.290	8.970	8.720	6.277	8.071	6.993	5.574	5.962	4.550
Al	0.145	0.091	0.211	0.237	0.212	0.178	0.090	0.130	0.139	0.105	0.141	0.039
Si	0.322	0.207	0.435	0.431	0.378	0.290	0.173	0.204	0.241	0.196	0.291	0.144
P	0.192	0.023	0.016	0.015	0.015	0.014	0.000	0.002	0.002	0.000	0.000	0.001
S	4.562	3.454	3.781	3.228	3.099	3.091	2.781	2.530	2.576	2.135	2.286	1.499
Cl	0.159	0.094	0.077	0.062	0.079	0.094	0.068	0.064	0.092	0.079	0.057	0.071
K	0.563	0.383	0.572	0.388	0.437	0.384	0.285	0.329	0.323	0.251	0.321	0.198
Ca	0.089	0.074	0.111	0.121	0.109	0.094	0.094	0.080	0.088	0.105	0.088	0.070
Ti	0.011	0.010	0.016	0.015	0.014	0.011	0.009	0.009	0.012	0.013	0.010	0.007
V	0.020	0.014	0.014	0.015	0.014	0.018	0.015	0.016	0.013	0.010	0.005	0.001
Cr	0.002	0.002	0.002	0.002	0.002	0.002	0.002	0.000	0.002	0.006	0.000	0.001
Mn	0.017	0.013	0.022	0.019	0.018	0.014	0.010	0.010	0.010	0.011	0.012	0.011
Fe	0.200	0.155	0.222	0.222	0.203	0.188	0.175	0.166	0.178	0.217	0.199	0.163
Co	0.000	0.000	0.000	0.000	0.000	0.000	0.000	0.000	0.000	0.000	0.000	0.000
Ni	0.007	0.004	0.005	0.005	0.005	0.005	0.004	0.004	0.004	0.003	0.002	0.003
Cu	0.011	0.017	0.023	0.017	0.038	0.032	0.013	0.011	0.011	0.009	0.009	0.005
Zn	0.238	0.160	0.219	0.188	0.152	0.118	0.105	0.096	0.078	0.073	0.070	0.078
Ga	0.002	0.000	0.000	0.000	0.000	0.000	0.000	0.000	0.000	0.000	0.000	0.000
As	0.008	0.002	0.006	0.003	0.004	0.002	0.003	0.000	0.000	0.000	0.000	0.000
Se	0.001	0.000	0.000	0.000	0.000	0.000	0.001	0.000	0.000	0.001	0.000	0.001
Br	0.012	0.014	0.017	0.012	0.013	0.012	0.011	0.006	0.009	0.007	0.002	0.005
Rb	0.003	0.002	0.002	0.001	0.001	0.001	0.001	0.001	0.001	0.001	0.000	0.001
Sr	0.002	0.002	0.003	0.001	0.002	0.001	0.002	0.001	0.001	0.002	0.001	0.002
Y	0.000	0.000	0.000	0.000	0.000	0.000	0.000	0.000	0.000	0.000	0.000	0.000
Zr	0.001	0.001	0.001	0.001	0.001	0.001	0.001	0.000	0.001	0.001	0.000	0.001
Mo	0.002	0.001	0.001	0.000	0.000	0.003	0.001	0.001	0.000	0.000	0.002	0.000
Pd	0.002	0.001	0.002	0.000	0.000	0.000	0.000	0.000	0.000	0.000	0.000	0.000
Ag	0.002	0.001	0.000	0.000	0.000	0.000	0.000	0.000	0.000	0.000	0.000	0.002
Cd	0.003	0.001	0.001	0.001	0.000	0.001	0.000	0.000	0.000	0.000	0.000	0.001
In	0.002	0.001	0.000	0.000	0.000	0.000	0.000	0.000	0.001	0.000	0.001	0.001
Sn	0.016	0.010	0.015	0.005	0.011	0.008	0.003	0.008	0.001	0.000	0.003	0.001
Sb	0.004	0.001	0.009	0.000	0.001	0.002	0.001	0.001	0.000	0.001	0.000	0.000
Ba	0.007	0.002	0.011	0.021	0.012	0.006	0.000	0.014	0.009	0.001	0.000	0.001
La	0.008	0.004	0.017	0.000	0.000	0.006	0.001	0.011	0.003	0.001	0.000	0.001
Au	0.000	0.000	0.000	0.000	0.000	0.000	0.000	0.000	0.000	0.000	0.000	0.001
Hg	0.000	0.000	0.000	0.000	0.000	0.000	0.000	0.000	0.000	0.000	0.001	0.000
Tl	0.000	0.000	0.000	0.000	0.000	0.000	0.000	0.000	0.000	0.000	0.000	0.000
Pb	0.062	0.044	0.067	0.038	0.043	0.036	0.021	0.021	0.018	0.012	0.013	0.009
U	0.002	0.001	0.004	0.000	0.000	0.000	0.000	0.000	0.000	0.000	0.000	0.001

Table 4-3. . Annual averages for PM<sub>2.5</sub> mass and chemical constituents( $\mu\text{g}/\text{m}^3$ ) at TW.

Site	TW	TW	TW	TW	TW	TW	TW	TW	TW	TW	TW	TW	TW
Year	2000-01	2004-05	2008-09	2011	2012	2013	2014	2015	2016	2017	2018	2019	2020
Teflon Mass	34.120	38.590	30.610	35.300	28.640	29.500	26.190	23.835	21.500	22.378	20.089	17.823	15.869
QMA Mass	37.280	40.750	34.000	40.560	48.260	33.970	28.660	26.344	22.915	24.746	21.672	20.731	18.010
Cl <sup>-</sup>	0.138	0.126	0.175	0.122	0.080	0.095	0.138	0.130	0.084	0.113	0.067	0.073	0.091
NO <sub>3</sub> <sup>-</sup>	1.340	1.640	2.030	1.800	1.010	1.170	0.930	1.006	0.756	0.993	0.907	0.859	0.770
SO <sub>4</sub> <sup>2-</sup>	9.170	13.170	10.480	10.910	9.410	8.880	8.660	7.452	6.617	6.597	5.438	5.072	3.821
NH <sub>4</sub> <sup>+</sup>	2.960	4.070	3.270	4.380	3.400	3.360	3.050	2.625	2.438	2.415	1.252	1.987	1.221
Na <sup>+</sup>	0.397	0.362	0.211	0.404	0.310	0.292	0.398	0.379	0.307	0.371	1.048	0.330	0.316
K <sup>+</sup>	0.492	0.486	0.308	0.492	0.320	0.309	0.294	0.186	0.221	0.235	0.165	0.167	0.094
OC	8.690	6.930	4.380	5.440	4.570	4.860	5.830	4.055	5.782	5.902	3.423	3.568	2.942
EC	5.370	6.260	3.760	4.240	3.590	4.010	2.610	2.147	2.182	1.601	1.874	1.284	1.379
TC	14.040	13.180	8.120	9.650	8.160	8.860	8.450	6.197	7.964	7.503	5.256	4.853	4.297
Al	0.115	0.141	0.083	0.191	0.212	0.192	0.168	0.086	0.119	0.140	0.094	0.0941	0.031
Si	0.387	0.314	0.185	0.389	0.390	0.344	0.273	0.157	0.187	0.247	0.173	0.1831	0.128
P	0.005	0.195	0.024	0.016	0.014	0.014	0.016	0.000	0.002	0.003	0.000	0.0003	0.001
S	3.379	4.584	3.431	3.764	3.151	3.137	3.068	2.801	2.568	2.568	2.109	2.1103	1.473
Cl	0.087	0.076	0.057	0.064	0.049	0.074	0.095	0.056	0.050	0.123	0.079	0.0796	0.078
K	0.586	0.508	0.328	0.480	0.321	0.362	0.319	0.236	0.246	0.291	0.201	0.2098	0.164
Ca	0.126	0.090	0.073	0.101	0.125	0.105	0.099	0.093	0.076	0.105	0.102	0.0662	0.074
Ti	0.009	0.010	0.008	0.012	0.013	0.011	0.009	0.008	0.007	0.008	0.010	0.0056	0.006
V	0.014	0.024	0.018	0.021	0.021	0.025	0.026	0.023	0.021	0.016	0.014	0.0061	0.002
Cr	0.001	0.002	0.001	0.002	0.002	0.002	0.002	0.002	0.000	0.002	0.006	0.0000	0.001
Mn	0.012	0.016	0.011	0.019	0.016	0.016	0.016	0.009	0.007	0.010	0.009	0.0063	0.008
Fe	0.187	0.186	0.133	0.193	0.196	0.178	0.180	0.163	0.147	0.176	0.195	0.1358	0.146
Co	0.000	0.000	0.000	0.000	0.000	0.000	0.000	0.000	0.000	0.000	0.000	0.0002	0.000
Ni	0.005	0.007	0.005	0.006	0.011	0.007	0.007	0.006	0.006	0.004	0.005	0.0021	0.003
Cu	0.009	0.010	0.019	0.021	0.015	0.021	0.018	0.012	0.009	0.012	0.008	0.0063	0.004
Zn	0.174	0.219	0.134	0.194	0.170	0.150	0.202	0.083	0.076	0.117	0.074	0.0506	0.041
Ga	0.000	0.003	0.000	0.000	0.000	0.000	0.000	0.000	0.000	0.000	0.000	0.0000	0.000
As	0.006	0.006	0.001	0.005	0.003	0.004	0.002	0.003	0.000	0.001	0.000	0.0000	0.000
Se	0.002	0.000	0.000	0.000	0.000	0.000	0.000	0.001	0.000	0.000	0.001	0.0000	0.001
Br	0.013	0.010	0.015	0.016	0.011	0.013	0.012	0.010	0.006	0.010	0.007	0.0000	0.005
Rb	0.004	0.003	0.001	0.001	0.001	0.001	0.000	0.001	0.001	0.000	0.001	0.0002	0.001
Sr	0.001	0.001	0.002	0.003	0.002	0.002	0.001	0.002	0.001	0.001	0.002	0.0007	0.001
Y	0.000	0.000	0.000	0.000	0.000	0.000	0.000	0.000	0.000	0.000	0.000	0.0001	0.000
Zr	0.001	0.001	0.001	0.000	0.001	0.001	0.001	0.001	0.000	0.000	0.001	0.0000	0.001
Mo	0.001	0.001	0.001	0.001	0.000	0.000	0.002	0.001	0.001	0.000	0.000	0.0016	0.000
Pd	0.002	0.001	0.001	0.002	0.000	0.000	0.000	0.000	0.001	0.000	0.000	0.0002	0.001
Ag	0.002	0.002	0.001	0.000	0.000	0.000	0.000	0.000	0.000	0.000	0.000	0.0001	0.002
Cd	0.002	0.002	0.001	0.000	0.001	0.001	0.000	0.000	0.000	0.000	0.000	0.0005	0.001
In	0.002	0.001	0.001	0.000	0.000	0.000	0.000	0.000	0.001	0.000	0.000	0.0018	0.001
Sn	0.020	0.019	0.010	0.012	0.003	0.006	0.006	0.003	0.008	0.003	0.000	0.0015	0.001
Sb	0.005	0.003	0.001	0.007	0.000	0.001	0.000	0.000	0.002	0.001	0.001	0.0000	0.001
Ba	0.017	0.008	0.003	0.010	0.012	0.006	0.005	0.000	0.016	0.009	0.001	0.0000	0.001
La	0.009	0.008	0.003	0.013	0.000	0.000	0.004	0.001	0.013	0.003	0.002	0.0000	0.000
Au	0.001	0.001	0.000	0.000	0.000	0.000	0.000	0.000	0.000	0.000	0.000	0.0000	0.001
Hg	0.000	0.000	0.000	0.000	0.000	0.000	0.000	0.000	0.000	0.000	0.000	0.0000	0.000
Tl	0.000	0.000	0.000	0.000	0.000	0.000	0.000	0.000	0.000	0.000	0.000	0.0000	0.000
Pb	0.073	0.050	0.041	0.060	0.035	0.037	0.031	0.018	0.016	0.018	0.009	0.0086	0.007
U	0.000	0.001	0.001	0.004	0.000	0.000	0.000	0.000	0.000	0.000	0.000	0.0000	0.001

Table 4-4. Annual averages for PM<sub>2.5</sub> mass and chemical constituents( $\mu\text{g}/\text{m}^3$ ) at KC.

Site	KC	KC	KC	KC	KC	KC
Year	2015	2016	2017	2018	2019	2020
Teflon Mass	24.458	20.740	22.076	19.512	18.893	15.549
QMA Mass	26.557	22.106	23.913	20.775	21.987	17.820
Cl <sup>-</sup>	0.098	0.072	0.087	0.057	0.077	0.076
NO <sub>3</sub> <sup>-</sup>	0.848	0.612	0.705	0.753	0.753	0.684
SO <sub>4</sub> <sup>2-</sup>	7.737	6.557	6.511	5.285	5.357	3.964
NH <sub>4</sub> <sup>+</sup>	2.679	2.420	2.287	1.270	2.038	1.271
Na <sup>+</sup>	0.364	0.294	0.395	0.969	0.322	0.300
K <sup>+</sup>	0.185	0.220	0.233	0.158	0.180	0.101
OC	4.055	5.171	5.140	3.090	3.523	2.861
EC	2.760	2.604	2.278	2.282	1.618	1.626
TC	6.810	7.775	7.418	5.331	5.141	4.461
Al	0.077	0.124	0.144	0.098	0.113	0.032
Si	0.154	0.191	0.260	0.187	0.232	0.126
P	0.000	0.003	0.003	0.000	0.001	0.000
S	2.933	2.552	2.577	2.082	2.235	1.493
Cl	0.044	0.052	0.109	0.078	0.061	0.064
K	0.227	0.243	0.293	0.202	0.254	0.168
Ca	0.092	0.084	0.133	0.109	0.081	0.074
Ti	0.008	0.008	0.010	0.011	0.008	0.007
V	0.037	0.025	0.020	0.017	0.006	0.003
Cr	0.002	0.000	0.003	0.003	0.000	0.001
Mn	0.009	0.006	0.012	0.009	0.010	0.009
Fe	0.185	0.171	0.212	0.216	0.193	0.173
Co	0.000	0.000	0.000	0.000	0.000	0.000
Ni	0.010	0.006	0.005	0.005	0.003	0.005
Cu	0.016	0.016	0.018	0.010	0.009	0.004
Zn	0.078	0.076	0.083	0.059	0.068	0.058
Ga	0.000	0.000	0.000	0.000	0.000	0.000
As	0.003	0.000	0.000	0.000	0.000	0.000
Se	0.001	0.000	0.000	0.001	0.000	0.001
Br	0.011	0.005	0.010	0.007	0.000	0.005
Rb	0.001	0.000	0.000	0.001	0.000	0.001
Sr	0.002	0.001	0.001	0.002	0.000	0.002
Y	0.000	0.000	0.000	0.000	0.000	0.000
Zr	0.001	0.000	0.001	0.001	0.000	0.001
Mo	0.001	0.001	0.000	0.000	0.001	0.001
Pd	0.000	0.001	0.000	0.000	0.000	0.001
Ag	0.000	0.000	0.000	0.000	0.000	0.001
Cd	0.000	0.000	0.000	0.000	0.001	0.001
In	0.000	0.000	0.001	0.000	0.001	0.001
Sn	0.002	0.004	0.003	0.000	0.001	0.001
Sb	0.001	0.001	0.000	0.001	0.000	0.000
Ba	0.000	0.021	0.013	0.001	0.000	0.001
La	0.001	0.016	0.001	0.003	0.000	0.001
Au	0.000	0.000	0.000	0.000	0.000	0.000
Hg	0.000	0.000	0.000	0.000	0.000	0.000
Tl	0.000	0.000	0.000	0.000	0.000	0.000
Pb	0.018	0.016	0.018	0.010	0.011	0.007
U	0.000	0.000	0.000	0.000	0.000	0.000



Table 4-5. Annual averages for PM<sub>2.5</sub> mass and chemical constituents(μg/m<sup>3</sup>) at WB..

Site	WB	WB	WB	WB	WB	WB	WB	WB	WB	WB
Year	2011	2012	2013	2014	2015	2016	2017	2018	2019	2020
Teflon Mass	31.320	25.480	26.080	23.120	21.082	16.985	18.665	16.720	16.652	13.201
QMA Mass	35.890	45.580	30.380	23.810	22.089	17.098	19.317	16.849	19.021	15.002
Cl <sup>-</sup>	0.105	0.070	0.093	0.123	0.083	0.035	0.072	0.034	0.074	0.099
NO <sub>3</sub> <sup>-</sup>	0.930	0.510	0.580	0.520	0.527	0.347	0.469	0.481	0.630	0.624
SO <sub>4</sub> <sup>2-</sup>	11.130	9.340	9.250	8.450	7.367	5.965	6.118	4.960	5.203	3.758
NH <sub>4</sub> <sup>+</sup>	4.090	3.130	3.160	2.850	2.370	2.157	2.123	1.111	1.941	1.196
Na <sup>+</sup>	0.510	0.390	0.401	0.482	0.453	0.211	0.376	0.915	0.319	0.316
K <sup>+</sup>	0.483	0.290	0.318	0.273	0.177	0.194	0.209	0.159	0.191	0.089
OC	3.910	3.070	3.370	4.390	2.661	3.572	3.730	1.912	2.349	1.877
EC	2.430	1.840	1.960	1.290	1.006	1.008	0.933	1.094	0.775	0.861
TC	6.310	4.920	5.330	5.680	3.663	4.581	4.663	2.965	3.123	2.712
Al	0.199	0.226	0.201	0.169	0.094	0.112	0.135	0.108	0.1250	0.038
Si	0.398	0.406	0.353	0.269	0.158	0.174	0.237	0.199	0.2509	0.140
P	0.015	0.013	0.012	0.013	0.000	0.002	0.002	0.000	0.0005	0.000
S	3.840	3.176	3.234	3.028	2.845	2.400	2.441	1.993	2.1624	1.398
Cl	0.072	0.024	0.095	0.132	0.074	0.044	0.105	0.069	0.0570	0.081
K	0.474	0.301	0.369	0.303	0.230	0.222	0.267	0.204	0.2540	0.158
Ca	0.091	0.109	0.085	0.072	0.075	0.052	0.077	0.090	0.0639	0.062
Ti	0.011	0.012	0.010	0.008	0.008	0.006	0.007	0.010	0.0065	0.005
V	0.012	0.013	0.015	0.015	0.013	0.014	0.012	0.009	0.0052	0.001
Cr	0.002	0.002	0.002	0.002	0.002	0.001	0.002	0.003	0.0000	0.001
Mn	0.017	0.013	0.013	0.010	0.007	0.005	0.007	0.007	0.0072	0.007
Fe	0.158	0.153	0.134	0.121	0.111	0.082	0.115	0.137	0.1046	0.099
Co	0.000	0.000	0.000	0.000	0.000	0.000	0.000	0.000	0.0001	0.000
Ni	0.004	0.005	0.005	0.004	0.004	0.004	0.004	0.003	0.0017	0.002
Cu	0.023	0.018	0.020	0.016	0.010	0.011	0.015	0.010	0.0076	0.003
Zn	0.195	0.134	0.140	0.106	0.074	0.057	0.076	0.043	0.0404	0.030
Ga	0.000	0.000	0.000	0.000	0.000	0.000	0.000	0.000	0.0000	0.000
As	0.005	0.003	0.004	0.002	0.004	0.000	0.001	0.000	0.0000	0.000
Se	0.000	0.000	0.000	0.000	0.001	0.000	0.000	0.001	0.0000	0.001
Br	0.019	0.016	0.016	0.014	0.013	0.006	0.011	0.006	0.0000	0.005
Rb	0.001	0.001	0.001	0.000	0.001	0.000	0.000	0.001	0.0002	0.001
Sr	0.003	0.002	0.002	0.001	0.002	0.001	0.001	0.003	0.0009	0.001
Y	0.000	0.000	0.000	0.000	0.000	0.000	0.000	0.000	0.0000	0.000
Zr	0.000	0.001	0.001	0.001	0.001	0.000	0.001	0.001	0.0001	0.001
Mo	0.001	0.000	0.000	0.001	0.001	0.002	0.000	0.000	0.0009	0.000
Pd	0.002	0.000	0.000	0.000	0.000	0.000	0.000	0.000	0.0001	0.001
Ag	0.000	0.000	0.000	0.000	0.000	0.000	0.000	0.000	0.0001	0.002
Cd	0.001	0.001	0.001	0.000	0.000	0.000	0.000	0.000	0.0003	0.001
In	0.001	0.000	0.000	0.000	0.000	0.000	0.001	0.000	0.0023	0.001
Sn	0.013	0.004	0.005	0.004	0.002	0.005	0.002	0.000	0.0012	0.001
Sb	0.007	0.001	0.001	0.002	0.000	0.001	0.000	0.001	0.0000	0.001
Ba	0.009	0.013	0.005	0.004	0.001	0.015	0.006	0.001	0.0015	0.000
La	0.015	0.000	0.000	0.004	0.001	0.014	0.001	0.003	0.0007	0.000
Au	0.000	0.000	0.000	0.000	0.000	0.000	0.000	0.000	0.0000	0.000
Hg	0.000	0.000	0.000	0.000	0.000	0.000	0.000	0.000	0.0000	0.000
Tl	0.000	0.000	0.000	0.000	0.000	0.000	0.000	0.000	0.0000	0.000
Pb	0.063	0.037	0.041	0.034	0.018	0.017	0.019	0.010	0.0112	0.006
U	0.004	0.000	0.000	0.000	0.000	0.000	0.000	0.000	0.0001	0.001

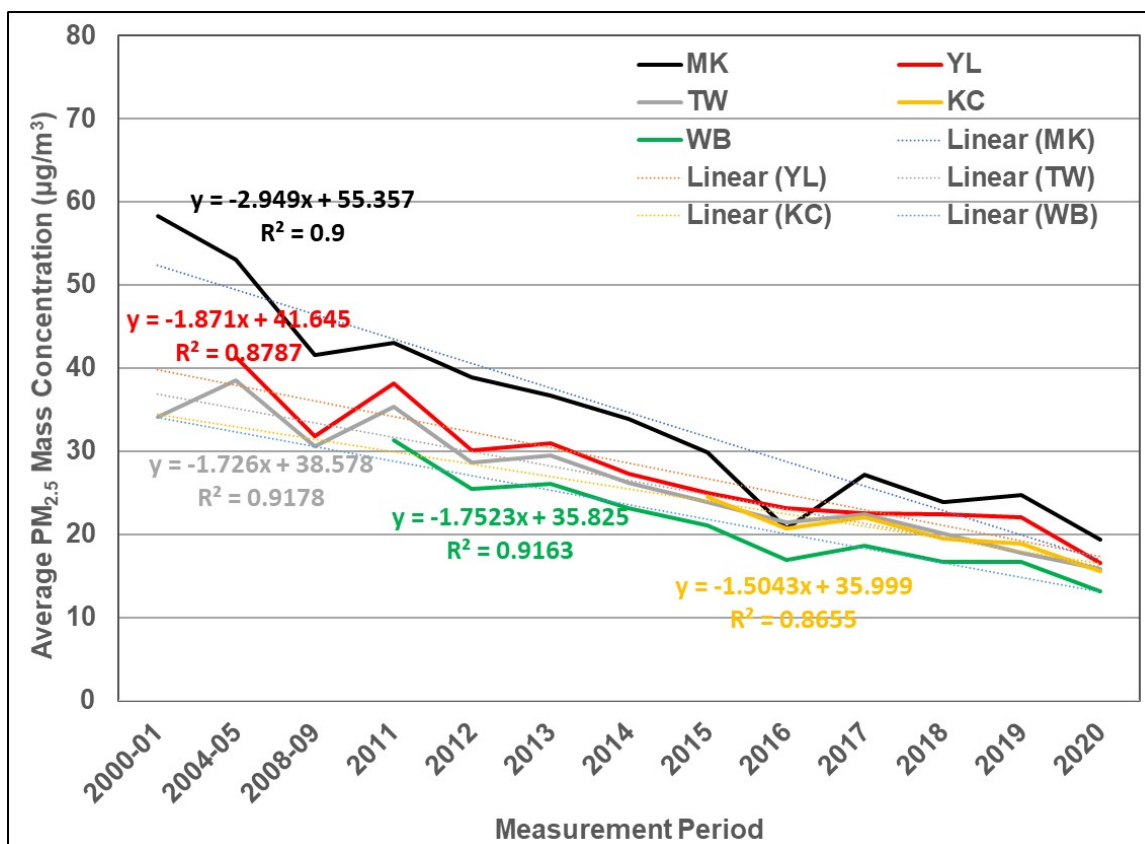


Figure 4-1. Trends in PM<sub>2.5</sub> annual averages at the five speciation sites.

Table 4-6. 2020 annual average contributions of major PM<sub>2.5</sub> components (µg/m<sup>3</sup>).

Component	MK	YL	KC	TW	WB	All
MeasMass	19.33	16.54	15.55	15.87	13.20	16.10
RecMass	16.55	13.75	12.93	12.66	10.36	13.26
OM	4.95	4.39	4.00	4.12	2.63	4.02
EC	3.27	1.44	1.63	1.38	0.86	1.72
Sulfate	4.05	4.06	3.96	3.82	3.76	3.93
Nitrate	1.18	1.03	0.68	0.77	0.62	0.86
Ammonium	1.40	1.39	1.27	1.22	1.20	1.29
Salt	0.50	0.36	0.38	0.41	0.42	0.41
Minerals	0.87	0.71	0.68	0.65	0.60	0.70
Trace	0.34	0.37	0.32	0.30	0.28	0.32
Unid	2.78	2.79	2.62	3.21	2.84	2.84

Table 4-7. 2020 annual average relative contributions (%) of major PM<sub>2.5</sub> components.

Component	MK	YL	KC	TW	WB	All
RecMass	85.62%	83.11%	83.13%	79.79%	78.47%	82.34%
OM	25.59%	26.56%	25.76%	25.95%	19.91%	24.94%
EC	16.92%	8.70%	10.46%	8.69%	6.52%	10.70%
Sulfate	20.93%	24.52%	25.49%	24.08%	28.46%	24.41%
Nitrate	6.12%	6.23%	4.40%	4.85%	4.73%	5.34%
Ammonium	7.22%	8.39%	8.17%	7.69%	9.06%	8.04%
Salt	2.59%	2.19%	2.42%	2.56%	3.15%	2.56%
Minerals	4.50%	4.31%	4.39%	4.07%	4.55%	4.37%
Trace	1.74%	2.22%	2.04%	1.90%	2.10%	1.99%
Unid	14.38%	16.89%	16.87%	20.21%	21.53%	17.66%

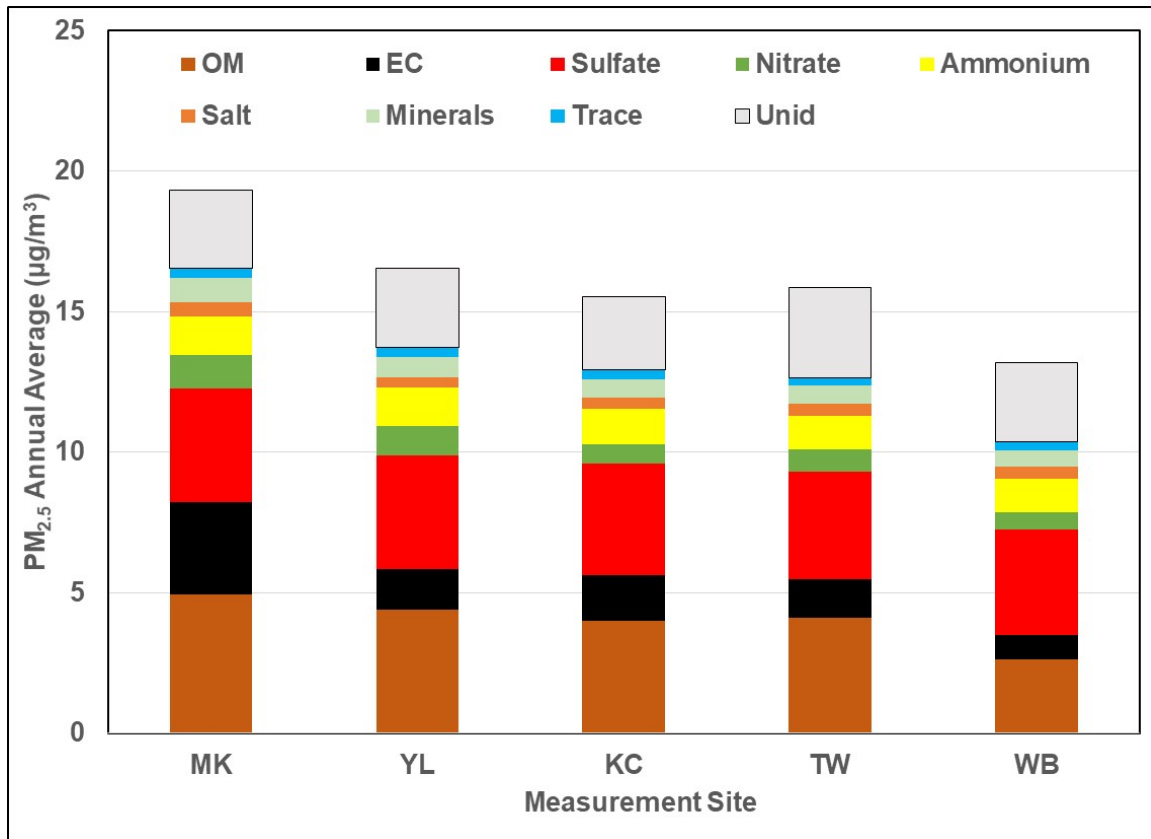


Figure 4-2. Contributions of major components to 2020 PM<sub>2.5</sub> average concentrations.

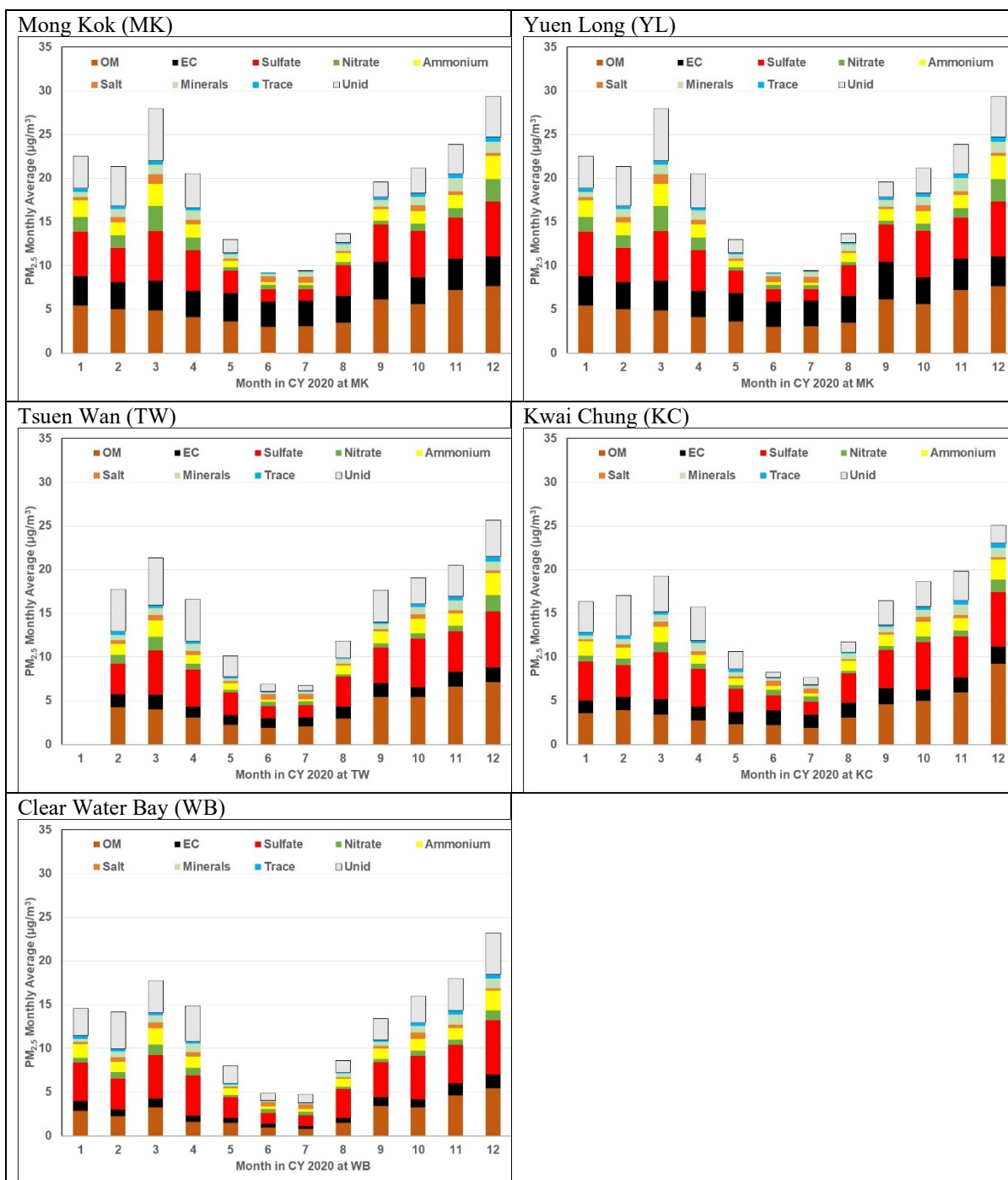


Figure 4-3. Monthly average contributions from major  $PM_{2.5}$  components at each site.

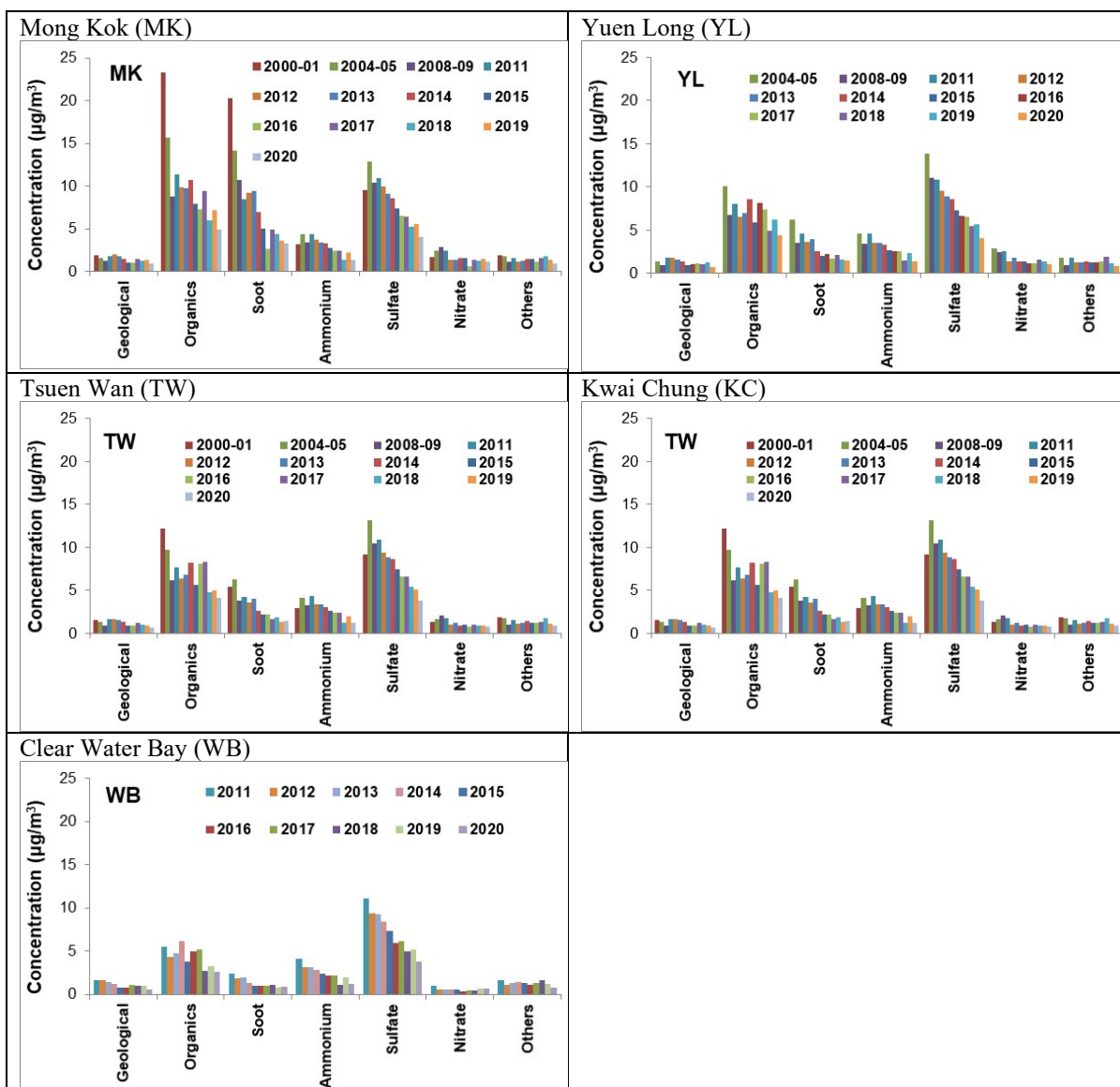


Figure 4-4. Trends in contributions from major components to PM<sub>2.5</sub>.

Table 4-8. Change in annual average contributions from 2019 to 2020 (µg/m<sup>3</sup>).

Category\Site	MK	YL	TW	KC	WB
Geological	-0.51	-0.58	-0.21	-0.42	-0.41
Organics	-2.24	-1.79	-0.88	-0.93	-0.66
Soot	-0.30	-0.11	0.10	0.01	0.09
Ammonium	-0.86	-0.98	-0.77	-0.77	-0.75
Sulfate	-1.48	-1.67	-1.25	-1.39	-1.45
Nitrate	-0.25	-0.40	-0.09	-0.07	-0.01
Others	-0.42	-0.35	-0.26	-0.39	-0.37
PM <sub>2.5</sub>	-5.42	-5.52	-1.95	-3.34	-3.45

## 5 Summary

This report summarizes the validation and quality assurance aspects of the chemical analysis of filter samples from the Hong Kong PM<sub>2.5</sub> speciation network from January 1 through December 31, 2020. Sampling was conducted at Mong Kok (MK), Yuen Long (YL), Tsuen Wan (TW), Kwai Chung (KC), and Clear Water Bay (WB) sites on a 1-in-6 day schedule which yielded a total of 60 sampling events at each site through the year. 298 filter sets out of 300 available were analyzed for the full complement of PM<sub>2.5</sub> mass, ions, carbon fractions and elements.

The data were evaluated by comparisons among different measurements that included comparing the sum of species concentrations to measured mass, comparisons of sulfur, chloride, and potassium measured by ion chromatography and x-ray fluorescence, comparison of colocated samples, and comparisons of reconstructed with measured mass.

Similar to the past years, sulfate and organic material were the most abundant PM<sub>2.5</sub> components across all sites, constituting more than or close to 50% of the mass. Average sulfate levels were homogeneous across the network while the organic material was highest at the MK and YL sites which are most influenced by Hong Kong traffic. Ammonium correlated with sulfate and nitrate concentrations, although there is evidence that some of the chloride in marine aerosols is being replaced by combination of sodium with nitric acid. This results in an overestimation of measured ammonium when nitrate is assumed to be only in the ammonium nitrate form.

The unidentified PM<sub>2.5</sub>, that is not assigned to the major categories, constitutes ~15% to ~20% of the PM<sub>2.5</sub> mass, exceeding that of or the EC, Nitrate, Ammonium, Salt, Minerals, and Trace categories. While this unexplained part of the mass is negligible during summer, it becomes an important contributor during other parts of the year. Potential causes are too low a multiplier to convert OC to OM (currently 1.4, but can exceed a factor of two for different aerosol compositions) and retention of liquid water associated with the ions. The causes can be narrowed with more specific analysis of the organic fraction and experiments that further desiccate the filters prior to gravimetric analysis.

Long-term trends show continued improvement in year-to-year PM<sub>2.5</sub> levels and the major contributors, indicating the success of HKEPD's emission reduction efforts in the SAR and improvements to emissions in the nearby mainland.

## 6 References

- Akhter, M.S., Chughtai, A.R., Smith, D.M., (1985a). The structure of hexane soot I. Spectroscopic studies. *Applied Spectroscopy*, 39, 143-153.
- Akhter, M.S., Chughtai, A.R., Smith, D.M., (1985b). The structure of hexane soot II. Extraction studies. *Applied Spectroscopy*, 39, 154-167.
- Ali, G., Abbas, S., Qamer, F.M., Irteza, S.M., (2021). Environmental spatial heterogeneity of the impacts of COVID-19 on the top-20 metropolitan cities of Asia-Pacific. *Scientific Reports*, 11, 20339-20347.
- Bevington, P.R., (1969). *Data Reduction and Error Analysis for the Physical Sciences*. McGraw Hill, New York, NY.
- Birch, M.E., Cary, R.A., (1996). Elemental carbon-based method for monitoring occupational exposures to particulate diesel exhaust. *Aerosol Science and Technology*, 25, 221-241.
- Chen, L.-W.A., Chow, J.C., Wang, X.L., Robles, J.A., Sumlin, B.J., Lowenthal, D.H., Zimmermann, R., Watson, J.G., (2015). Multi-wavelength optical measurement to enhance thermal/optical analysis for carbonaceous aerosol. *Atmospheric Measurement Techniques*, 8, 451-461. <http://www.atmos-meas-tech.net/8/451/2015/amt-8-451-2015.html>
- Chen, L.-W.A., Chow, J.C., Wang, X.L., Cao, J.J., Mao, J.Q., Watson, J.G., (2021). Brownness of organic aerosol over the United States: Evidence for seasonal biomass burning and photobleaching effects. *Environmental Science & Technology*, 55, 8561-8572. 10.1021/acs.est.0c08706. <https://doi.org/10.1021/acs.est.0c08706>
- Chow, J.C., Watson, J.G., (1989). Summary of particulate data bases for receptor modeling in the United States, Watson, J.G. (Ed.) *Transactions, Receptor Models in Air Resources Management*, Air & Waste Management Association, Pittsburgh, PA, pp. 108-133.
- Chow, J.C., Watson, J.G., Pritchett, L.C., Pierson, W.R., Frazier, C.A., Purcell, R.G., (1993). The DRI Thermal/Optical Reflectance carbon analysis system: Description, evaluation and applications in U.S. air quality studies. *Atmospheric Environment*, 27A, 1185-1201.
- Chow, J.C., Watson, J.G., (1994). Contemporary source profiles for geological material and motor vehicle emissions. Desert Research Institute, Reno, NV. [https://www.researchgate.net/publication/235341474\\_Contemporary\\_source\\_profiles\\_for\\_geological\\_material\\_and\\_motor\\_vehicle\\_emissions](https://www.researchgate.net/publication/235341474_Contemporary_source_profiles_for_geological_material_and_motor_vehicle_emissions)
- Chow, J.C., (1995). Critical review: Measurement methods to determine compliance with ambient air quality standards for suspended particles. *Journal of the Air & Waste Management Association*, 45, 320-382. <http://www.tandfonline.com/doi/pdf/10.1080/10473289.1995.10467369>
- Chow, J.C., Watson, J.G., (1999). Ion chromatography in elemental analysis of airborne particles, Landsberger, S., Creatchman, M. (Eds.), *Elemental Analysis of Airborne Particles*, Vol. 1, Gordon and Breach Science, Amsterdam, pp. 97-137.
- Chow, J.C., Watson, J.G., Crow, D., Lowenthal, D.H., Merrifield, T.M., (2001). Comparison of IMPROVE and NIOSH carbon measurements. *Aerosol Science and Technology*, 34, 23-34. 10.1080/02786820600623711. <http://www.tandfonline.com/doi/pdf/10.1080/02786820600623711>
- Chow, J.C., Watson, J.G., Chen, L.-W.A., Arnott, W.P., Moosmüller, H., Fung, K.K., (2004). Equivalence of elemental carbon by Thermal/Optical Reflectance and Transmittance with different temperature protocols. *Environmental Science & Technology*, 38, 4414-4422. [https://www.researchgate.net/publication/8331878\\_Equivalence\\_of\\_Elemental\\_Carbon\\_by\\_ThermalOptical\\_Reflectance\\_and\\_Transmittance\\_with\\_Different\\_Temperature\\_Protocols](https://www.researchgate.net/publication/8331878_Equivalence_of_Elemental_Carbon_by_ThermalOptical_Reflectance_and_Transmittance_with_Different_Temperature_Protocols)
- Chow, J.C., Watson, J.G., Chen, L.-W.A., Chang, M.-C.O., Robinson, N.F., Trimble, D.L., Kohl, S.D., (2007). The IMPROVE\_A temperature protocol for thermal/optical carbon analysis: Maintaining consistency with a long-term database. *Journal of the Air & Waste Management Association*, 57, 1014-1023. <http://www.tandfonline.com/doi/pdf/10.3155/1047-3289.57.9.1014>
- Chow, J.C., Watson, J.G., Chen, L.-W.A., Rice, J., Frank, N.H., (2010). Quantification of PM<sub>2.5</sub> organic carbon sampling artifacts in US networks. *Atmospheric Chemistry and Physics*, 10, 5223-5239. <http://www.atmos-chem-phys.net/10/5223/2010/acp-10-5223-2010.pdf>
- Chow, J.C., Watson, J.G., Robles, J., Wang, X.L., Chen, L.-W.A., Trimble, D.L., Kohl, S.D., Tropp, R.J., Fung, K.K., (2011). Quality assurance and quality control for thermal/optical analysis of aerosol samples for organic and elemental carbon. *Analytical and Bioanalytical Chemistry*, 401, 3141-3152. DOI 10.1007/s00216-011-5103-3.

- [https://www.researchgate.net/publication/51178259\\_Quality\\_assurance\\_and\\_quality\\_control\\_for\\_thermaloptical\\_analysis\\_of\\_aerosol\\_samples\\_for\\_organic\\_and\\_elemental\\_carbon](https://www.researchgate.net/publication/51178259_Quality_assurance_and_quality_control_for_thermaloptical_analysis_of_aerosol_samples_for_organic_and_elemental_carbon)
- Chow, J.C., Lowenthal, D.H., Chen, L.-W.A., Wang, X.L., Watson, J.G., (2015a). Mass reconstruction methods for PM<sub>2.5</sub>: A review. *Air Qual. Atmos. Health*, 8, 243-263.  
<http://link.springer.com/article/10.1007%2Fs11869-015-0338-3#page-1>
- Chow, J.C., Wang, X.L., Sumlin, B.J., Gronstal, S.B., Chen, L.-W.A., Trimble, D.L., Kohl, S.D., Mayorga, S.R., Riggio, G.M., Hurbain, P.R., Johnson, M., Zimmermann, R., Watson, J.G., (2015b). Optical calibration and equivalence of a multiwavelength thermal/optical carbon analyzer. *Aerosol and Air Quality Research*, 15, 1145-1159. doi:10.4209/aaqr.2015.02.0106.  
[http://aaqr.org/VOL15\\_No4\\_August2015/1\\_AAQR-15-02-OA-0106\\_1145-1159.pdf](http://aaqr.org/VOL15_No4_August2015/1_AAQR-15-02-OA-0106_1145-1159.pdf)
- Chow, J.C., Watson, J.G., (2017). Enhanced ion chromatographic speciation of water-soluble PM<sub>2.5</sub> to improve aerosol source apportionment. *Aerosol Science and Engineering*, 1, 7-24. doi:10.1007/s41810-017-0002-4.  
<http://link.springer.com/article/10.1007/s41810-017-0002-4>
- Chow, J.C., Watson, J.G., Green, M.C., Wang, X.L., Chen, L.-W.A., Trimble, D.L., Cropper, P.M., Kohl, S.D., Gronstal, S.B., (2018). Separation of brown carbon from black carbon for IMPROVE and CSN PM<sub>2.5</sub> samples. *Journal of the Air & Waste Management Association*, 68, 494-510.
- Chow, J.C., Chen, L.-W.A., Wang, X.L., Green, M.C., Watson, J.G., (2021). Improved estimation of PM<sub>2.5</sub> brown carbon contributions to filter light attenuation. *Particuology*, 56, 1-9. 10.1016/j.partic.2021.01.001.  
<https://www.sciencedirect.com/science/article/pii/S1674200121000158>
- Cui, L., Wang, X.L., Ho, K.F., Gao, Y., Liu, C., Ho, S.S.H., Li, H.W., Lee, S.C., Wang, X.M., Jiang, B.Q., Huang, Y., Chow, J.C., Watson, J.G., Chen, L.-W.A., (2018). Decrease of VOC emissions from vehicular emissions' in Hong Kong from 2003 to 2015: Results from a tunnel study. *Atmospheric Environment*, 177, 64-74. 10.1016/j.atmosenv.2018.01.020.
- Fitz, D.R., (1990). Reduction of the positive organic artifact on quartz filters. *Aerosol Science and Technology*, 12, 142-148.
- Hidy, G.M., (1985). Jekyll Island meeting report: George Hidy reports on the acquisition of reliable atmospheric data. *Environmental Science & Technology*, 19, 1032-1033.
- HKEPD, (2021a). Hong Kong air pollutant emission inventory. Hong Kong Department of Environmental Protection, Hong Kong, SAR.  
[https://www.epd.gov.hk/epd/english/environmentinhk/air/air\\_quality\\_objectives/air\\_quality\\_objectives.html](https://www.epd.gov.hk/epd/english/environmentinhk/air/air_quality_objectives/air_quality_objectives.html)
- HKEPD, (2021b). PM<sub>2.5</sub> speciation study in Hong Kong. Hong Kong Environmental Protection Department, Wan Chai, HongKong.  
[https://www.epd.gov.hk/epd/english/environmentinhk/air/studyrrpts/pm25\\_study.html](https://www.epd.gov.hk/epd/english/environmentinhk/air/studyrrpts/pm25_study.html)
- Huang, Y., Zhou, J.L., Yang, Y., Wai-chuen, M., Lee, C.F.C., Yam, Y.S., (2020). Uncertainty in the impact of the COVID-19 pandemic on air quality in Hong Kong, China. *Atmosphere*, 11, 914-922.
- Kenny, L.C., Merrifield, T.M., Mark, D., Gussman, R.A., Thorpe, A., (2004). The development and designation testing of a new USEPA-approved fine particle inlet: A study of the USEPA designation process. *Aerosol Science and Technology*, 38, 15-22. <http://www.tandfonline.com/doi/pdf/10.1080/027868290502290>
- Lee, K.W., Ramamurthi, M., (1993). Filter collection, Willeke, K., Baron, P.A. (Eds.), *Aerosol Measurement: Principles, Techniques and Applications*, Van Nostrand, Reinhold, New York, NY, pp. 179-205.
- Lioy, P.J., Watson, J.G., Spengler, J.D., (1980). APCA specialty conference workshop on baseline data for inhalable particulate matter. *Journal of the Air Pollution Control Association*, 30, 1126-1130.  
<http://www.tandfonline.com/doi/pdf/10.1080/00022470.1980.10465158>
- Lippmann, M., (1989). Sampling aerosols by filtration, Hering, S.V. (Ed.) *Air Sampling Instruments for Evaluation of Atmospheric Contaminants*, 7 ed. American Conference of Governmental Industrial Hygienists, Cincinnati, OH, pp. 305-336.
- Louie, P.K.K., G.S.P., L., B.T.W., Y., Sin, D.W.M., Yu, J.Z., Lau, A., Bergin, M., Zheng, M., Chow, J.C., Watson, J.G., (2002). Twelve-month particulate matter study in Hong Kong. Hong Kong Environmental Protection Department, Wan Chai, Hong Kong, SAR, China.  
<http://www.epd.gov.hk/epd/english/environmentinhk/air/studyrrpts/files/content.pdf>
- Louie, P.K.K., Chow, J.C., Chen, L.-W.A., Watson, J.G., Leung, G., Sin, D., (2005a). PM<sub>2.5</sub> chemical composition in Hong Kong: Urban and regional variations. *Science of the Total Environment*, 338, 267-281.
- Louie, P.K.K., Watson, J.G., Chow, J.C., Chen, L.-W.A., Sin, D.W.M., Lau, A.K.H., (2005b). Seasonal characteristics and regional transport of PM<sub>2.5</sub> in Hong Kong. *Atmospheric Environment*, 39, 1695-1710.



- Lyu, X.P., Guo, H., Simpson, I.J., Meinardi, S., Louie, P.K.K., Ling, Z.H., Wang, Y., Liu, M., Luk, C.W.Y., Wang, N., Blake, D.R., (2016). Effectiveness of replacing catalytic converters in LPG-fueled vehicles in Hong Kong. *Atmospheric Chemistry and Physics*, 16, 6609-6626. 10.5194/acp-16-6609-2016.
- Niu, X.Y., Chuang, H.C., Wang, X.L., Ho, S.S.H., Li, L.J., Qu, L.L., Chow, J.C., Watson, J.G., Sun, J., Lee, S.C., Cao, J.J., Ho, K.F., (2020). Cytotoxicity of PM<sub>2.5</sub> vehicular emissions in the Shing Mun Tunnel, Hong Kong. *Environmental Pollution*, 263, 114386. 10.1016/j.envpol.2020.114386.  
<http://www.sciencedirect.com/science/article/pii/S0269749119370253>
- Pitchford, M.L., Malm, W.C., Schichtel, B.A., Kumar, N.K., Lowenthal, D.H., Hand, J.L., (2007). Revised algorithm for estimating light extinction from IMPROVE particle speciation data. *Journal of the Air & Waste Management Association*, 57, 1326-1336.
- Root, R.A., (2000). Lead loading of urban streets by motor vehicle wheel weights. *Environ. Health Perspect*, 108, 937-940.
- Turpin, B.J., Huntzicker, J.J., Hering, S.V., (1994). Investigation of organic aerosol sampling artifacts in the Los Angeles Basin. *Atmospheric Environment*, 28, 3061-3071. Research & Development.
- Turpin, B.J., Lim, H.J., (2001). Species contributions to PM<sub>2.5</sub> mass concentrations: Revisiting common assumptions for estimating organic mass. *Aerosol Science and Technology*, 35, 602-610.
- U.S.EPA, (2012). Quality assurance project plan: PM<sub>2.5</sub> chemical speciation sampling at Trends, NCore, supplemental and tribal sites. U.S. Environmental Protection Agency, Research Triangle Park, NC.  
[https://www3.epa.gov/ttnamtl/files/ambient/pm25/spec/CSN\\_QAPP\\_v120\\_05-2012.pdf](https://www3.epa.gov/ttnamtl/files/ambient/pm25/spec/CSN_QAPP_v120_05-2012.pdf)
- U.S.EPA, (2021). Sampling schedule calendar. U.S. Environmental Protection Agency, Research Triangle Park, NC. <https://www.epa.gov/amtic/sampling-schedule-calendar>
- Wang, X.L., Ho, K.F., Chow, J.C., Kohl, S.D., Chan, C.S., Cui, L., Lee, S.C., Chen, L.-W.A., Ho, S.S.H., Cheng, Y., Watson, J.G., (2018). Hong Kong vehicle emission changes from 2003 to 2015 in the Shing Mun Tunnel. *Aerosol Science and Technology*, 52, 1085–1098. 10.1080/02786826.2018.1456650.
- Wang, X.L., Chen, L.-W.A., Ho, K.F., Chan, C.S., Zhang, Z.Z., Lee, S.C., Chow, J.C., Watson, J.G., (2021). Comparison of vehicle emissions by EMFAC-HK model and tunnel measurement in Hong Kong. *Atmospheric Environment*, 256, 118452. 10.1016/j.atmosenv.2021.118452.  
<https://www.sciencedirect.com/science/article/pii/S1352231021002739>
- Watson, J.G., Lioy, P.J., Mueller, P.K., (1989). The measurement process: Precision, accuracy, and validity, Hering, S.V. (Ed.) *Air Sampling Instruments for Evaluation of Atmospheric Contaminants*, Seventh Edition, 7th ed. American Conference of Governmental Industrial Hygienists, Cincinnati, OH, pp. 51-57.
- Watson, J.G., Chow, J.C., (1992). Data bases for PM<sub>10</sub> and PM<sub>2.5</sub> chemical compositions and source profiles, Chow, J.C., Ono, D.M. (Eds.), *Transactions, PM10 Standards and Nontraditional Particulate Source Controls*, Air & Waste Management Association, Pittsburgh, PA, pp. 61-91.
- Watson, J.G., Chow, J.C., (1993). *Ambient air sampling*, Willeke, K., Baron, P.A. (Eds.), *Aerosol Measurement: Principles, Techniques and Applications*, Van Nostrand, Reinhold, New York, NY, pp. 622-639.
- Watson, J.G., Chow, J.C., (1994). Particle and gas measurements on filters, Markert, B. (Ed.) *Environmental Sampling for Trace Analysis*, VCH, New York, pp. 125-161.
- Watson, J.G., Chow, J.C., Frazier, C.A., (1999). X-ray fluorescence analysis of ambient air samples, Landsberger, S., Creatchman, M. (Eds.), *Elemental Analysis of Airborne Particles*, Vol. 1, Gordon and Breach Science, Amsterdam, The Netherlands, pp. 67-96.
- Watson, J.G., Turpin, B.J., Chow, J.C., (2001). The measurement process: Precision, accuracy, and validity, Cohen, B.S., McCammon, C.S., Jr (Eds.), *Air Sampling Instruments for Evaluation of Atmospheric Contaminants*, Ninth Edition, 9th ed. American Conference of Governmental Industrial Hygienists, Cincinnati, OH, pp. 201-216.  
[https://www.researchgate.net/publication/235341825\\_The\\_measurement\\_process\\_Precision\\_accuracy\\_and\\_validity](https://www.researchgate.net/publication/235341825_The_measurement_process_Precision_accuracy_and_validity)
- Watson, J.G., Chow, J.C., Chen, L.-W.A., (2005). Summary of organic and elemental carbon/black carbon analysis methods and intercomparisons. *Aerosol and Air Quality Research*, 5, 65-102. 10.4209/aaqr.2005.06.0006 [http://aaqr.org/VOL5\\_No1\\_June2005/6\\_AAQR-05-06-OA-0006\\_65-102.pdf](http://aaqr.org/VOL5_No1_June2005/6_AAQR-05-06-OA-0006_65-102.pdf)
- Watson, J.G., Chow, J.C., Chen, L.-W.A., Frank, N.H., (2009). Methods to assess carbonaceous aerosol sampling artifacts for IMPROVE and other long-term networks. *Journal of the Air & Waste Management Association*, 59, 898-911. <http://www.tandfonline.com/doi/pdf/10.3155/1047-3289.59.8.898>

- Watson, J.G., Chow, J.C., (2011). Ambient aerosol sampling, Kulkarni, P., Baron, P.A., Willeke, K. (Eds.), Aerosol Measurement: Principles, Techniques and Applications, Third Edition, Wiley, Hoboken, NJ, USA, pp. 591-614. [https://www.researchgate.net/publication/229760686\\_Ambient\\_Aerosol\\_Sampling](https://www.researchgate.net/publication/229760686_Ambient_Aerosol_Sampling)
- Watson, J.G., Tropp, R.J., Kohl, S.D., Wang, X.L., Chow, J.C., (2017). Filter processing and gravimetric analysis for suspended particulate matter samples. Aerosol Science and Engineering, 1, 193-205.
- Yao, D.W., Lyu, X.P., Murray, F., Morawska, L., Yu, W., Wang, J.Y., Guo, H., (2019). Continuous effectiveness of replacing catalytic converters on liquified petroleum gas-fueled vehicles in Hong Kong. Science of the Total Environment, 648, 830-838. 10.1016/j.scitotenv.2018.08.191.
- Yu, Y.Z., Wong, Y.K., Zhang, T., (2020). Chemical speciation of PM<sub>2.5</sub> filter samples January 1 through December 31, 2019. Hong Kong Institute of Science and Technology, Clearwater Bay, Hong Kong. [https://www.epd.gov.hk/epd/sites/default/files/epd/english/environmentinhk/air/study/rpts/files/final\\_report\\_mvtmpms\\_2019.pdf](https://www.epd.gov.hk/epd/sites/default/files/epd/english/environmentinhk/air/study/rpts/files/final_report_mvtmpms_2019.pdf)